CATALYTIC OXIDATION OF ISOBUTYLENE

by

Denis J. Rouleau

A thesis submitted in partial fulfillment of the requirements for

the degree of

DOCTOR OF PHILOSOPHY

in the

DEPARTMENT OF CHEMICAL ENGINEERING
UNIVERSITY OF OTTAWA

Ottawa, Canada

April, 1964

Approved by

Ph.D. Candidate

ACKNOWLEDGMENT

The author wishes to acknowledge his sincere gratitude to Dr. B. C. -Y. Lu for providing the facilities for this research work, to Dr. R.S. Mann, who directed its course, for his advice and encouragement, to Messrs. F. Giacobbi and G. Gasperetti, for their technical assistance, to Mrs. Carriere for typing the manuscript, and to Mr. S. C. Naik, for proof reading the manuscript.

The author is much indebted to the members of the teaching staff of the Chemical Engineering Department for stimulating discussions and suggestions.

Finally, the author wishes to express his sincere thanks to the National Research Council, Ottawa for providing financial assistance.

TABLE OF CONTENTS

		PAGE
I.	ABSTRACT	viii
II.	INTRODUCTION	1
III.	LITERATURE SURVEY	4
	A. Literature Related to Propylene	4
	B. Literature Related to Isobutylene	11
IV.	EXPERIMENTAL	16
	A. Apparatus	16
	B. Reactants	21
	C. Catalyst	22
	D. Operating Procedure	27
	E. Analysis of the Products	28
V.	EFFECT OF PROCESS VARIABLES	35
VI.	KINETIC ANALYSIS OF THE DATA	41
	A. Rate Steps in Heterogeneous Catalysis	41
	B. Exterior Heat and Mass Transfer Effects	42
	C. Internal Diffusion and Effectiveness Factor	51
	D. Method of Initial Rates	54
	E. Adsorption and the Adsorption Isotherm	57
	F. Surface Reactions	64
	G. Correlation of Initial Rate Data	80
	H. Correlation of Conversion Data	89
VII.	DISCUSSION OF THE FINAL CORRELATION	117
	A. The Isobutylene Adsorption Constant $K_{C_4H_8}$	117
	B. The Methacrolein Adsorption Constant $K_{C_4H_6O}$	117

		PAGE
	C. The Rate Constant α	118
	D. The Rate Equation	118
VIII.	CONCLUSIONS AND RECOMMENDATIONS	121
IX.	NOMENCLATURE	124
X.	BIBLIOGRAPHY	131
XI.	APPENDICES	134
	A. Instrument Calibrations and Analysis of Products	135
	B. Density Determination of Methacrolein	142
	C. Experimental Data	144
	D. Effect of Process Variables on Conversion and Yield	167
	E. Calculation of Drops of Partial Pressures and Temperature from Ambient Gas Stream to the External Surface of Catalyst	172
	F. Conversion Curves as Calculated by Equation (68)	181
	G. Calculations of $f(r_o)$ and $f(r)$	193
	H. Temperature Dependence of α, $K_{C_4H_8}$ and $K_{C_4H_6O}$	198
	I. Conversions and Yields for Different Catalysts	200

LIST OF TABLES

TABLE		PAGE
1	Properties of the Pumice Supported Copper Oxide Catalyst	26
2	Data Sheet	33
3	Calculated Results	34
4	Rate Equations for Fluid Reactions Catalyzed by Solids	68
5	Compositions of Feeds and Products and Conversions in Air Oxidation of Isobutylene over Catalyst 1	145
6	Effect of Feed Ratio on Conversion and Yield at 400° C for W/F = 1.0 over Catalyst 1	168
7	Effect of Temperature on Conversion and Yield for R = 2.0, W/F = 1.20 over Catalyst 1	169
8	Effect of Copper Concentration on Conversion and Yield at 400° C for W/F = 1.71 and R = 3.0	170
9	Effect of Velocity on Conversion at 400° C for R = 2.0 over Catalyst 1	171
10	Conversion Data as Calculated by Equation (68)	182
11	$f(r_o)$ as Calculated From the Different Rate Equations	194
12	Calculated Slopes from Curves of Figure 17	195
13	f(r) as Calculated From the Different Rate Equations	196
14	Temperature Dependence of α, $K_{C_4H_8}$ and $K_{C_4H_6O}$	199

LIST OF TABLES

TABLE		PAGE
15	Conversions and Yields For Different Catalysts at 400° C For R = 2.0 and W/F = 1.71	201

LIST OF FIGURES

FIGURE		PAGE
1	View of the Experimental Apparatus	17
2	Schematic diagram of the apparatus	18
3	Reactor and Preheater	20
4	Effect of Feed Ratio on Conversion and Yield	36
5	Effect of Temperature on Conversion and Yield	38
6	Effect of Copper Concentration on Conversion and Yield	39
7	Effect of Velocity on Conversion	50
8	Initial Rate Versus $P_{C_4H_8}$ in Feed at 400° C	55
9	Activated State for Adsorption of gas molecule A_2 on two adjacent sites (s_2)	61
10	Activated State for jump of an atom (A) from one adsorption site to another	62
11	Potential-energy curves for the same reaction as a homogeneous and as a heterogeneous process	75
12	$f(r_o)$ Versus P_{O_2} in Feed for Equation (53a)	84
13	$f(r_o)$ Versus $P_{C_4H_8}$ in Feed for Equation (55a)	85
14	$f(r_o)$ Versus $P_{C_4H_8}$ in Feed for Equation (57a)	86
15	$f(r_o)$ Versus $P_{C_4H_8}$ in Feed for Equation (58a)	87
16	$f(r_o)$ Versus P_{O_2} in Feed for Equation (59a)	88
17	Conversion of Isobutylene Versus Conversion of Methacrolein at 400° C	91

LIST OF FIGURES

FIGURE		PAGE
18	Slope of Curves in Fig. 17 Versus Mole Ratio of Oxygen to Isobutylene at 400° C	92
19	f(r) Versus Conversion for Equation (53b)	96
20	f(r) Versus Conversion for Equation (57b)	97
21	f(r) Versus Conversion for Equations (58b) and (59b)	98
22	Intercept of Fig. 19 Versus P_{O_2} in Feed	99
23	Intercept of Fig. 21 Versus $P_{C_4H_8}$ in Feed	100
24	Intercept of Fig. 21 Versus P_{O_2} in Feed	101
25	Conversion Curves at 400° C for R = 0.25	105
26	Conversion Curves at 400° C for R = 0.50	106
27	Conversion Curves at 400° C for R = 1.0	107
28	Conversion Curves at 400° C for R = 2.0	108
29	Conversion Curves at 400° C for R = 3.0	109
30	Conversion Curves at 400° C for R = 4.0	110
31	Conversion Curves at 350° C for R = 4.0	111
32	Conversion Curves at 375° C for R = 4.0	112
33	Conversion Curves at 425° C for R = 4.0	113
34	Conversion Curves at 450° C for R = 4.0	114
35	Temperature Dependence of α, $K_{C_4H_8}$ and $K_{C_4H_6O}$	116
36	Air Calibration 1 Atm and 75° F	136
37	Isobutylene Calibration 1 Atm. and 75° F	137
38	Calibration of Gases 1 Atm. and 75° F	138
39	Methacrolein Calibration Sensitivity, 16 Temp. 110° C	139

LIST OF FIGURES

FIGURE		PAGE
40	Typical Analysis of the Gaseous Products	140
41	Typical Analysis of the Liquid Products	141

ABSTRACT

The air oxidation of isobutylene was investigated over supported and unsupported copper oxide catalysts in an isothermal integral flow reactor. The effect of various variables, that is ratio of oxygen to isobutylene in the feed, process temperature, copper concentration on the catalyst, and reciprocal of space velocity on the conversion and yield, were determined.

It was found that out of several models proposed, only one correlated the data satisfactorily. This model described the rate-controlling step as the surface reaction between adsorbed isobutylene and gaseous oxygen or between strongly adsorbed isobutylene and weakly adsorbed oxygen. On the basis that the oxidation of isobutylene to methacrolein and carbon dioxide was a consecutive reaction, the following Hougen-Watson type rate equation was developed:

$$r = \frac{a\, K_{C_4H_8} P_{C_4H_8} P_{O_2}}{1 + K_{C_4H_8} P_{C_4H_8} + K_{C_4H_6O} P_{C_4H_6O}}$$

where $\ln a = \frac{-12,100}{RT} + \frac{20.1}{R}$

$$\ln K_{C_4H_8} = \frac{22,800}{RT} - \frac{26.8}{R}$$

$$\ln K_{C_4H_6O} = \frac{22,800}{RT} - \frac{26.8}{R}$$

The partial pressures in the rate equation were expressed in terms of conversion and the rate equation integrated to give:

$$W/F = \frac{1}{\alpha K_1 a(e-d)} \left[-\ln \left(\frac{1 - eX/d}{1 - X} \right) \right] + \frac{1}{\alpha} \left[-\frac{1}{e} \ln (1 - eX/d) \right]$$

$$+ \frac{K_3 b}{\alpha K_1 a(e-d)} \left[\ln (1-X) - \frac{d}{e} \ln (1 - eX/d) \right]$$

where a, b, d, and e are constants. The final accepted model reproduced the experimental data within the limits of experimental accuracy.

II INTRODUCTION

The oxidation of unsaturated hydrocarbons without rupture of the C-C double bond is of great theoretical interest and industrial importance. The oxidation of ethylene to ethylene oxide in particular, has received much attention in recent years. However, the catalytic oxidation of propylene and butylenes to unsaturated carbonyl compounds has received very little attention. Commercial interest in the production of methacrolein from isobutylene has been demonstrated by the patents existing in the literature. Methacrolein is already in production in the U. S. A. and some of the European countries.

The scarcity of published scientific data and the apparently anomalous nature of the patent claims indicated a definite need for further work. In order to reconcile the very meagre data and to get an insight into the mechanism of the reaction, detailed kinetic studies of the catalytic oxidation of isobutylene to methacrolein were undertaken.

The partial oxidation of isobutylene on a copper oxide catalyst was carried out under atmospheric pressure in an isothermal, integral flow reactor over a wide range of temperatures, reactant ratios and conversions. The course of the individual reaction was followed from the composition of the reaction products. The purpose of this investigation was:

(1) to determine the effects of the process variables on the conversion and yield, and

(2) to develop a reaction model similar to the one proposed by Hougen and Watson (1) which may describe a possible reaction mechanism and the rate controlling step in the reaction.

In fixed bed catalytic processes, a major part of the problem of a mathematical description is the determination of the kinetics; that is, the development of a model which could predict reaction rates under actual operating conditions. This is generally achieved by obtaining reaction rate data from a small scale differential or integral reactor under various conditions of flow rate, pressure, temperature, and reactant feed compositions. These data are then used to develop a mathematical model which could hopefully be extrapolated with confidence outside the range of the data for which it was developed. These models usually contain several constants, each a function of temperature. These must be determined from the experimental data.

One difficulty in determining the best model for a process is the large number of admissible models which should be tested before any reliance is placed in a particular model or class of models. Another difficulty stems from the economic as well as technical desirability of using integral reactors for obtaining data. Technically, reaction rates obtained from a differential reactor are usually more reliable than rates obtained by differentiation of integral reactor data. However, there is an economic advantage in obtaining kinetic data in an integral reactor at the same time when sufficient product is being prepared for evaluation and testing. In addition, the collection of kinetic data from integral reactors, while

concentrations of important side products build up in the reaction stream, permits more reliable extrapolation of any accepted model.

This dissertation describes a method which was developed to determine a rate controlling step and a possible mechanism of reaction for the oxidation of isobutylene to methacrolein over a copper oxide catalyst using an integral type flow reactor.

III. LITERATURE SURVEY

Although the oxidation of olefins to unsaturated carbonyl compounds has great industrial importance, very little scientific literature is available on the subject. The difficulty of making a kinetic analysis when simultaneous and consecutive reactions take place has been a major reason for this lack of information. However, a number of patents on the oxidation of propylene to acrolein have appeared in the last 10 years. This reaction is very similar to the oxidation of isobutylene to methacrolein. For this reason and because the scientific literature related to the oxidation of isobutylene to methacrolein is very scarce, a survey of the patents and scientific literature pertaining to the partial oxidation of propylene is presented first. This is then followed by a similar review for isobutylene.

A. Literature Related to Propylene

Isaev and Margolis (2) made a kinetic study of the air oxidation of propylene at atmospheric pressure in a dynamic unit. The copper-catalyzed oxidation of propylene yielded acrolein, carbon dioxide, water and a small quantity of acetaldehyde. At higher process temperatures, they observed a significant quantity of carbon monoxide in the gas. An organic coating that formed on the surface of the catalyst probably due to adsorption and polymerization of acrolein was also detected. These investigators found that the propylene oxidation rate was proportional to oxygen concentration and was independent of propylene concentration. They obtained an apparent activation energy of 30 k cal./gm. mole for carbon dioxide formation over a silite supported copper catalyst and 23-25 k cal./gm. mole over a pumice supported copper catalyst. Similarly, the acrolein oxidation rate was found to be proportional to oxygen concentration and independent of acrolein concentration and that the presence of propylene reduced

considerably the acrolein oxidation rate.

Later, Enikeev, Isaev and Margolis (3) studied the oxidation of propylene to acrolein on pumice supported copper oxide catalyst. The oxidation products were found to be the same, namely acrolein, carbon dioxide, water and traces of acetaldehyde and carbon monoxide. From experimental data on oxygen and propylene adsorption and results obtained while investigating the nature of the intermediary products by an isotope method, a stage scheme was proposed for the oxidation of propylene on semiconducting metal oxides. The following mechanism was postulated by these investigators for the oxidation of propylene to acrolein Oxygen in either atomic or molecular form is first adsorbed on the surface of the catalyst. Next propylene is adsorbed with its methyl group on the adsorbed oxygen without the rupture of the C-C double bond and the formation of a hydroperoxide. This hydroperoxide decomposes into acrolein and water. The adsorbed acrolein interacts with oxygen from the gas phase giving a charged intermediary complex, which decomposes into carbon dioxide, water and a hydrocarbon radical adsorbed on the surface. The latter reacts again with oxygen (chain reaction). Roginskii (4) has shown that such closed chains on the surface are characteristic for many catalytic processes. By analogy, they postulated that propylene might be adsorbed on the cuprous oxide surface with the rupture of the C-C double bond and be converted into a radical, which would react with adsorbed oxygen. The intermediary complex thus formed then decomposes into carbon dioxide, water and a hydrocarbon radical with a smaller number of carbon and hydrogen atoms. They observed that the surface of cuprous oxide was charged, when oxygen, propylene and acrolein

were adsorbed. This change in work function caused by the adsorption enabled them to determine the sign of the charge on the adsorbed molecules. They were able to establish that propylene and acrolein, like most of the organic substances, were electron donors on the cuprous oxide surface and oxygen an acceptor and that water lowered insignificantly the work function and was also a donor.

Ishikawa (5) studied the catalytic oxidation of propylene with air using cupric oxide on silica gel as catalyst in a flow system. In all experiments, the propylene concentration in the feed was about 10%, and space velocity was 0.1 l./hr./gm. catalyst. The activity of the catalyst (0.1 gm. atoms Cu/100 gm. catalyst) was studied between 200° and 300° C. He observed that in all cases, the activity of the catalyst became constant after two to four hours and that the highest conversion to acrolein, about 10% of the propylene in the feed, was obtained at a temperature of 250° C. The formation of carbon dioxide, the greater part of the side reaction, was suppressed by adding nitrogen to propylene - air mixture i.e. by lowering the mole ratio of oxygen to propylene in the feed. This resulted in higher yields. The effect of copper concentration in the catalyst on the conversion to acrolein was also studied.

Acrolein is now produced on a commercial scale in Italy by a process developed by M. Agamennone (6) whereby propylene is oxidized directly to acrolein with oxygen. The reaction is catalyzed by a thin layer of copper oxide on the walls of the reactor tube without diluent in the feed stream. According to him, the high

yields were due to a uniform temperature of the reaction zone and suppression of the combustion products in favour of catalyzed reaction. Agamennone has concluded that fast removal of the heat of reaction plus a large catalyst surface relative to free volume would be desirable.

The mechanism of catalytic oxidation of propylene to acrolein and acrylonitrile has been investigated by Adams and Jennings (7). They selectively oxidized deuterated propylene with molecular oxygen in vapor phase over two catalysts, cuprous oxide and bismuth molybdate to acrolein, and in the presence of ammonia, to acrylonitrile. Both cuprous oxide and bismuth molybdate were supported on 10-20 mesh granular SA-101 Alundum. They found that there was considerable retention of deuterium in both products. Though 61% of the acrolein formed at 350°C was monodeuterated and 1.3% dideuterated, at 410°C, 41% of the acrylonitrile formed was monodeuterated and 2.9% dideuterated over a cuprous oxide catalyst. With the bismuth molybdate catalyst at 450°C, while 62% of the acrolein was monodeuterated and 1.6% dideuterated, 44% of the acrylonitrile was monodeuterated and 0.3% dideuterated. These results suggested that the mechanism of propylene oxidation with these two catalysts was the same. Adams and Jennings showed that a mechanism consistent with the data involved the formation of an allyl intermediate by abstraction of a hydrogen or deuterium from the methyl group, followed by further abstraction at either end of this symmetric intermediate. The isotope discrimination effect k_D/k_H, assumed to be the same for all the abstractions was calculated to be 0.58 and 0.49 for acrolein and acrylonitrile on copper oxide,

and 0.50 and 0.49 respectively on bismuth molybdate. From the constancy of the results they concluded that the same mechanism was inherent in the formation of acrolein or acrylonitrile.

The mechanism of the catalytic oxidations of propylene to acrolein and of isomeric butylenes to butadiene was studied by Sachtler (8). He found that the oxidation of propylene to acrolein catalyzed by various transition metal oxides was of zero order with respect to oxygen pressure and of first order with respect to propylene pressure. Two possibilities were envisaged for the rate determining adsorption of the substrate:

(A) associative adsorption at the double bond leading to:

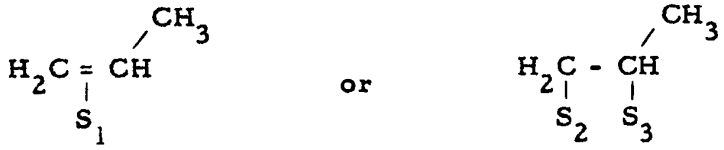

(B) dissociative adsorption, resulting in allylic adsorbate:

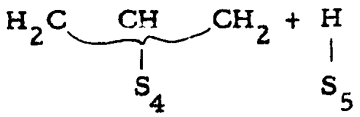

where $S_1 \ldots S_5$ represent surface sites. In case A, the C-atom of the aldehyde group in acrolein stem from the original methyl group; in case B, however, both terminal C-atoms have an equal chance to end up in the aldehyde group. In order to choose between the two mechanisms, C^{14} labelled propylenes were oxidized under flow conditions over a bismuth molybdate catalyst. After separation of the products, the acrolein was decomposed photochemically in a quartz reactor. The decomposition products were separated by gas

liquid chromatography and their specific radioactivities (r) determined. According to Sachtler, reaction conditions favoured the formation of an allylic adsorbate (case B) as the true reaction intermediate. He observed that isomerization of the butylenes took place to a small degree only, and that after incomplete oxidation, the unreacted butylenes were not in isomeric equilibrium, but the original isomer always prevailed. On the basis that the rate of oxidation was different for the three n-butylenes and highest for n-butylene-1, Sachtler concluded that oxidation of butylenes did not proceed by fast isomerization.

Voge, Wagner and Stevenson (9) also studied the mechanism of the oxidation of propylene to acrolein by reaction with molecular oxygen over cuprous oxide catalyst supported on 8-14 mesh Johns-Manville Celite VIII (a bonded diatomite). The reaction could conceivably involve several alternatives, including initial removal of a hydrogen atom from the methyl group, or addition of an oxygen atom to the double bond. Tagging one end of the propylene molecule, permitted them to determine which end was converted to a carbonyl group. They prepared $CH_2=CH-C^{13}H_3$ and oxidized it to acrolein over a cuprous oxide catalyst The amount of C^{13} in the CHO group of the recovered acrolein was determined by a mass spectrometer. They found that half of the heavy carbon in the acrolein product was in the carbonyl group. Isomerization of unreacted propylene was incomplete, proceeding to 38% of the equilibrium value. The distribution of C^{13} in the acrolein indicated to them that the initial removal of a hydrogen atom from the methyl group led to an allyl intermediate, which then is rapidly isomerized by exchange of ends,

prior to the addition of oxygen atom. They noted that the carbon dioxide ($C^{13}O_2$) by-product from the oxidation of propylene to acrolein was 17.4%. This is in complete agreement with 53.3/3 = 17.8% expected if the carbon dioxide came exclusively from the complete oxidation of a portion of acrolein or propylene rather than from the selective oxidation of an end carbon. Since the selectivity declined with conversion as required for consecutive reactions, Voge, Wagner and Stevenson concluded that the carbon dioxide was a secondary product, formed mainly by complete oxidation of part of the acrolein. A similar conclusion was reached by others (10, 3).

From the literature cited above, it appears that when propylene is oxidized over a copper catalyst, the only products formed are acrolein, water and carbon dioxide. The adsorption of propylene on the catalyst surface apparently takes place without the rupture of the C-C double bond to form an intermediary complex which then decomposes into acrolein and water. The carbon dioxide would result from a chain reaction between acrolein and oxygen. It also appears that higher yields of acrolein could be obtained by lowering the mole ratio of oxygen to propylene and by maintaining a uniform temperature within the reactor.

However, there are conflicting opinions regarding the order of the reaction with respect to oxygen and propylene. The rate controlling step in the partial oxidation of propylene and rate equation for a flow system has not been established yet.

B. Literature Related to Isobutylene

Bretton, Wan and Dodge (11), found that the vapor-phase oxidation of four carbon hydrocarbons over a vanadium pentoxide catalyst can for the most part be explained by a scheme of atomic dehydrogenation and peroxidation similar to that suggested by Waters (12) and by peroxide decomposition. The first step according to this scheme was the removal of a hydrogen atom from the hydrocarbon forming a free radical which then reacted with a molecule of oxygen to form a peroxide radical. This last product then became a peroxide by gaining a hydrogen atom. According to Waters' mechanism, the peroxide radical abstracted a hydrogen atom from another hydrocarbon molecule and the reaction proceeded in a chain like fashion. The experimental results were explained by considering the catalyst as a hydrogen atom abstractor and donor. This role of the catalyst is represented by the following reaction:

$$RH + X \longrightarrow HX + R- \qquad (1)$$

$$R- + O_2 \longrightarrow R-O-O- \qquad (2)$$

$$R-O-O- + HX \longrightarrow ROOH + X \qquad (3)$$

where X represents the catalyst. The decomposition of the peroxide occurs by scission at the O-O bond followed by scission of an adjacent C-H or the weakest adjacent C-C bond. The presence of methacrolein in the products of oxidation of isobutylene indicated that the initial point of oxidative attack on the mono-olefins might be at the α-methyl or methylenic carbon atom. The first step would involve the formation of the hydroperoxide by equations 1, 2 and 3, the peroxide

group being attached to one of the alpha carbon atoms. The second step would involve the decomposition of this peroxide. Scission of the O-O bond and adjacent C-H bond could lead to methacrolein.

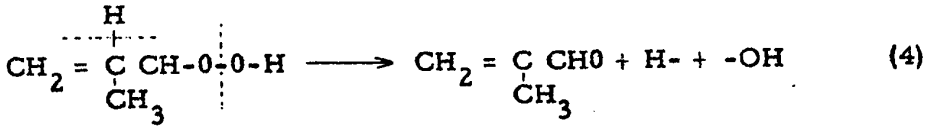

(4)

Baldwin (13) described a method whereby isobutylene could be oxidized to methacrolein. A list of possible metals, their organic compounds and common supports, which form useful catalysts were mentioned.

Dowden and Caldwell (14) studied the effect of reactant ratio, contact time and temperature on the conversion and yield of isobutylene to methacrolein. They claim that by passing 100 l./hr. of a mixture of 85% air and 15% by volume of isobutylene through a flow reactor packed with 30 ml. of a silite supported copper catalyst, a conversion of 17% per pass with a 95% yield of methacrolein could be obtained at 400° C.

Kitahara and Moriya (15) investigated the catalytic oxidation of isobutylene to methacrolein over various metal oxides and their mixtures. They found that a V_2O_5: MoO_3: P_2O_5 catalyst supported on an AL-sponge was the most effective catalyst for oxidation. They studied the effects of various types of supports, grain size of AL-sponge, space velocity, isobutylene/oxygen ratio in the feed, and the promotional effect of steam. Several undesirable by-products were obtained as liquid substances in the catalytic vapor phase oxidation of isobutylene to methacrolein. Methacrolein, and other

liquid products (aldehydes, ketones, acids and ethers) were obtained by condensing the reaction products in ice cooled traps and an absorption train containing methanol. The products which were collected in condensation and absorption trains contained 90% methacrolein. Most of the acidic substances in the product were condensed at the ice cooled traps separately from methacrolein, together with formaldehyde. The acid fraction was found to consist of formic acid, acetic acid, acrylic acid, methacrylic acid and trace of maleic acid. They found that the unsaturated aldehyde could be selectively oxidized and esterified to the corresponding acid ester in one process by using the lower aliphatic alcohols as solvent and reacting at low temperatures. The methacrolein absorbed in methanol obtained by the catalytic air oxidation of isobutylene was oxidized to yield 70% methyl methacrylate by this method.

Popova, Mil'man and Latysheva (16) studied the oxidation of isobutylene with oxygen over a 0.1 - 1.5% copper oxide (70% Cu_2O + 30% Cu 0) catalyst supported on silite, at 350° - 370° C. They used an isobutylene/oxygen ratio of 5.6 over a wide range of space velocities. 3.8% of the isobutylene was converted to carbonyl compounds; 82.5% of which was methacrolein, 7.2% propion-aldehyde, 6.2% acetaldehyde and 4.1% acrolein.

Skirrow and Williams (17) examined the gas-phase oxidation of isobutylene by a static method between 252° and 320° C. They found that the reaction proceeded with an initial pressure decrease during which formaldehyde and acetone were produced in equivalent amounts. They suggested that the isobutyraldehyde detected at

lower temperatures was probably formed by the isomerization of isobutylene oxide. Much of the pressure decrease during the course of the reaction was attributed to the overall process,

$$(CH_3)_2\ C = CH_2 + 1/2\ O_2 \longrightarrow (CH_3)_2\ CHCHO$$

rather than to peroxide formation since under certain conditions, the yield of peroxide was much too small to provide a satisfactory explanation. The more important primary products could be accounted for in terms of a radical addition mechanism initiated by addition of a hydroxyl radical to the terminal CH_2 group, and followed by peroxy radical formation and its subsequent decomposition. The formation of methyl allyl hydroperoxide and methacrolein showed that some abstraction of methyl hydrogen occured, although to be less important than the addition attack. The carbon oxides, water and propylene were formed by reactions of the primary products. It has been suggested that the branching occured by aldehyde oxidation.

Popova, Vermel, and Mil'man (18) followed the oxidation of isobutylene in a flow reactor on 0.5% and 1.5% cupric oxide supported on silite with and without the addition of Mo O_3 and W O_3. They found that the reaction was first order relative to oxygen for the formation of aldehydes and carbon dioxide. The formation rate of the unsaturated aldehydes depended on the structure of the oxidized hydrocarbons and the reactivity of the aldehydes formed. Addition of Mo O_3 and W O_3 did not change the activation energy E of the dienals but increased E of carbon dioxide formation and the oxidation selectivity of the dienes, which was relatively lower than that of the mono-olefins. Electronic considerations of these

experimental data showed that the formation rate of unsaturated aldehydes on the copper catalyst was determined by the degree of polarization of hydrogen in the methyl groups conjugated with a double bond as well as by space difficulties while being oriented toward the catalyst surface.

The scientific literature published on the partial oxidation of isobutylene is still very sketchy and mostly qualitative in nature. Some patents have appeared discussing the preparation of several catalysts and the effect of process variables on the conversion and yield, but very little information is available on the kinetics of the reaction. Few attempts have been made to explain the mechanism of the reaction and the theories advanced so far are mostly in disagreement. A careful search of the literature has revealed that no information exists about the possible mechanism, rate controlling step of the reaction or the rate equation for the catalytic oxidation of isobutylene to methacrolein in a flow reactor.

IV. EXPERIMENTAL

A. Apparatus

The partial oxidation of isobutylene to methacrolein was investigated in a flow system. A view of the experimental apparatus used in the study of the reaction is shown in Figure 1. This same apparatus is shown schematically in Figure 2.

The reactants, dry air and chemically pure isobutylene (minimum purity 99%) were obtained from high pressure cylinders, through a series of high pressure diaphram type regulators, whereby the pressure of air and isobutylene were reduced to 20 lb/sq. in gauge at the entrance to the rotameters. The gas lines were made out of 1/8 in. O.D. 316 stainless steel tubing. The various pressure fittings used in the equipment were made of 316 stainless steel, and were capable to withstand pressures of 5000 lbs/sq. in. The ratesof the flow of air and isobutylene were controlled by valves supplied by Autoclave Engineers Inc. The flow rates were measured by Brooks rotameters, which were calibrated against an American Gas Company's Wet test Gas meter. The calibration curves for the air and the isobutylene are given in appendix A. The streams of isobutylene and air leaving the rotameters, were mixed before they entered the preheating section.

The preheating section, which was immersed in a constant temperature liquid metal bath, consisted of a 3 ft. length 1/8 in. O.D. 316 stainless steel tubing wound around the reactor. Details of the preheater are shown in Figure 3. The liquid metal bath consisted of a mixture of 50% bismuth and 50% lead by weight. The metal

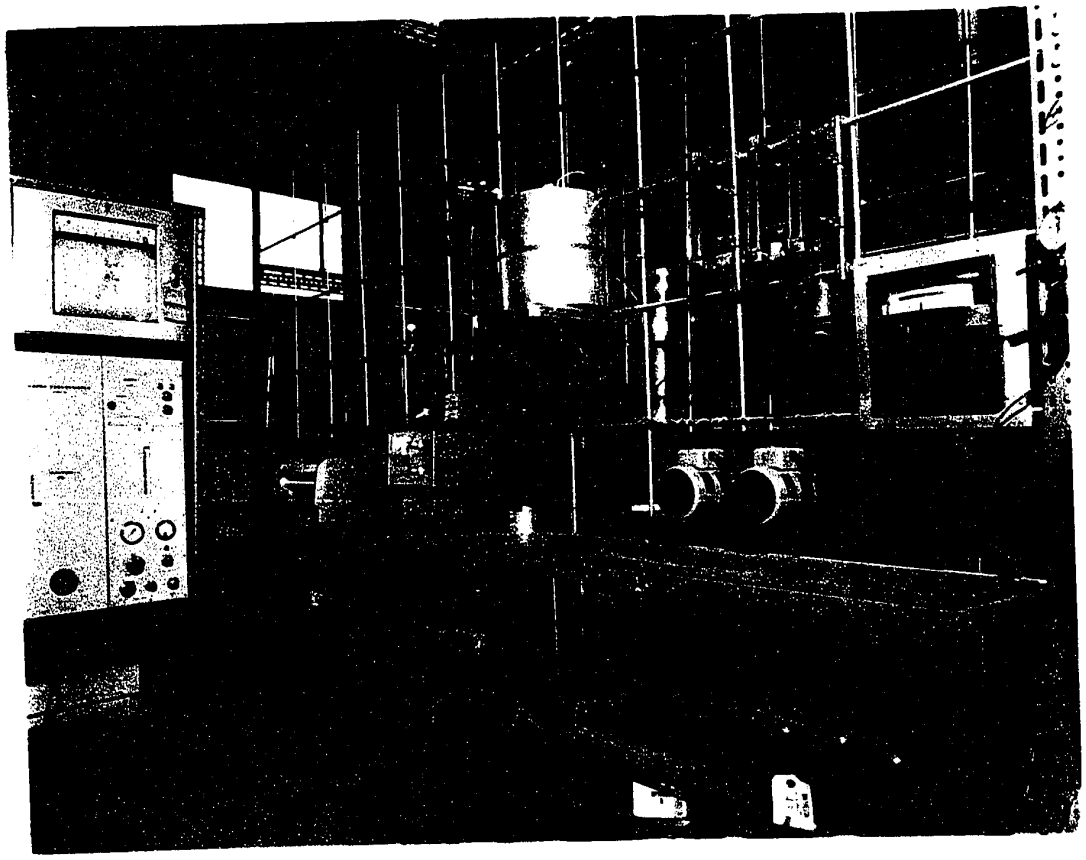

Figure 1 View of the Experimental Apparatus

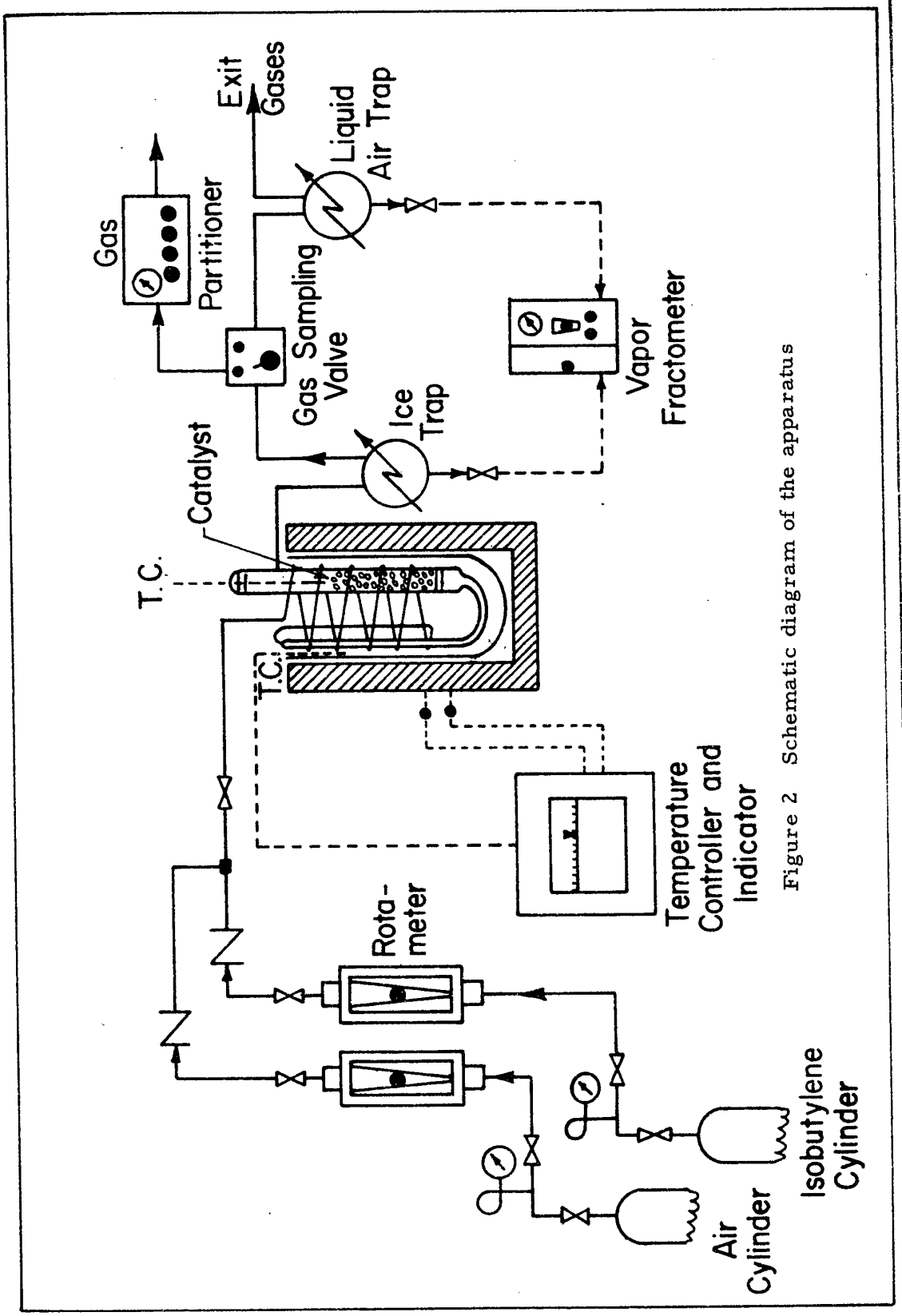

Figure 2 Schematic diagram of the apparatus

mixture was heated by an electrical furnace. The temperature of the furnace was controlled to within ± 3° C by a Honeywell Pyrovane temperature controller.

The design of the reactor was such that the reaction took place more or less under isothermal conditions. Blank runs were made with an iron-constantan thermocouple inserted inside the reactor. At high flow rates of gases, no temperature difference was observed between the metal bath and inside the reactor, which indicated that the preheating section was long enough to heat the gases entering the reactor to the desired reaction temperature. Runs were also made with the reactor filled with the catalyst, and the thermocouple inserted in it. The highest temperature difference obtained in this case was 5° C. Although the oxidation of isobutylene to methacrolein is a highly exothermic reaction, the rate of heat transfer through the metal wall of the reactor was high enough to maintain the reaction near isothermal conditions.

The gases entered the reactor at the bottom through a porous stainless steel plate which served as a support for the catalyst. The catalyst granules of 20-40 mesh size were kept in place by plugging loosely some stainless steel wool at the top. The reactor (Figure 3) consisted of a 5 in. long x 1/2 in. O. D. diameter 304 stainless steel tubing.

The exit gases from the reactor were led to an ice cooled trap, whereby acids, water and a small portion of the aldehydes were condensed. The non condensed gases were passed through a

Fig. 3. REACTOR and PREHEATER

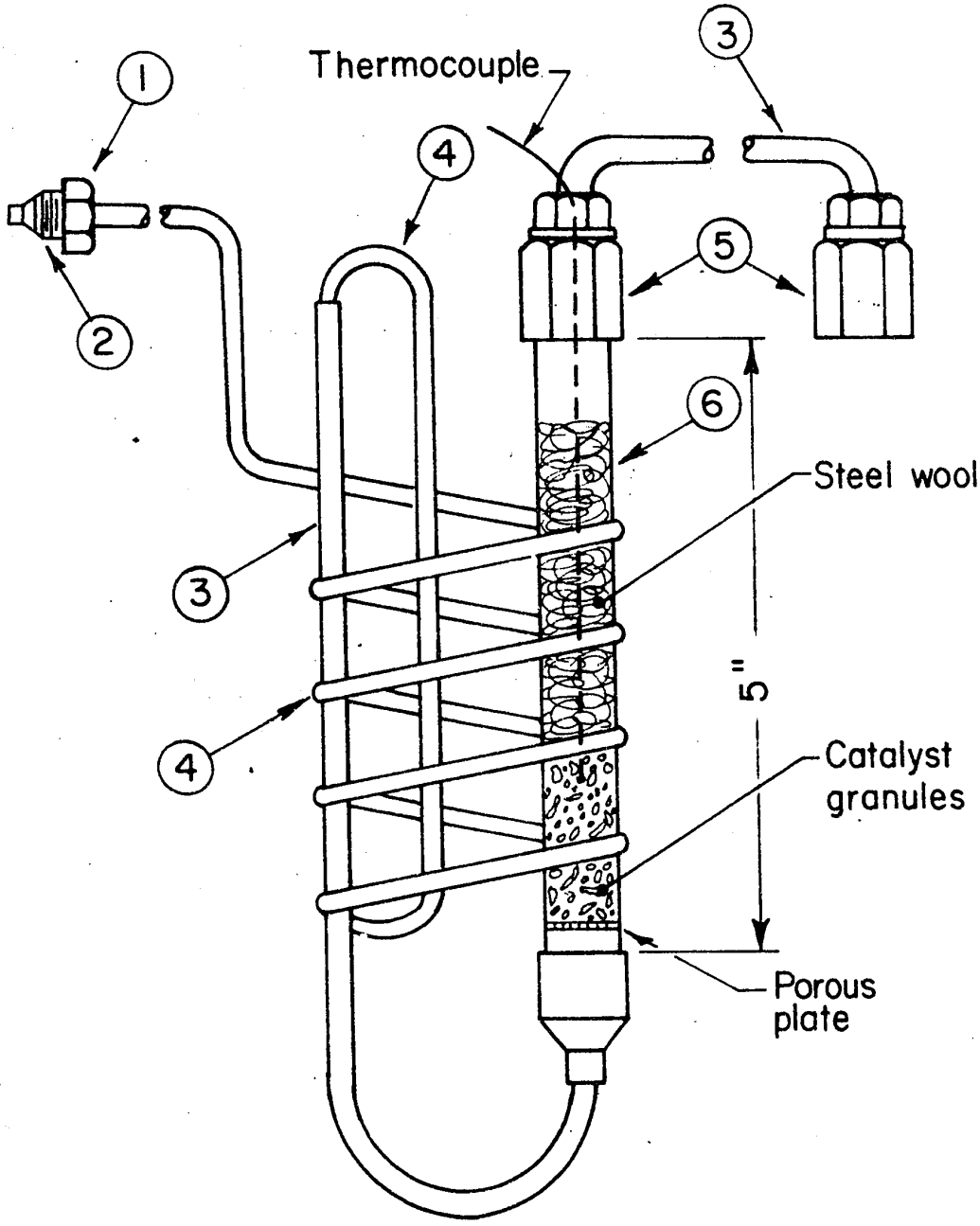

1	1/4"	Nut	4	1/8"	S.S. Pipe
2	1/8"	Sleeve	5	1/4"	Coupling
3	1/4"	S.S. Pipe	6	1/2"	S.S. Pipe

sampling valve leading to a Fisher gas partitioner, which could analyze carbon dioxide, carbon monoxide, isobutylene, oxygen and nitrogen. The off gases from the sampling valve were passed through a liquid air trap, where the remainder of the aldehydes, which did not condense at ice temperature, condensed.

B. Reactants

1. Isobutylene

A Matheson C.P. grade isobutylene gas with a minimum purity of 99% was used. The gas was received in cylinders containing 40 lbs. of liquid isobutylene at a pressure of 23 p. s. i. g. (70° F). Analysis of isobutylene on the gas chromatograph showed that the main impurities were isobutane, n-butane and 2 butylenes. These impurities were in such minor quantities, that they did not interfere with the experimental accuracy.

2. Air

The air used was supplied by the Linde company in compressed cylinders at a pressure of 2500 p. s. i. g. Analysis of the air on the gas chromatograph showed that it contained 20.95% oxygen, 0.05% carbon dioxide and 79% nitrogen.

Compressed air and isobutylene from the cylinders were passed through a tube containing drierite to remove moisture from the gases prior to their passing through the rotameters.

C. Catalyst

In order to investigate the kinetics of the catalytic oxidation of isobutylene to methacrolein, it was considered essential first to develop a catalyst, which would be highly selective towards the formation of methacrolein with least amounts of undesirable by-products, in addition to being stable, and its catalytic activity remaining constant under severe operating conditions for several days. Several catalysts, copper oxide on pumice, molybdenum oxide on pumice, copper-molybdenum oxides on pumice, copper on alumina and a molybdenum-vanadium-phosphorous oxide catalyst supported on alumina were tested for their catalytic activity. Step by step procedure for the preparation and evaluation of these catalysts is described below.

1. Preparation and Evaluation of Catalysts

Since all the catalysts were prepared in a similar way, the procedure for the preparation of only one of them is described in detail.

Catalyst 1

The pumice supported copper oxide catalyst (16% by weight of copper) was prepared by impregnating 20-40 mesh crushed pumice stone, supplied by Fisher Scientific Company, with copper nitrate solution. The required weight of pumice was added to a 750 ml. dilute solution of Analar grade copper nitrate, $Cu(NO_3)_2 \cdot 6\ H_2O$ and the mixture vigorously stirred for 2 hours. The resulting mixture was slowly evaporated to dryness. The impregnated

material was dried overnight at 105° C and calcined at 550° C for 6 hours in a muffle furnace. A weighed amount of the catalyst was charged into the reactor and activated by passing air over it for 12 hours at 450° C.

This catalyst appeared to be highly selective and seemed suitable for the kinetic study of the catalytic oxidation of isobutylene, as in spite of high conversions, the major products were methacrolein, carbon dioxide and water. The concentration of the acids, carbon monoxide and the other aldehydes in the products was found to be too low to affect the material balance In view of the selective and stable nature of this catalyst, it was used throughout the kinetic investigation except where noted otherwise.

Catalyst 2

This catalyst contained 2% by weight of copper on pumice.

Catalyst 3

This catalyst contained 8% by weight of copper on pumice.

Catalyst 4

This catalyst contained 32% by weight of copper on pumice.

Catalyst 5

The unsupported copper oxide catalyst was prepared by calcining Analar grade copper nitrate, $Cu(NO_3)_2 . 6 H_2O$ for 2 hours at 200° C and 4 hours at 550°C. Though no additional products were

obtained with this catalyst, the oxidation of isobutylene to carbon dioxide was greatly enhanced.

Catalyst 6

Molybdenum oxide supported on pumice (8% by weight of MoO_3) was prepared by impregnating the pumice stone with a dilute solution of Analar grade ammonium paramolybdate, (82% MoO_3). This catalyst was rejected as no noticeable conversion was observed even at 450° C.

Catalyst 7

The copper molybdenum oxide (25% MoO_3 + 75% Cu O) catalyst was prepared by impregnating the 20-40 mesh pumice stones with a solution containing copper nitrate and ammonium paramolybdate in the desired ratio. The only effect of the molybdenum oxide was to reduce the concentration of the copper on the catalyst. It did not in any way change the yield of methacrolein.

Catalyst 8

The catalyst, containing 16% by weight of copper, was prepared by impregnating the known weight of alumina with copper nitrate solution. Alumina in the shape of cylindrical pellets was supplied by the American Cyanamid Co., Stamford, Conn. The pellets were ground to 20-40 mesh and activated by heating overnight before being impregnated. High conversions were obtained with this catalyst. The amounts of total acid, carbon monoxide and other aldehydes in the products were greatly increased. Such large amounts

of by-products made the alumina supported copper catalyst undesirable for this work.

Catalyst 9

The mixed oxide catalyst containing MoO_3: V_2O_5: P_2O_5 in a ratio of 5:1:0.6 was prepared by impregnating alumina with a solution containing $(NH_4)_6 Mo_7 . 4H_2O$, NH_4VO_3 and $(NH_4)_2 HPO_4$ in such amounts as to give the desired ratios of molybdenum, vanadium and phosphorous oxides on the support. The catalyst contained 8% by weight of the mixture of the oxides. This catalyst was highly active and gave higher conversions of isobutylene and better yields of methacrolein. However, as numerous by-products in significant amounts were formed, this catalyst was discarded as being unsuitable for mechanistic kinetic study.

2. Selection of the Catalyst

A preliminary investigation on the oxidation of the isobutylene and analysis of the reaction products showed that copper oxide supported on pumice granules of 20-40 mesh size was very suitable for obtaining rate data and establishing of a possible mechanism and rate controlling step. The concentration of copper oxide on pumice as being 16% was arbitrarily chosen.

3. Properties of the Catalyst

Only those properties of the catalyst (particle diameter, particle density, surface area of the particle and catalytic activity) which have a direct bearing on the rate of catalytic oxidation of

isobutylene, were determined, and are summarized in Table 1.

Table 1: Properties of the Pumice Supported Copper Oxide Catalyst

Copper Concentration	= 16% by weight
Particle Diameter (D_p)	= 0.0286 inches
Particle Density (ρ_p)	= 43.4 lb/ft^3
Specific Surface (a_m)	= 0.04 m^2/gm.
Thermal Conductivity of Copper (k_c)	= 210 Btu/hr. ft.^{2} °F
Thermal Conductivity of Pumice (k_p)	= 0.3 Btu/hr. ft.^{2} °F

The particle diameter (D_p) was determined by measurement with a micrometer. A random sample of 25 granules were taken and the diameter of each measured with a micrometer. An arithmetic average of these measurements gave the value of particle diameter as 0.0286 in.

The particle density (ρ_p) was determined by measuring the weight and volume occupied by 100 granules of pumice. Since the granules were relatively small, the sphericity (S) was taken as 0.8 and the density calculated as follows:

Volume of a single granule	= $\frac{\pi D^3_p S}{6}$
Volume of 100 granules	= 100 x 1.225 x 10^{-5} x 0.8
	= 0.000980 ft^3
Weight of 100 granules	= 0.04253 lbs.
Particle density, ρ_p	= $\frac{0.04253}{0.000980}$ = 43.3 lb/ft^3

The area of the particle per unit mass, a_m was determined by the Fuel Research Laboratories of the Department of Mines and Technical Surveys, Ottawa on a gravimetric B. E. T. apparatus. They reported that the surface area of the particles was less than 1 $m.^2/gm.$ and that it was too low for accurate measurement by this method. However, Emmett (19) reported a surface area of 0.04 $m.^2/gm.$ for pumice.

The activity of the catalyst was verified periodically by passing a specified mixture of isobutylene and air over the catalyst and determining the percentage conversion of isobutylene. In each case, the conversion of isobutylene never varied by more than 5%, therefore no correction for change in catalytic activity was deemed necessary.

D. Operating Procedure

For the start of a run, air was slowly passed through the reactor, while the catalyst was brought to the required temperature. When the required temperature was attained, isobutylene was added to the feed and the flow rates of isobutylene and air were adjusted so as to give the desired total flow rate and molar ratios of oxygen to isobutylene in the feed. The gases were maintained at their specified rates, over a period of 30 minutes in which steady state conditions at the required temperature was reached. After the steady state conditions had been reached, the first trap (condenser) was immersed in a freezing mixture of ice and water, and the second in liquid air.

The steady state run was continued for one hour during which

time the isobutylene and air flow rates were constantly kept at their specified values. During the course of reaction, the exit gases from the reactor were periodically injected into the Fisher gas partitioner. In this way the composition of the product gases were determined from time to time. An average value of these compositions were used for calculation of rates. At the end of one hour the isobutylene feed was shut off. The samples from the two traps were collected, measured and analyzed. The air was kept flowing through the catalyst bed for another hour and a half, before the start of the second run.

E. Analysis of the Products

1. Acids

The total acid content was obtained by titration of the condensate from the ice cooled trap with 0.055 N. KOH solution. The total acid content was very low and too insignificant to affect the material balance. Therefore, it was not included in the analysis of the products. The condensate contained very minor quantities of aldehydes. Phenolphthalein was used as indicator in the titrations.

2. Gases

The inlet feed gas and the product gases were analyzed for isobutylene, carbon monoxide, carbon dioxide, and oxygen by periodic injection of 0.5 ml sample into the Fisher gas partitioner containing a 6 ft. hexamethyl phosphoramide column and a 13 ft. 13 X molecular sieve column connected in series. Nitrogen was usually obtained by difference. A typical analysis of the products from the gas partitioner is given in appendix A. Also included is a calibration curve for the percent compositions of isobutylene,

carbon monoxide, carbon dioxide and oxygen as determined from the gas partitioner.

The composition of various gases from the reactor was determined by measuring the peak heights instead of the area under the peak. This was done as the peaks for all gases were very sharp and narrow. The product gases thus could be analyzed within an accuracy of $\pm$ 2%.

3. Aldehydes

The sample from the liquid air trap was diluted with approximately 8 ml diethyl ether and placed in a refrigerator which was kept at approximately 5° C. Once temperature equilibrium was reached, 5 microlitre of the mixture was injected into a 154 D Perkin-Elmer gas chromatograph containing two 4 meter columns of carbowax 1500 on teflon. The aldehydes were separated at 110° C using 16 X as the sensitivity. The chromatograph could separate acetone, acetaldehyde, propionaldehyde, crotonaldehyde, butyraldehyde, acrolein, water and methacrolein. Methacrolein was the only product observed in the liquid sample except for traces of acrolein. A typical analysis of methacrolein from the Perkin-Elmer gas chromatograph is shown in Figure 41 in appendix A. Also included is a calibration curve for methacrolein which is given in Figure 39. The percent composition by volume of methacrolein was determined from the area under the peak. A Philips PT 1600 integrator was used to obtain the area under each peak. Two readings were taken from the integrator, one prior to the start of a peak and another immediately after the completion of this peak. The difference between these two readings was a measure of the area under that peak.

The density of methacrolein at 5° C (temperature of the refrigerator) was calculated to be 0.9425 gm/cc. The procedure for the determination of the density is given in appendix B. The moles of methacrolein produced per hour was calculated from the density of this liquid, and its percent composition by volume. The percent composition by volume was accurate to within $\pm$ 2%.

Feed rates were calculated on the basis of the rotameter reading which had been calibrated at 75° F* and one atmosphere pressure. Temperature corrections were applied to the feed rates if the room temperature varied by more than 5° F. The effluent rates were computed on the basis of the nitrogen fed and on the percent composition of the reaction products. Since the moles of nitrogen in the feed and in the effluent stream were the same, the percent composition of nitrogen in the product gas was used as a constant denominator in calculating the molal effluent rate of the gases. All the experiments were carried out at atmospheric pressure. Though air was used for oxidation, the calculations are based on the oxygen rate so that the effect of oxygen on the course of the reaction can be easily visualized.

A typical set of data as obtained for a particular experimental run is given in Table 2. From such data, the number of moles per hour and the composition of the reactants and products were calculated in a manner as given in sample calculation, and were recorded as shown in Table 3.

* These readings were corrected to S.T.P.

Sample Calculation

Moles In:

Moles C_4H_8/hr

$$= \frac{180 \text{ cc/min} \times 60 \text{ min/hr}}{22,414 \text{ cc/mole}} = 0.4821 \text{ moles/hr}$$

Moles O_2/hr

$$= \frac{890 \text{ cc/min} \times 60 \text{ min/hr} \times 20.95\%}{22,414 \text{ cc/mole}} = 0.5000 \text{ moles/hr}$$

Moles N_2/hr

$$= \frac{890 \text{ cc/min} \times 60 \text{ min/hr} \times 79.0\%}{22,414 \text{ cc/mole}} = 1.8833 \text{ moles/hr}$$

Moles Out:

Moles C_4H_8/hr

$$= \frac{1.8833}{72.4} \times 14.4 = 0.3744 \text{ moles/hr}$$

Moles O_2/hr

$$= \frac{1.8833}{72.4} \times 4.1 = 0.1066 \text{ moles/hr}$$

Moles N_2/hr = 1.8833 moles/hr

Moles CO_2/hr

$$= \frac{1.8833}{72.4} \times 8.8 = 0.2289 \text{ moles/hr}$$

Moles CO/hr

$$= \frac{1.8833}{72.4} \times 0.1 = 0.0026 \text{ moles/hr}$$

Moles H_2O/hr

$$= \frac{5.09 \text{ cc} \times .997 \text{ gm/cc}}{18.02} = 0.282 \text{ moles/hr}$$

Moles C_4H_6O/hr

$$= \frac{12.30 \text{ cc} \times .9425 \text{ gm/cc} \times 29.3\%}{70.09} = 0.0484 \text{ moles/hr}$$

These calculated results are given in Table 5 in appendix C.

Table 2: DATA SHEET

Date Feb. 5/63

Room temp. 75° F

Catalyst No. 1

Run No. 361

Time: Start 9:20 End 10:20

Duration of Run 60 minutes

Temperature of Reactor 400°C

Feed Rates:

Butylene flow meter 6.0 M mms.

Air flow meter 5.95 M mms.

Butylene 180 ccs/min. Air 890 ccs/min.

Liquid product volume 5.09 ml. (ice trap)

Color of product colourless Ratio of $0_2/C_4H_8$ 1.0

Weight of Catalyst .5785 gms.

Analysis:

A. Gas

Butylene	14.4%
CO_2	8.8
N_2	72.4
0_2	4.1
CO	0.1
CH_4	—

B. Liquid

Methacrolein 29.3%

Total Vol. 12.30 ml. (Liquid air trap)

Table 3: Calculated Results

MOLES IN:	Butylene	0.4821	$W/F = \frac{.5785}{.4821} = 1.20$
	O_2	0.5000	
	N_2	1.8833	
			% conversion
MOLES OUT:	Butylene	0.3744	22.3
	O_2	0.1066	
	N_2	1.8833	
	CO_2	0.2289	11.9
	CO	0.0026	
	CH_4	-	
	H_2O	0.282	
	C_4H_6O	0.0484	10.0
	CH_3COOH	-	

	IN	OUT	% dev.
C-Bal.	1.9284	1.9227	0.3
O-Bal.	1.0000	1.0030	0.3
H-Bal.	3.8568	3.8496	0.2

V. EFFECT OF PROCESS VARIABLES

The effect of oxygen (in the air)/isobutylene ratio in the feed, operating temperature and copper concentration of the catalyst on the conversion of isobutylene, and the yield of methacrolein were investigated. While conversion is referred to as the ratio of moles of isobutylene reacted per hour to the moles of isobutylene fed per hour, the ratio of the moles of methacrolein produced per hour to the moles of isobutylene reacted (converted) per hour has been defined as yield. The effect of several catalysts on the conversion and yield was also studied. The results obtained with several catalysts have already been discussed in the section, "Preparation and Evaluation of Catalysts", and are tabulated in Appendix I.

The effect of oxygen/isobutylene ratio in the feed on the conversion and yield for a W/F ratio of 1.0 at 400° C over catalyst 1 is shown in Figure 4, and data for this is given in Appendix D. The data for other W/F ratios and temperatures can be calculated from Appendix C. The ratio of oxygen to isobutylene in the feed was varied between 0.25 and 4.0. The conversion of isobutylene increased rapidly with reactant ratio up to an oxygen/isobutylene ratio of 2, and then seemed to become independent of the reactant ratio. The yield on the other hand decreased rapidly with an increase in oxygen/isobutylene ratio, which is in agreement with the stoichiometry of the reaction, that is, the higher the mole ratio of oxygen to isobutylene in the feed, the lower the yield of methacrolein would be.

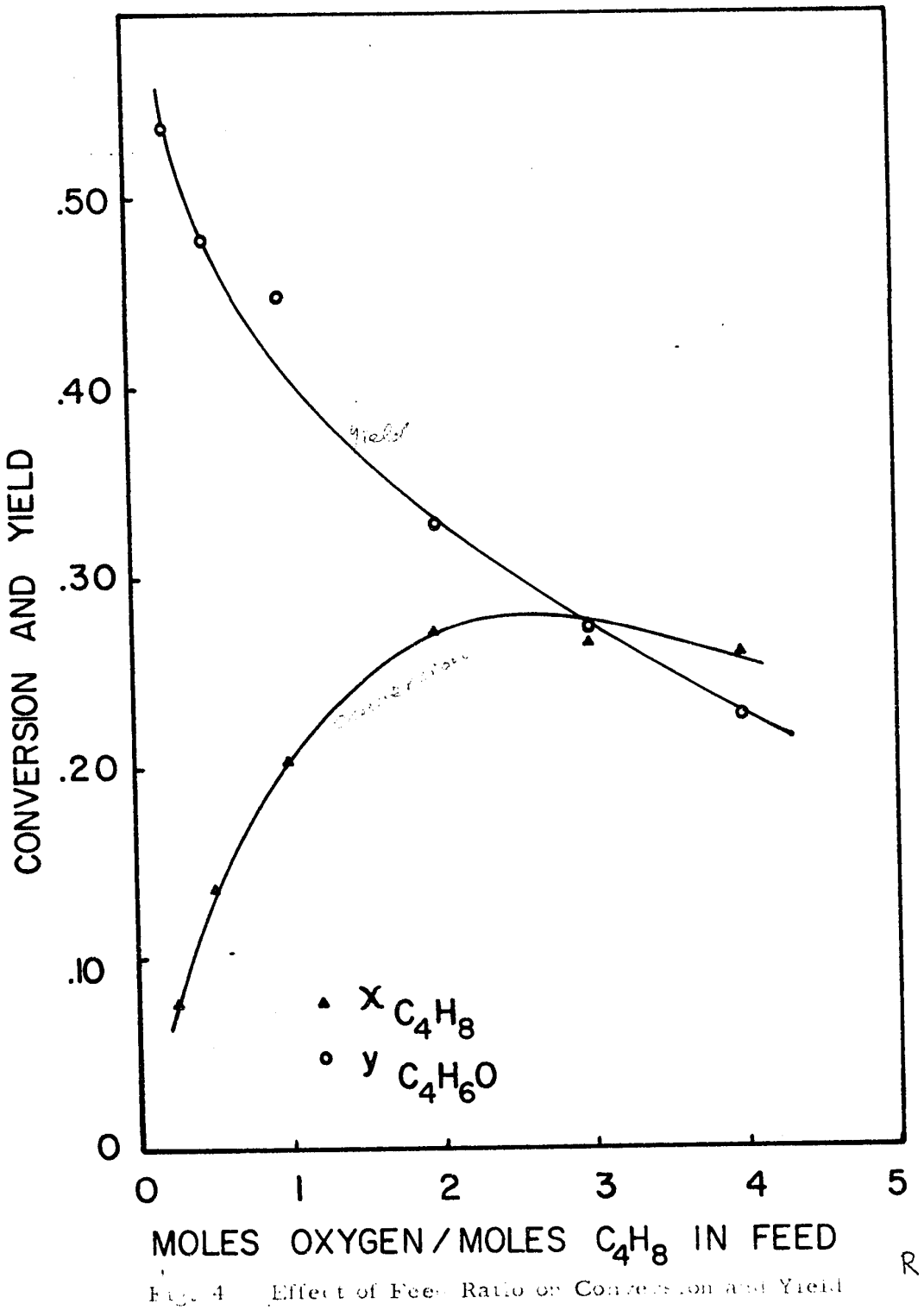

Fig. 4 Effect of Feed Ratio on Conversion and Yield

The influence of temperature on the conversion and yield was investigated in the temperature range of 350° to 450° C, and the results are tabulated in Appendix D. Figure 5 shows the effect of temperature on the oxidation reaction at a W/F ratio of 1.2, an oxygen/isobutylene ratio of 2.0 over catalyst 1. With increasing temperature from 350° to 450° C, the conversion increases, but the yield decreases. At temperatures of 425° C and above, much over oxidation occurs as is evidenced by a higher percentage of carbon dioxide formation in the product. The yield decreases slowly at first from 350° C to 400° C, and then drops off sharply with increasing temperatures.

The oxidation of isobutylene was carried out over several copper oxide catalysts containing varying amounts of copper oxide/support ratios, so as to determine the effect of the concentration of copper on the conversion and yield for W/F = 1 at 400° C. Figure 6 shows the effect of the copper concentration on the conversion of isobutylene. The conversion of isobutylene sharply increased with an increase in copper oxide concentration up to a value of 10% copper by weight of the catalyst. For higher concentrations of copper, the effect on the conversion was not very pronounced but increased steadily up to a value of 0.467 for unsupported copper oxide. An increase in copper content of the catalyst on the other hand adversely affected the yield of methacrolein. The decrease in the yield of methacrolein seems to be directly proportional to an increase in copper concentration of the catalyst.

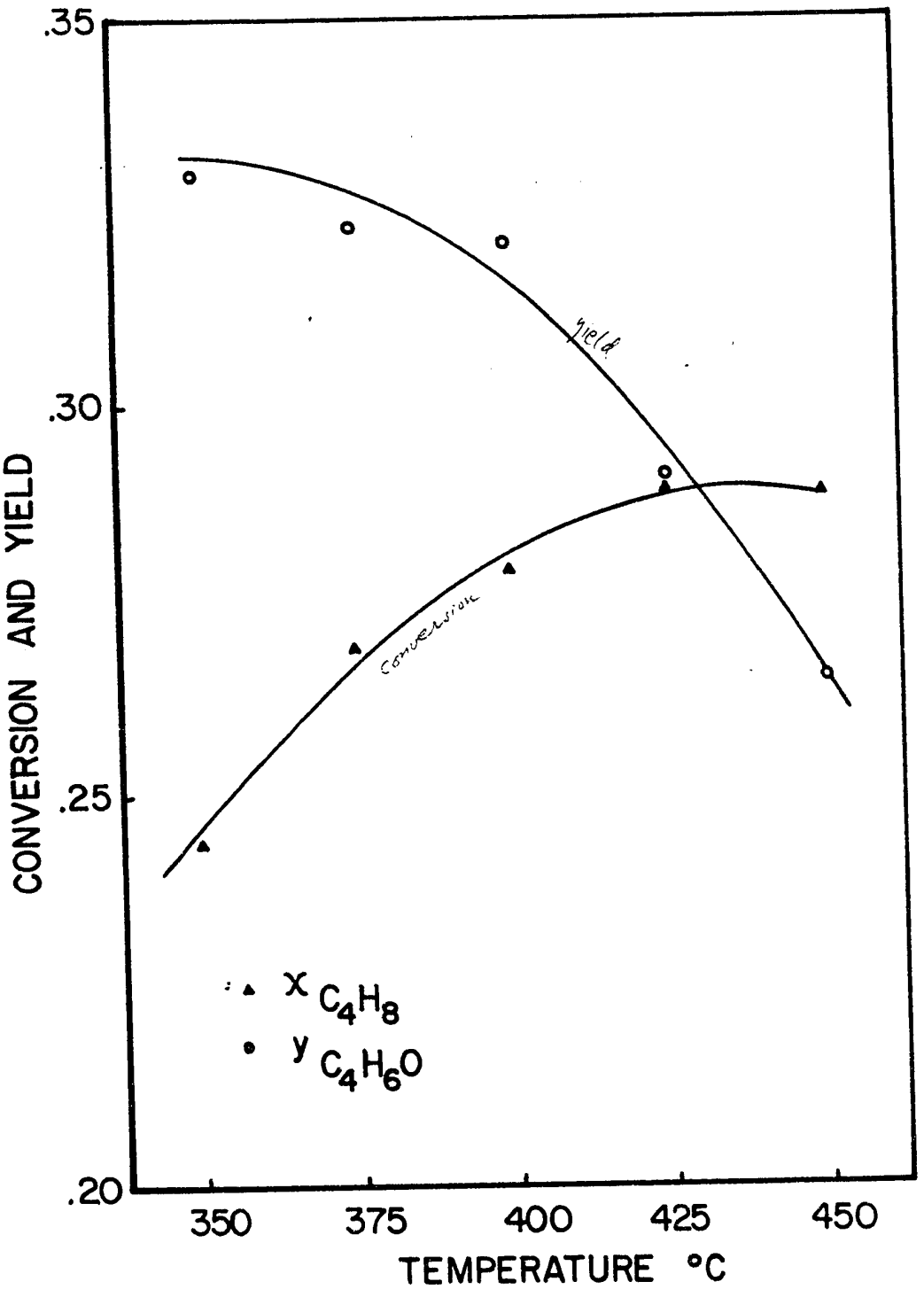

Fig. 5 — Effect of Temperature on Conversion and Yield

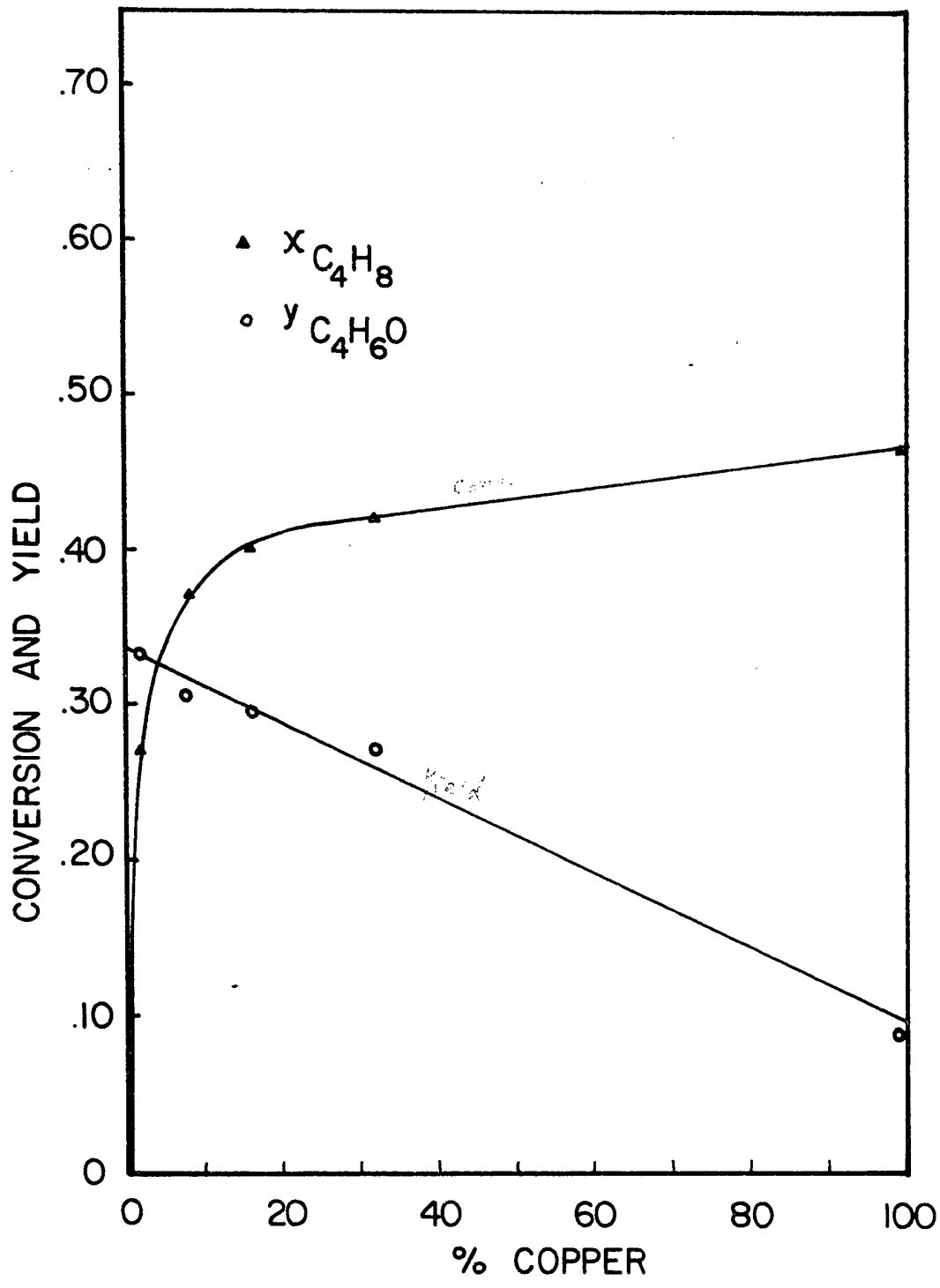

Effect of Copper Content on Conversion and Yield

Keeping all the process variables constant, when the reciprocal of space velocity, W/F, was increased systematically, the conversions of isobutylene to methacrolein and carbon dioxide, increased parabolically as shown in Figure 25, and the data in Appendix C. The yield of methacrolein ($Y_{C_4H_6O}$) can also be calculated from this figure as the product of $X_{C_4H_6O}$ and $1/X_{C_4H_8}$.

From the foregoing results it could be concluded therefore that with the increase in the process variables of temperature, reactant ratio, copper concentration and reciprocal of space velocity, the conversion would increase and the yield of methacrolein decrease. As required for consecutive reactions, the selectivity of the reaction towards the formation of methacrolein decreased with increasing isobutylene conversion.

VI. KINETIC ANALYSIS OF THE DATA

A. Rate Steps in Heterogeneous Catalysis

The Hougen-Watson type rate equations represent a methodical and systematic way of describing the relationship among the experimental variables including the reaction velocity and adsorption constants. Together with the theory of absolute reaction rates, they give satisfactory explanations for many catalytic reactions and are particularly convenient in reactor design. These theories and mechanisms, as applied to catalytic oxidation are described in this section.

Chemical reactions involving a fluid-solid system, that is, reactions in which the reactants and products are fluids and the catalyst a porous solid, involve the following seven successive steps:

Step 1: Diffusion of the reactant molecules from the main gas stream to the external surface of the catalyst.

Step 2: Diffusion of the reactant molecules through the catalyst pores into the interior of the porous catalyst.

Step 3: Adsorption of one or more or all of the reactants on the catalyst surface.

Step 4: Reaction of the adsorbed reactants on the catalyst surface with one another or with other components not adsorbed.

Step 5: Desorption of the products from the catalyst surface.

Step 6: Diffusion of the product molecules back to the surface of the porous catalyst.

Step 7: Transfer of the product molecules from the external surface of the catalyst to the main gas stream.

Each of these steps offerssome resistance to the overall process. If all these resistances were considered, the resulting rate equations would be very complicated. The diffusion steps (1, 2, 6 and 7) are physical processes which can be minimized or accounted for independently as will be described later. The chemical steps (3, 4 and 5) contribute significant resistances which cannot be reduced by altering physical conditions and hence are the most important ones to consider. Inclusion of only these three types results in equations of high complexity. Usually only one of these three, offers a much higher resistance than the other two, and is therefore considered to be the rate controlling, or rate determining step, while the other two are considered to be at equilibrium.

The different processes taking place during the chemical reaction involving gases over a solid catalyst are considered separately to see if a rate controlling step can be found. The selection or exclusion of the steps are determined by the results of the present investigation on the oxidation of isobutylene to methacrolein over a pumice supported copper oxide catalyst, and by reference to the paper of Yang and Hougen (20).

B. Exterior Heat and Mass Transfer Effects

In the rate equations for reactions catalyzed by solid surfaces, the partial pressures and temperatures should represent values at gas-solid interface. These interfacial partial pressures can be significantly different from those in the ambient stream because of the resistance in the gas film to the diffusion of reactants towards and products away from the exterior catalyst surface. Similarly,

temperature differences could exist between the exterior catalyst surface and the ambient stream due to the release of large amounts of heat of reaction in highly exothermic reactions at the catalyst surface.

It is desirable, in an experimental packed-bed reactor, to establish very large heat and mass transfer coefficients such that the conditions at the surface of the catalyst particle are very close to those measured in the ambient stream. The rates of heat and mass transfer can be evaluated from the following equations.

$$q_m = h_G a_m (T_i - T) \tag{5}$$

$$r_A = k_G a_m (P_{A_i} - P_A) \tag{6}$$

where T_i = temperature of the gas-solid interface

T = temperature of the bulk stream

q_m = heat transfer due to heat of reaction per unit mass of catalyst

h_G = heat transfer coefficient of the gas film

P_{A_i} = partial pressure of component A at gas-solid surface

P_A = partial pressure of component A in the bulk stream

r_A = rate of reaction or mass transfer of A per unit mass of catalyst.

k_G = mass transfer coefficient of the gas film

a_m = surface area of the particle per unit mass of catalyst

The transfer coefficients, h_G and k_G, can be calculated by using the following j-factor correlation of Chilton and Colburn (21).

$$j_h = \left(\frac{h_G}{C_p G}\right)\left(\frac{C_p \mu}{k}\right)^{2/3}_f \qquad (7)$$

$$j_d = \left(\frac{k_G M_m P_{f_A}}{G}\right)\left(\frac{\mu}{\rho D_{Am}}\right)^{2/3}_f \qquad (8)$$

where j_h = a factor for heat transfer

j_d = a factor for mass transfer

C_p = specific heat of the gas

G = mass velocity of flow based on total cross-sectional area of the bed, mass per unit time per unit area

μ = viscosity of the gas

k = thermal conductivity of the gas

$\frac{C_p \mu}{k}$ = the dimensionless Prandtl number

M_m = mean molecular weight of the gas film

P_{f_A} = film pressure factor defined by equation (13)

ρ = density of gas

D_{Am} = average diffusivity of component A

$\frac{\mu}{\rho D_{Am}}$ = the dimensionless Schmidt number

Subscript f = properties at average condition of the gas film

Gamson, Thodos, and Hougen (22), suggest the use of the following equation for determining j_h and j_d

for $\frac{D_p G}{\mu} > 350$

$$j_h = 1.06 \left(\frac{D_p G}{\mu}\right)^{-0.41} \quad (9)$$

$$j_d = 0.99 \left(\frac{D_p G}{\mu}\right)^{-0.41} \quad (10)$$

and for $\frac{D_p G}{\mu} < 350$, Wilkie and Hougen (23) recommend the following

$$j_h = 1.95 \left(\frac{D_p G}{\mu}\right)^{-0.51} \quad (11)$$

$$j_d = 1.82 \left(\frac{D_p G}{\mu}\right)^{-0.51} \quad (12)$$

where $\frac{D_p G}{\mu}$ = modified Reynolds number, D_p = effective particle diameter. The film pressure factor for component A, P_{f_A} in equation (8) is defined by:

$$P_{f_A} = \Pi - P_A \frac{(a + b - r - s)}{a} \quad (13)$$

where Π = total pressure, and

r, s, ..., a, b, ..., are the coefficients of the components R, S, ..., A, B, ..., respectively, in the reaction equation

$$aA + bB + \ldots \rightleftharpoons rR + sS + \ldots$$

Recently, Yoshida, Ramaswami and Hougen (24) have published a new j-factor correlation for determining the partial pressure

and temperature gradients across the fluid film surrounding the catalyst particle, in a fixed bed catalytic reactor. They describe a new type of more compact and general chart, where the temperature and pressure gradients are related to a modified Reynolds number based on such parameters as the Schmidt and Prandtl numbers. Allowance for void fraction and packing shape is also included. The temperature and pressure gradients can be easily determined from these charts using calculated values of the constants and dimensionless numbers for the particular system. In essence, they can be represented by:

$$\Delta T = Q(j_h)^{-1} (Pr)_f^{2/3} \tag{14}$$

$$\Delta Y_A = \frac{\Delta P_A}{P_A} = R(j_d)^{-1} Y_{f_A} (Sc)_f^{2/3} \tag{15}$$

where ΔT = temperature drop across the film

$Q = \dfrac{r \Delta H_A}{a_m \phi C_p G_M}$

ΔH_A = heat of reaction per mole of A reacted

Pr = Prandtl number = $\dfrac{C_p \mu}{k}$

ΔP_A = partial pressure difference of component A across the gas film

$R = \dfrac{r_A}{a_m \phi G_M}$

$Y_{f_A} = \dfrac{P_{f_A}}{\pi}$

Sc = Schmidt number = $\frac{\mu}{\rho D_{Am}}$

G_M = molal mass velocity of gas based on total cross section of bed

ϕ = shape factor, (ratio of actual external surface area available for mass and heat transfers to the total external surface area) assumed to be 0.90 for irregular granules

The j-factors are related to the modified Reynolds number by:

for $0.01 < Re < 50$

$$j_d = 0.84\ Re^{-0.51} \tag{16}$$

for $50 < Re < 1000$

$$j_d = 0.57\ Re^{-0.41} \tag{17}$$

and $j_h = 1.076\ j_d$ (18)

where $Re = \frac{G}{a_v \phi \mu}$

Ramaswami (24) has successfully correlated the data of several investigators using this correlation. It was found that the gradients fall in a narrow band on a Δy_A vs. R or ΔT vs. Q plot, indicating that R and Q are the most significant factors in controlling the pressure and temperature gradients respectively.

Both the temperature and partial pressure differences across the film were found to be proportional to $r_A D_p^{n+1} G^{n-1}$. Since n is either 0.51 or 0.41, the heat and mass transfer resistances can be effectively eliminated by decreasing the particle size and increasing the flow rates.

The effects of diffusion are kept at a minimum by using a high velocity of the gases through the catalyst bed. Some preliminary runs were made to study the effect of the rate of gas flow on the conversion. The reciprocal of space velocity W/F, was kept constant while varying the total feed rate, F from 0.7180 moles/hr. to 2.8661 moles/hr. The results are given in Table 9 and represented in Fig. 7. The fair constancy of conversion indicated that in this range of low rates, the mass and heat transfer resistances were negligible.

The partial pressure gradients between the flowing fluid and the exterior surface of the catalyst particles were evaluated by the method of Yoshida, Ramaswami and Hougen (24). The values of $\Delta P_j/P_j$ (pressure gradient for component j) were calculated for each component from the charts of Yoshida, Ramaswami and Hougen so as to obtain a rough guide of the relative magnitudes of partial pressure drops. The highest partial pressure gradient thus calculated was for carbon dioxide and was of the order of 0.001-0.009. A more precise value of the partial pressure gradient of carbon dioxide ($\Delta P_{CO_2}/P_{CO_2}$) between the main stream and the catalyst surface was calculated from equation (15) to be 0.0019. These calculations were carried out for run number 362 and are presented in Appendix E. This particular run was chosen because it was made at one of the highest experimental reaction rates. The partial pressure drop across the gas film would be even more insignificant for other rates.

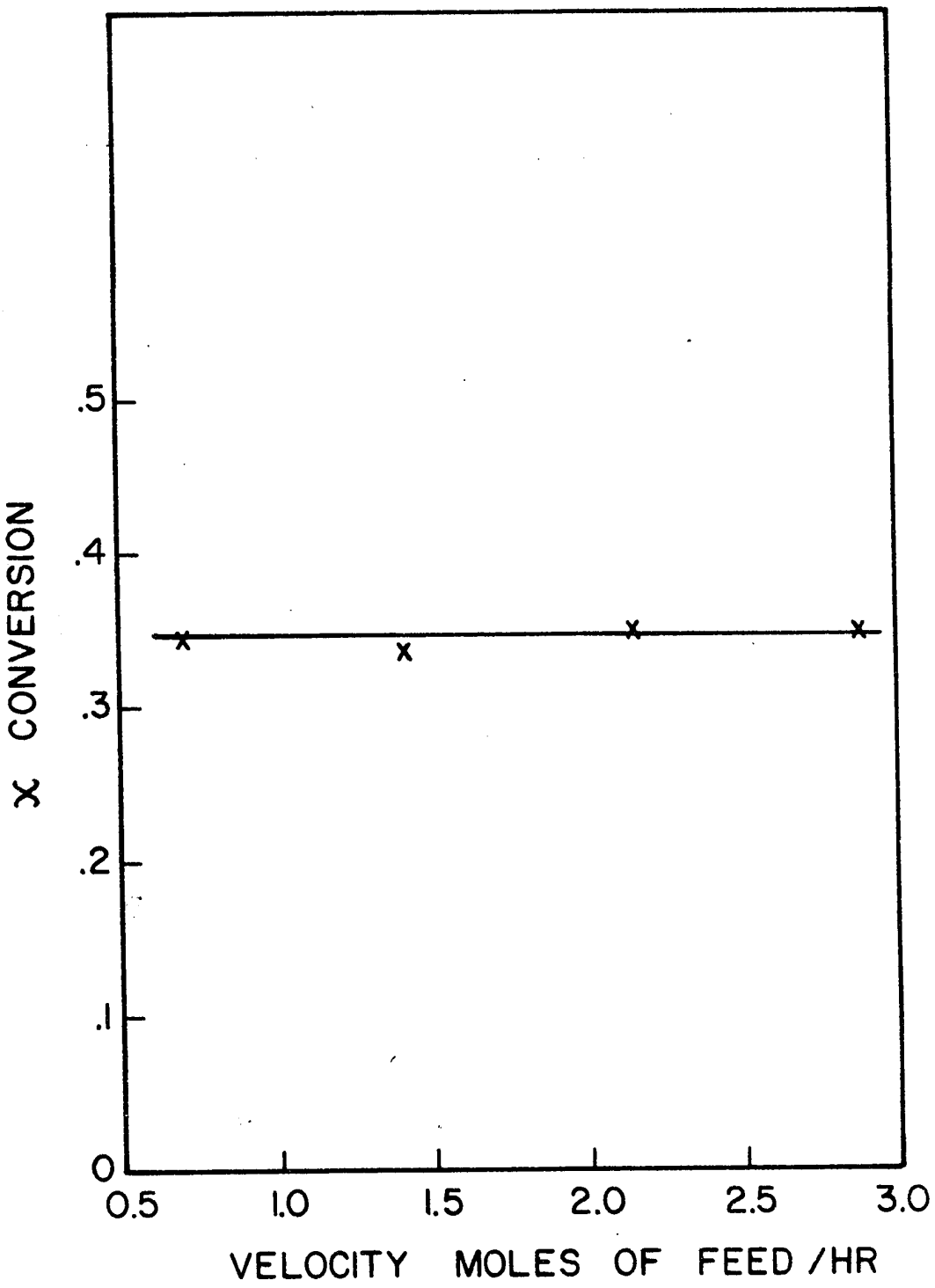

Fig. 7 Effect of Velocity on Conversion

The temperature difference across the gas film surrounding the catalyst particle was also considered. Using the method of Yoshida, Ramaswami and Hougen (24), for run 362, the temperature at the catalyst surface was calculated to be a maximum of 7° C higher than that of the main gas stream. This run probably offered the highest resistance to heat transfer from the granule surface to ambient gas. The temperature gradient from the main gas stream to the liquid metal bath was also determined by placing a thermocouple in the centre of the reactor at the top of the catalyst bed. The temperature difference between the main gas stream and the liquid metal bath never varied by more than 5° C. The temperature gradient from the main gas stream to the liquid metal was also estimated from a heat balance using run no. 362. The maximum temperature drop of 15° C was calculated by assuming a parallel heat transfer scheme based on an effective thermal conductivity (k_e). Calculations for the temperature difference across the gas film surrounding the catalyst particle and for the temperature gradient from the main gas stream to the liquid metal bath are given in apprendix E.

C. Internal Diffusion and Effectiveness Factor

As most catalysts are porous, their external surface area only constitutes a small fraction of the total surface area on which the reaction takes place. Most of the reaction occurs on the inner surfaces of the porous structure. The diffusion of the reactants into and of the product out of them could be important factors in

controlling reaction rate. Even if the exact concentrations of the reactants at the gas-solid interface are known, the condition existing in the interior surface may be quite different due to resistance offered by internal diffusion and heat transfer.

The effectiveness factor (E_A) is defined as the ratio of the actual rate of reaction per unit mass of catalyst to the rate which would exist if the concentrations at all interior interfaces were the same as those at the gross exterior interface (1).

Although much effort has been spent on the correlation of this factor with the physical properties of the system, the success has not been great. Only relatively simple cases have been treated. With the assumptions of uniform density and porosity and negligible adsorption and external surface, Thiele (25) developed the following expression for a first-order reaction:

$$E_A = \frac{3}{m_T^2} (m_T \coth m_T - 1) \qquad (19)$$

where m_T = the Thiele modulus $= \frac{D_p'}{2} \sqrt{\frac{k}{c D_v}}$

D_p' = effective particle diameter for Thiele modulus

c = average radius of pores in the particle

D_v = diffusion coefficient

k = reaction velocity constant

The activity of a catalyst for some reactions is not constant and not reproducible. For such reactions, the use of reaction rate

data for different sizes of the catalyst would be meaningless. It is therefore best to obtain kinetic data under such conditions that E_A approaches unity. This is generally accomplished by decreasing the particle size and using catalyst with large and well-connected pores. For this reason, a catalyst 20-40 mesh in size was employed for the kinetic study. The use of an inert porous support having small particle size and surface area thus ruled out the possibility of the diffusion in the pores controlling the reaction rate.

The diffusion steps (1, 2, 6 and 7) which are physical processes, were found not to be rate controlling. The remaining steps (3, 4 and 5), which are chemical processes, were examined in detail in order to determine which one offered the greatest resistance to the overall reaction. For each of the three chemical steps, namely absorption of reactants, surface reaction and desorption of products, several mechanisms can be postulated depending on whether one or both of the reacting substances are adsorbed on the catalyst surface. Three methods of approach were used to test the validity of each mechanism. First, the method of initial rates as described by Yang and Hougen (20) was applied to the experimental data with the hope of eliminating one and possibly two of the three chemical steps. Next, for each of the postulated mechanisms, functions of initial rate $f(r_o)$ were plotted against the partial pressure of one of the reactants in the feed. The validity of a particular reaction mechanism was verified by determining whether a plot of $f(r_o)$ vs. the partial pressure of isobutylene or oxygen gave a straight line or not.

Finally functions of reaction rate f(r) were calculated for each remaining mechanism and represented graphically as a function of conversion. The intercepts from these graphs were then plotted against the partial pressure of one of the reactants in the feed. The numerical values for the constants in the rate equation were obtained from the slope and intercept of these curves. For the particular mechanism to be valid, the values of the constants thus determined should be positive.

D. Method of Initial Rates

Integral-reactor data were plotted in the form of W/F versus X with feed composition as parameter. The rate of reaction corresponding to any given value of W/F was taken as the slope of the tangent to the curve at that point. The initial rate (when no products are present) was obtained by determining the slope of the curve at W/F = O and X = O. The initial rates were determined for a series of reactant ratios ranging from 0.25 to 4.0 moles oxygen/moles isobutylene and plotted in Figure 8 against the partial pressure of isobutylene in the feed. From the charts of Yang and Hougen (20), which show the effect of feed composition upon initial rates for various mechanisms, and the information derived from Figure 8, it was concluded that desorption of the products was definitely not rate controlling. Further, from a comparison of Fig. 8 with those of Yang and Hougen, it appeared that most likely surface reaction was rate controlling. However, due to the possibility of significant errors in the determination of initial rates (especially in the region of low values of R) both adsorption of reactants and surface reaction were considered as possible rate controlling steps.

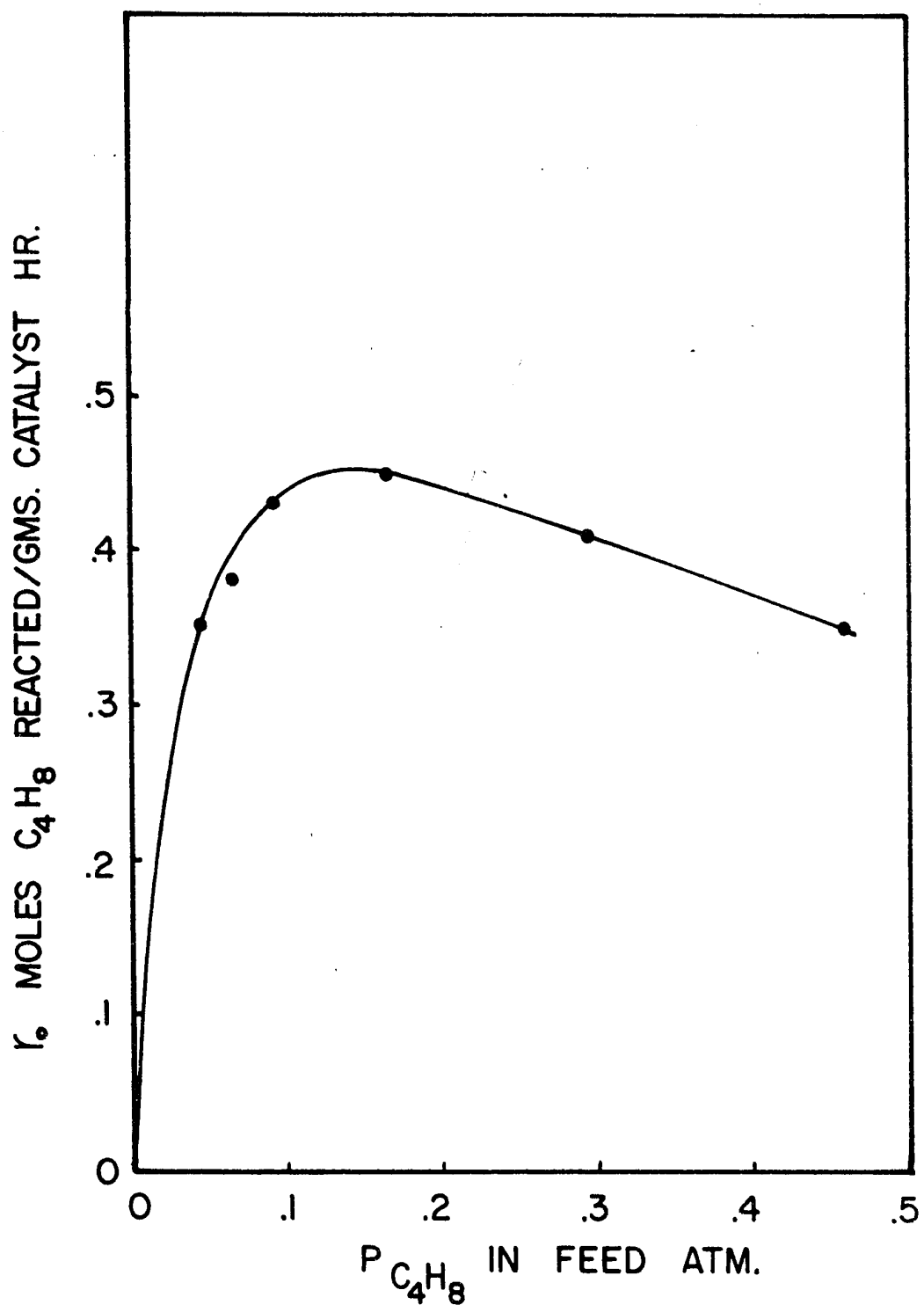

Fig. 8 Initial Rate Versus $P_{C_4H_8}$ in Feed at 400 C

Plausible mechanisms were then postulated for these two chemical steps and rate equations derived for each one. In the following pages, the various theories pertaining to the derivation of the rate equations are considered.

E. Adsorption and the Adsorption Isotherm

Adsorption plays an essential role in heterogeneous catalysis since one or more of the reactants must be adsorbed in order for the reaction to be catalyzed by the solid. Adsorption can be conveniently studied according to the different mechanisms involved.

Van der Waal adsorption is a physical phenomenon, analogous to vapor condensation. The activated adsorption is a chemical phenomenon. Both types of adsorption take place with a decrease in free energy and a decrease in entropy due to the loss of certain degrees of freedom by restricting the translational and rotational motions of the adsorbed molecule.

Chemisorption requires an energy of activation. In physical adsorption the activation energy is negligible (26). Thus physical adsorption proceeds much more rapidly than chemisorption. Chemisorption involves the strong bonding between adsorbed molecules and the active centers of the solid catalyst. The adsorbed molecules are thus much less mobile than those physically adsorbed.

In deriving the adsorption mechanisms for the Hougen-Watson type rate equations it is generally assumed that all the active centers available for the chemical adsorption behave similarly, or are equally active, and that the chemisorption may take place either with or without dissociation of the adsorbed molecules. These two cases are considered separately.

1. Chemisorption Without Dissociation

Chemical adsorption can be considered as a reaction between a vacant active site on the catalyst surface and a gaseous molecule. The forward rate of adsorption for species A can then be written as:

$$r_A = k_A a_{A_i} C_v \qquad (20)$$

where r_A = forward rate of adsorption of reactant A, moles per unit time per unit mass

k_A = adsorption velocity constant of A

a_{A_i} = activity of A in the gas phase at the gas-solid interface

C_v = molal concentration of vacant sites, moles per unit mass

The rate of desorption is:

$$r'_A = k'_A c_A \qquad (21)$$

where r'_A = rate of desorption of A, moles per unit time per unit mass

k'_A = desorption velocity constant of A

c_A = molal concentration of adsorbed A, moles per unit mass

The net rate of adsorption is then:

$$r = r_A - r'_A = k_A a_{A_i} C_v - k'_A c_A \qquad (22)$$

Since any process can be considered as reversible, the equilibrium condition for it can be established by equating the rate of the forward and reverse processes. At equilibrium r = 0, hence

$$\frac{c_A}{a_{A_i} C_v} = \frac{k_A}{k'_A} = K_A \qquad (23)$$

where K_A = adsorption equilibrium constant of A

or $$c_A = K_A a_{A_i} C_v \qquad (24)$$

At this point the assumption is made that the adsorption equilibrium does not depend on the surface coverage. The isotherms thus correspond to Langmuir adsorption which is based on the same assumption. According to this simplified theory the heat of adsorption is independent of the surface coverage. This assumption is justified by assuming that catalytic adsorption is limited to a small fraction of the total atoms present. Substituting equation (24) into equation (22) gives:

$$r = k_A(a_{A_i} C_v - \frac{c_A}{K_A}) \qquad (25)$$

Let L be the molal concentration of active sites, i.e., the number of active sites per unit mass of catalyst divided by the Avogadro number; and c_B, c_I ... are the molal concentration of B, I .... respectively, where I denotes adsorption of an inert component, then the concentration of available active centers

is

$$C_v = L - (c_A + c_B + c_I + \ldots.) \qquad (26)$$

Substituting equation (24) and similar expressions for B, I .... into equation (26) one obtains:

$$C_v = L - C_v (a_{A_i} K_A + a_{B_i} K_B + a_{I_i} K_I + \ldots) \qquad (27)$$

Rearranging one then has:

$$c_A = \frac{a_{A_i} \cdot K_A \cdot L}{1 + a_{A_i} K_A + a_{B_i} K_B + a_{I_i} K_I + \ldots} \qquad (28)$$

and the fraction coverage of A is:

$$\theta_A = \frac{c_A}{L} = \frac{a_{A_i} K_A}{1 + a_{A_i} K_A + a_{B_i} K_B + a_{I_i} K_I + \ldots} \qquad (29)$$

In addition to being in agreement with the Langmuir isotherm, equation (29) also agrees with the form derived by Glasstone, Laidler and Eyring (27) through the use of partition functions.

Equation (29) has been derived in terms of the activities of the components of the reaction. The activity, a, may be defined as the ratio of the fugacity, f, in any given state to the fugacity, f°, in some standard state generally taken at the same temperature. For gases the activity is referred to the standard state, at any fixed temperature, in which the gas has a fugacity of one atmosphere. Consequently, the activity and fugacity of a gas are identical numerically. Therefore, in equation (29) activities may be replaced by fugacities. The fugacity and pressure

are identical for an ideal gas. Assuming that the components of the system under investigation behave like ideal gases in the range of temperatures used in this study, then the partial pressures of these components can be substituted for their fugacities. Then equation (29) becomes

$$\theta_A = \frac{c_A}{L} = \frac{K_A P_A}{1 + K_A P_A + K_B p_B + K_I p_I + \ldots} \qquad (30)$$

2. Chemisorption With Dissociation

Where adsorption is accompanied by dissociation, the distance between the adsorbed atoms is much greater than in a normal molecule. There are two main types of dissociation:

a) The molecule undergoes dissociation in the course of adsorption but the atoms remain on adjacent sites. This may be described as shown in Figure 9 where A_2 is the adsorbed gas molecule and s_2 represents the two adjacent sites. The

Figure 9 Activated State for Adsorption of gas molecule A_2 on two adjacent sites (s_2)

equilibrium between initial, activated and final states may be written as:

$$A_2 \quad + \quad s_2 \rightleftharpoons (A_2 s_2)^{\neq} \rightleftharpoons A - s \ldots . s - A$$

gas — surface — activated state — adsorbed atoms

The adsorption isotherm thus obtained is identical with that for no dissociation

b) Dissociation results from the jump of one or both of the atoms constituting the molecule from one site to another. Still two possibilities may arise:

Case 1. The actual adsorption of the molecule is rapid and the jump of the atoms slow. In this case the activated state may be depicted in Figure 10 so that the adsorption and desorption equilibrium can be represented as:

$$\frac{1}{2} A_2 \quad + \quad s_2 \rightleftharpoons (A s_2)^{\neq} \rightleftharpoons A - s_2$$

gas — surface — activated state — adsorbed atom

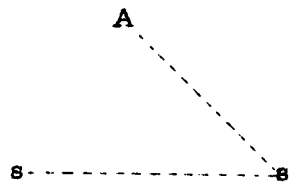

Figure 10 Activated state for jump of an atom (A) from one adsorption site to another

Through the use of partition functions (27), the adsorption isotherm obtained is:

$$\theta = \frac{bp^{1/2}}{1 + bp^{1/2}} \tag{31}$$

Case 2. The adsorption of the molecule is the rate-controlling step. The processes may be represented by

$$A_2 + s_2 \rightleftharpoons (A_2 s_2)^{\neq}$$

$$(A_2 s_2)^{\neq} + 2s' \rightleftharpoons 2 A s' + s_2$$

where s_2 is a dual site on which the molecule A_2 is first adsorbed and s' represents a site to which each atom finally jumps. For the first step,

$$r = k_{A_2} a_{A_i} c_{s_2} - k'_{A_2} c_{(A_2 s_2)^{\neq}} \tag{32}$$

For the second step which is in equilibrium

$$c_{(A_2 s_2)^{\neq}} = \frac{c^2_{As} c_{s_2}}{K'_A c^2_{s'}} \tag{33}$$

where K'_A = equilibrium constant for the dissociation step

With the assumption that the active centers are arranged on the surface in a regular geometric pattern such that each site is surrounded by s equidistant adjacent sites, the following relation can be derived:

$$c_A = c_{As'} = c_V \sqrt{a_{A_{2i}} K_{A_2}} \qquad (34)$$

where $K_{A_2} = \dfrac{k_{A_2} K'_A}{k'_{A_2}}$

By substituting equation (34) into equation (26), one can obtain an expression for adsorption equilibrium conditions for a gaseous mixture consisting of components A, B, I..., in which A is adsorbed with dissociation:

$$\theta_A = \frac{c_A}{L} = \frac{\sqrt{a_{A_{2_i}} K_{A_2}}}{1 + \sqrt{a_{A_{2_i}} K_{A_2}} + a_{B_i} K_B + a_{I_i} K_I \quad \ldots} \qquad (35)$$

If the gaseous activities are again replaced by partial pressures, with the understanding that A represents the gaseous component A_2, then:

$$\theta_A = \frac{c_A}{L} = \frac{\sqrt{K_A P_A}}{1 + \sqrt{K_A P_A} + K_B p_B + K_I p_I \quad \ldots} \qquad (36)$$

This result again agrees with the Langmuir isotherm for adsorption with dissociation and the result obtained by use of partition functions. It may be noted that both, Cases 1 and 2, in this "jump type" dissociation yield similar results.

F. Surface Reactions

1. Rate Equations

With the expression for surface coverages θ_A, θ_B, ... etc. available, it is now possible to derive the Hougen-Watson rate equations for the various possible mechanisms. As a specific example, a rate equation can be developed for the reaction

$$A + B \rightleftharpoons R + S$$

The rate controlling step of the reaction is the surface reaction between adsorbed A and adsorbed B to give R and S. Since in a Hougen-Watson rate equation, only one of the successive steps is considered rate-controlling, the adsorption and desorption stages in this case are assumed to be at equilibrium. The forward reaction rate is proportional to the concentration of adjacently adsorbed AB pairs, c_{AB}:

$$r_f = k\, c_{AB} \tag{37}$$

where r_f = forward reaction rate, moles product formed per unit time per unit catalyst weight

k = reaction velocity constant for the surface reaction

c_{AB} = molal concentration of adjacent A and B molecules per unit mass of catalyst

Since the surface concentration of adsorbed A is c_A and each adsorbed A is surrounded by s active sites including vacant and occupied, also, on the average, coverage of sites by B is θ_B, the surface concentration of AB pairs is:

$$c_{AB} = c_A \cdot s\theta_B = c_A \cdot s \frac{c_B}{L} = \frac{s}{L}\, c_A\, c_B \tag{38}$$

Substituting equation (38) into equation (37) gives

$$r_f = \frac{ks}{L}\, c_A\, c_B \tag{39}$$

Substituting for c_A from equation (30) and a similar one for c_B, gives

$$r_f = \frac{k\, s\, L\, K_A\, K_B\, P_A\, P_B}{(1 + K_A P_A + K_B P_B + K_R P_R + K_S P_S)^2} \qquad (40)$$

If the reverse reaction is included, the net forward reaction rate is:

$$r = \frac{k\, s\, L\, K_A\, K_B\, (P_A P_B - P_R P_S/K)}{(1 + K_A P_A + K_B P_B + K_R P_R + K_S P_S)^2} \qquad (41)$$

where K = thermodynamic equilibrium constant for the overall reaction

The initial rate of a differential reaction where conversion is extremely small, P_R and P_S are negligible can be written as:

$$r_o = \frac{k\, s\, L\, K_A\, K_B\, P_A\, P_B}{(1 + K_A P_A + K_B P_B)^2} \qquad (42)$$

where subscript o signifies "initial".

Equations of the above form (equation 41) have been systematically developed and compiled for various adsorption mechanisms and controlling steps. Hougen (28) suggested that the right hand side of the rate equation be divided into three parts, namely, the kinetic term which includes the reaction velocity constant, the potential term which consists of the activity (or partial pressure) difference, and the adsorption terms which gives the adsorption isotherms. The proper rate

equation for a certain reaction and mechanism can be easily and readily composed by selecting and modifying proper terms. Table 4 shows how this convenient form appears.

Table 4: Rate Equations for Fluid Reactions Catalyzed by Solids

Reaction rate = [Kinetic Term] [Absorption Term] [Potential Term] *

r = reaction rate = moles of reactant A converted/(unit mass catalyst)/(unit time)

$$r = \frac{Fdx}{dW}$$

F = feed rate, mass (or moles) of A per unit time

W = mass of catalyst

x = moles of A converted per moles of A in feed

E = effectiveness factor of catalyst pellets

L = total active molal sites per unit mass of catalyst

f(s) = adjacency of sites

ELf(s) = constant for any given catalyst (This term may be used as a multiplying factor in either the kinetic term or adsorption term).

K = overall equilibrium constant - uncatalyzed reaction (obtained where the potential term is 0)

a = activity - may also be used for concentration (gas or liquid) of partial pressure (gases)

---

* Not including resistance due to mass transfer.

I. Kinetic term

Each reaction velocity constant should be multiplied by ELf(s) to allow for the population and availability of active sites.

Rate-controlling chemical step	$A \rightleftharpoons R$	$A \rightleftharpoons R + S$	$A + B \rightleftharpoons R$	$A + B \rightleftharpoons R + S$
Surface reaction	k_s	k_s	k_s	k_s
Adsorption of A	k_a	k_a	k_a	k_a
Desorption of R	k'_d	k'_d	k'_d	k'_d

II. Potential term

The potential term assumes that the forward and reverse reactions proceed by the same reversible step.

Rate-controlling chemical step	$A \rightleftharpoons R$	$A \rightleftharpoons R + S$	$A + B \rightleftharpoons R$	$A + B \rightleftharpoons R + S$
Surface reaction	$a_A - \frac{a_R}{K}$	$a_A - \frac{a_R a_S}{K}$	$a_A a_B - \frac{a_R}{K}$	$a_A a_B - \frac{a_R a_S}{K}$
Adsorption of A	$a_A - \frac{a_R}{K}$	$a_A - \frac{a_R a_S}{K}$	$a_A - \frac{a_R}{a_B K}$	$a_A - \frac{a_R a_S}{a_B K}$
Desorption of R	$Ka_A - a_R \frac{Ka_A}{a_S} - a_R$		$Ka_A a_B - a_R$	$\frac{Ka_A a_B}{a_S} - a_R$

III. Adsorption term

The kinetic adsorption constants are obtained from kinetic data and not from separate adsorption equilibrium experiments and are applicable only to the active sites engaged in the catalytic reaction. Where extensive coverage is involved the kinetic

ADSORPTION TERMS

The cases tabulated herewith are limited to a single and dual site adsorptions.

ate-ntrolling emical eps	$A \rightleftharpoons R$	$A \rightleftharpoons R + S$	$A + B \rightleftharpoons R$	$A + B \rightleftharpoons R + S$
rface action ntrolling	$\frac{K_A}{(1 + K_A a_A + K_R a_R)}$ **(single site)**	$\frac{K_A}{(1 + K_A a_A + K_R a_R + K_S a_S)}$ **(single site)**	$\frac{K_A K_B}{(1 + K_A a_A + K_B a_B + K_R a_R)^2}$	$\frac{K_A K_B}{(1 + K_A a_A + K_B a_B + K_R a_R + K_S a_S)^2}$
ll compo-nts are ad-rbed with dissocia-ons)	$\frac{K_A}{(1 + K_A a_A + K_R a_R)^2}$ **(dual sites for A)**	$\frac{K_A}{(1 + K_A a_A + K_R a_R + K_S a_S)^2}$ **(dual sites for A)**		
lsorption A control-g without ssociation of A	$\frac{1}{(1 + \frac{K_A a_R}{K} + K_R a_R)}$	$\frac{1}{(1 + \frac{K_A a_R a_S}{K} + K_R a_R)}$	$\frac{1}{(1 + \frac{K_A a_R}{K a_B} + K_B a_B + K_R a_R)}$	$\frac{1}{(1 + \frac{K_A}{K}\frac{a_R a_S}{a_B} + K_B a_B + K_R a_R + K_S a_S}$

Rate-controlling chemical steps	$A \rightleftharpoons R$	$A \rightleftharpoons R + S$	$A + B \rightleftharpoons R$	$A + B \rightleftharpoons R + S$
Adsorption of A controlling with dissociation of A (all components other than A are at equilibrium adsorption without dissociation)	$\frac{1}{\left(1+\sqrt{\frac{K_A a_R}{K}}+K_R a_R\right)^2}$	$\frac{1}{\left(1+\sqrt{\frac{K_A a_R a_S}{K}}+K_R a_R\right)^2}$	$\frac{1}{\left(1+\sqrt{\frac{K_A a_R}{K a_B}}+K_B a_B+K_R a_R\right)^2}$	$\frac{1}{\left(1+\sqrt{\frac{K_A}{K}\frac{a_R a_S}{a_B}}+K_B a_B+K_R a_R+K_S a_S\right)^2}$
Desorption of R (all components other than R are at equilibrium adsorption without dissociation)	$\frac{1}{(1+K_A a_A+K K_R a_A)}$	$\frac{1}{(1+K_A a_A+K\frac{K_R a_A}{a_S}+K_S a_S)}$	$\frac{1}{(1+K_A a_A+K_B a_B+K K_R a_A a_B}$	$\frac{1}{1+K_A a_A+K_B a_B+K K_R \frac{a_A a_B}{a_S}+K_S a_S)}$

adsorption constants decrease with extent of coverage or the exponents of concentrations in the adsorption term become less than unity.

The cases of dissociation tabulated under adsorption terms are limited to dissociation of molecules into two parts with adsorption on adjacent sites.

Special Cases

Adsorption Terms

IV. A. Surface Reaction rate controlling

1. Where dissociation of A occurs
   a. replace $k_A a_A$ by $\sqrt{K_A a_A}$ and
   b. increase exponent of denominator term by 1
2. Where dissociation of B occurs
   a. replace $K_B a_B$ by $\sqrt{K_B a_B}$ and
   b. increase exponent of denominator term by 1
3. Where B is not adsorbed
   a. replace K_B by 1 in numerator
   b. replace $K_B a_B$ by 0 in denominator
   c. reduce exponent in denominator by 1
4. Where R or S are dissociated
   a. replace $K_R a_R$ by $\sqrt{K_R a_R}$ and $K_S a_S$ by $\sqrt{K_S a_S}$
5. Where R or S are not adsorbed
   a. replace $K_R a_R$ by 0 and $K_S a_S$ by 0

B. Adsorption of A rate controlling

1. Where dissociation of B occurs
   a. replace $K_B a_B$ by $\sqrt{K_B a_B}$ and

b. increase exponent of denominator by 1

2. Where B is not adsorbed
   a. replace K_B by 1 in numerator
   b. replace $K_B a_B$ by 0 in denominator
   c. reduced exponent of denominator by 1
3. Where R is not adsorbed replace $K_R a_R$ by 0
4. Where S is not adsorbed replace $K_S a_S$ by 0
5. Where dissociation of R occurs replace $K_R a_R$ by $\sqrt{K_R a_R}$
6. Where dissociation of S occurs replace $K_S a_S$ by $\sqrt{K_S a_S}$

C. This table covers only cases of single rate-controlling steps and where adsorption is restricted to single or dual sites. Where two surface reactions occur simultaneously on different types of active sites the two reaction rates are additive requiring independent kinetic and adsorption terms.

2. The Theory of Absolute Reaction Rates

The Eyring theory of absolute reaction rates (27, 29) offers an excellent explanation for the function of catalyst. In its simplest version, this theory postulates that in order for a chemical reaction to occur, the reacting atoms or molecules must form an "activated complex" located at the top of an "energy barrier" which corresponds to the peak in a potential energy curve (Figure 11) between the initial and final states. The rate of reaction is controlled by the rate at which the complex forms and travels over the top of the "hill".

In the case of a slow, non-catalyzed reaction (full curve in Figure 11), it is regarded that the barrier is so high that forming of the activated complex is very slow. In terms of potential energy, we say that it requires a very high energy of activation. If the same reaction occurs in the presence of a catalyst, it follows a different path corresponding to the dotted curve in Figure 11. Although the number of barriers is increased from one to three in this case, each of these barriers requires a much lower energy of activation and hence is more easily crossed. Therefore the activated complex is formed more rapidly and the reaction rate increased. There are two significant points in observing these paths. The first is that the adsorbed state is always at a lower energy level than the gaseous state of the same species. The second is that the initial and final states remain unchanged despite the presence of catalyst. This is in line with the fact that a catalyst can only speed up a reaction but never shift the equilibrium of the overall reaction.

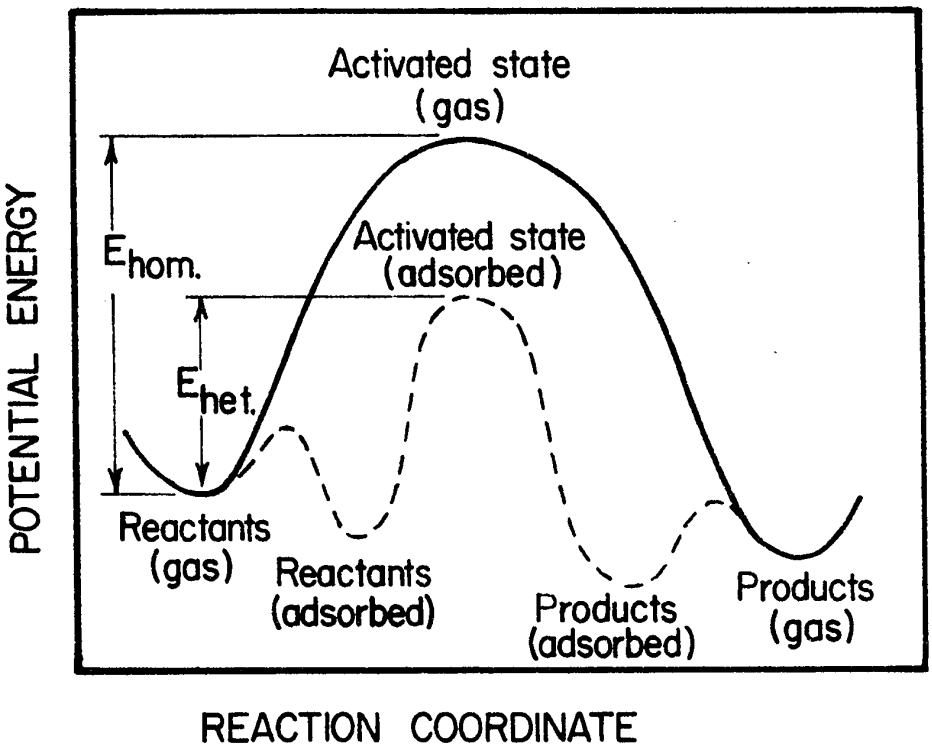

Figure 11 Potential energy curves for the same reaction as a homogeneous and as a heterogeneous process. (27)

3. Temperature Dependence of Constants

The most universal expression representing the temperature effect on the kinetic rate constant is the Arrhenius form

$$A e^{B/T}$$

named after Svante Arrhenius, original spark of chemical kinetics. With the knowledge of the theory of absolute reaction rates and with the assistance of statistical mechanics, this expression can be further analyzed with added significance.

For the surface reaction and its rate constant, we can write the process, according to the theory of absolute reaction rates in the last section, as

$$A^* + B^* \rightleftharpoons X^{\neq} \longrightarrow R^* + S^*$$

where $X^{\neq}$ represents the activated complex and * indicates the adsorbed state. For the equilibrium part of the process, forward reaction rate is (same as Equation 39)

$$r_f = k c_{AB} = k c_A \frac{s}{L} c_B = \frac{ks}{L} c_A c_B \qquad (43)$$

The reverse reaction rate

$$r' = k' c_{X^{\neq}}$$

At $r_f = r'$, equilibrium constant for the activation process is then

$$K^{\neq} = \frac{k}{k'} = \frac{c_{X^{\neq}}}{\frac{s}{L} c_A c_B} = \frac{f^{\neq}}{f_A f_B} e^{-\epsilon_1/kT} \qquad (44)$$

where $f^{\neq}$, f_A and f_B are the total partition functions of the activated complex, adsorbed A and adsorbed B , respectively. ϵ_1 is the energy of the complex with reference to the reactants, at absolute zero, or simply the activation energy at that temperature, and $\underline{k}$ is the Boltzmann constant. Now we consider the partition function of the activated complex. Among the various modes of vibration motion, there is one with a very different nature from the rest. It corresponds to a very loose vibration allowing the complex to dissociate into the products of the surface reaction. We may then evaluate the partition function for this vibrational degree of freedom by letting it approach the limit of zero frequency, i.e.:

$$f_{l.v.} = \lim_{\nu \to 0} \frac{1}{1 - e^{-h\nu/\underline{k}T}} = \frac{1}{1 - (1 - h\nu/kT)} = \frac{kT}{h\nu} \qquad (45)$$

where h = Planck constant

ν = frequency of vibration

and $f_{l.v.}$ represents the partition function for the loose vibrational degree of freedom

We can now replace the partition function of the activated complex by

$$f^{\neq} = f_{l.v.} \quad f = \frac{kT}{h\nu} \quad f_{\neq} \qquad (46)$$

where $f_{\neq}$ = partition function of the activated complex with one less vibrational degree of freedom

Then, Equation (44) can be rewritten as:

$$c_{X^{\neq}} = \frac{s}{L}\, c_A c_B \frac{f^{\neq}}{f_A f_B} \left(\frac{kT}{hy}\right) e^{-\epsilon_1/\underline{k}T}$$

or

$$yc_{X^{\neq}} = \frac{s}{L}\, c_A c_B \frac{f^{\neq}}{f_A f_B} \left(\frac{kT}{h}\right) e^{-\epsilon_1/\underline{k}T} \qquad (47)$$

Since y is the frequency of vibration of the activated complex in the transformation into products, $yc_{X^{\neq}}$ is then the rate of the process and therefore one obtains

$$r = \frac{s}{L} \left[\frac{f^{\neq}}{f_A f_B} \left(\frac{kT}{h}\right) e^{-\epsilon_1/\underline{k}T}\right] c_A c_B \qquad (48)$$

The ϵ_1 and $\underline{k}$ in exponent on e in Equation (48) are both on per molecule basis, ϵ_1 the activation energy per molecule and $\underline{k}$ the gas constant R divided by the Avogadro number. The exponential term can then be rewritten in the more familiar form

$$e^{-\Delta H^{\neq}/RT}$$

where $\Delta H^{\neq}$ is the activation energy per mole
Equation (48) is then

$$r = \frac{s}{L} \left[\frac{f^{\neq}}{f_A f_B} \left(\frac{kT}{h}\right) e^{-\Delta H^{\neq}/RT}\right] c_A c_B \qquad (49)$$

$$= \frac{s}{L}\, k\, c_A\, c_B$$

where k = rate constant for the surface reaction

$$= \left[\left(\frac{kT}{h}\right) \frac{f^{\neq}}{f_A f_B}\right] e^{-\Delta H^{\neq}/RT}$$

Since the partition functions are associated with the various degrees of freedom, their ratio can be related to the entropy change during the activation process as follows:

$$\frac{f^{\neq}}{f_A f_B} = e^{\frac{\Delta S^{\neq}}{R}}$$

and

$$k = \left[\frac{kT}{h} e^{\frac{\Delta S^{\neq}}{R}}\right] e^{-\Delta H^{\neq}/RT} \qquad (50)$$

The expression in the bracket in Equation (50) is known as the "frequency factor" and corresponds to A in the Arrhenius equation. Since it changes much more slowly with temperature than does the exponential term $e^{-\Delta H^{\neq}/RT}$, it can be considered constant over a moderate temperature range. Therefore an Arrhenius plot for the constants should approximately give straight lines. One also notes that, since $\frac{s}{L}$ is usually unknown for porous catalyst, $\Delta S^{\neq}$ can only be calculated from the surface reaction rate constants, not the rates, at different temperatures.

For the adsorption equilibrium constants, the familiar thermodynamic relation

$$\Delta G^\circ = \Delta H^\circ - T\Delta S^\circ = -RT \ln K \qquad (51)$$

holds. In this equation ΔG° is the Gibbs free energy change for the reaction when the reactants and products are in their standard states, ΔH° is the standard state enthalpy change, ΔS° is the standard state entropy change and K is the equilibrium constant for the

reaction. When applied to the adsorption of a certain component A, we have:

$$K_A = e\left(\frac{-\Delta H^\circ_A}{RT} + \frac{\Delta S^\circ_A}{R}\right) = e^{\frac{+\Delta S^\circ_A}{R}} e^{\frac{-\Delta H^\circ_A}{RT}} \qquad (52)$$

This equation suggests that if $\ln K_A$ is plotted against $1/T$, it will produce a straight line with slope $-\frac{\Delta H^\circ_A}{R}$ and intercept $\frac{\Delta S^\circ_A}{R}$. The theory of absolute reaction rates can be similarly applied as described above for the kinetic rate constant and will not be elaborated here.

G. Correlation of Initial Rate Data

Since mass transfer from the gas stream to the catalyst surface and diffusion through the catalyst pores, and desorption of the products were not rate controlling, it left for consideration the possibility of the adsorption of the reactants and surface reaction as rate controlling. By combining the equations for adsorption and surface reaction, it was possible to develop several rate equations (1) based on a particular rate controlling step. Seven such mechanisms were postulated. For each mechanism of reaction, a rate equation was developed based on the rate controlling step. The rate equations thus developed were rearranged in the form:

$$f(r_o) = f \text{ (partial pressure)}$$

When testing the validity of an equation for a particular mechanism, the term $(P_{C_4H_6O})(P_{H_2O})/K$ was omitted as the equilibrium constant (K) for the gas phase oxidation of isobutylene

was very large ($\ln K > 20$). Furthermore, the adsorption term for nitrogen ($K_I P_I$) was not included in the rate equations, since, according to Dowden (30), the chemisorption of nitrogen on copper oxide was negligible.

1. Adsorption of Isobutylene Controlling

Mechanism 1

Surface reaction between adsorbed isobutylene and adsorbed oxygen.

$$r = \frac{a\, P_{C_4H_8}}{1 + K_2 P_{O_2} + K_3 P_{C_4H_6O} + K_4 P_{H_2O}} \qquad (53)$$

$$\frac{P_{C_4H_8}}{r_o} = 1/a + K_2 P_{O_2}/a \qquad (53a)$$

where a = reaction rate constant, combined with surface parameters.

Mechanism 2

Surface reaction between adsorbed isobutylene and oxygen in the gas phase.

$$r = \frac{a\, P_{C_4H_8}}{1 + K_3 P_{C_4H_6O}} \qquad (54)$$

$$\frac{P_{C_4H_8}}{r_o} = 1/a \qquad (54a)$$

2. Adsorption of Oxygen Controlling

Mechanism 3

Surface reaction between adsorbed isobutylene and

adsorbed oxygen

$$r = \frac{a P_{O_2}}{1 + K_1 P_{C_4H_8} + K_3 P_{C_4H_6O} + K_4 P_{H_2O}} \qquad (55)$$

$$\frac{P_{O_2}}{r_o} = 1/a + K_1 P_{C_4H_8}/a \qquad (55a)$$

Mechanism 4

Surface reaction between adsorbed oxygen and isobutylene in the gas phase

$$r = \frac{a P_{O_2}}{1 + K_3 P_{C_4H_6O}} \qquad (56)$$

$$\frac{P_{O_2}}{r_o} = 1/a \qquad (56a)$$

3. Surface Reaction Controlling

Mechanism 5

Surface reaction between adsorbed isobutylene and adsorbed oxygen.

$$r = \frac{a K_1 K_2 P_{C_4H_8} P_{O_2}}{(1 + K_1 P_{C_4H_8} + K_2 P_{O_2} + K_3 P_{C_4H_6O} + K_4 P_{H_2O})^2} \qquad (57)$$

$$\left[\frac{P_{C_4H_8} P_{O_2}}{r_o}\right]^{1/2} = \frac{1 + K_1 P_{C_4H_8} + K_2 P_{O_2}}{\sqrt{a K_1 K_2}} \qquad (57a)$$

Mechanism 6

Surface reaction between adsorbed isobutylene and oxygen in the gas phase.

$$r = \frac{\alpha \quad K_1 P_{C_4H_8} P_{O_2}}{1 + K_1 P_{C_4H_8} + K_3 P_{C_4H_6O}} \qquad (58)$$

$$\frac{P_{C_4H_8} P_{O_2}}{r_o} = 1/\alpha K_1 + P_{C_4H_8}/\alpha \qquad (58a)$$

Mechanism 7

Surface reaction between adsorbed oxygen and isobutylene in the gas phase.

$$r = \frac{\alpha K_2 P_{C_4H_8} P_{O_2}}{1 + K_2 P_{O_2} + K_3 P_{C_4H_6O}} \qquad (59)$$

$$\frac{P_{C_4H_8} P_{O_2}}{r_o} = 1/\alpha K_2 + P_{O_2}/\alpha \qquad (59a)$$

Function of initial rates $f(r_o)$ were plotted versus the partial pressure of one of the reactants in the feed for mechanism 1, 3, 5, 6, and 7 and are shown in Figures 12, 13, 14, 15 and 16 respectively. The data for these graphs are given in Table 8.

From Figures 12, 14, 15 and 16 it can be seen that mechanisms 1, 5, 6 and 7 meet the necessary condition that a plot of $f(r_o)$ versus

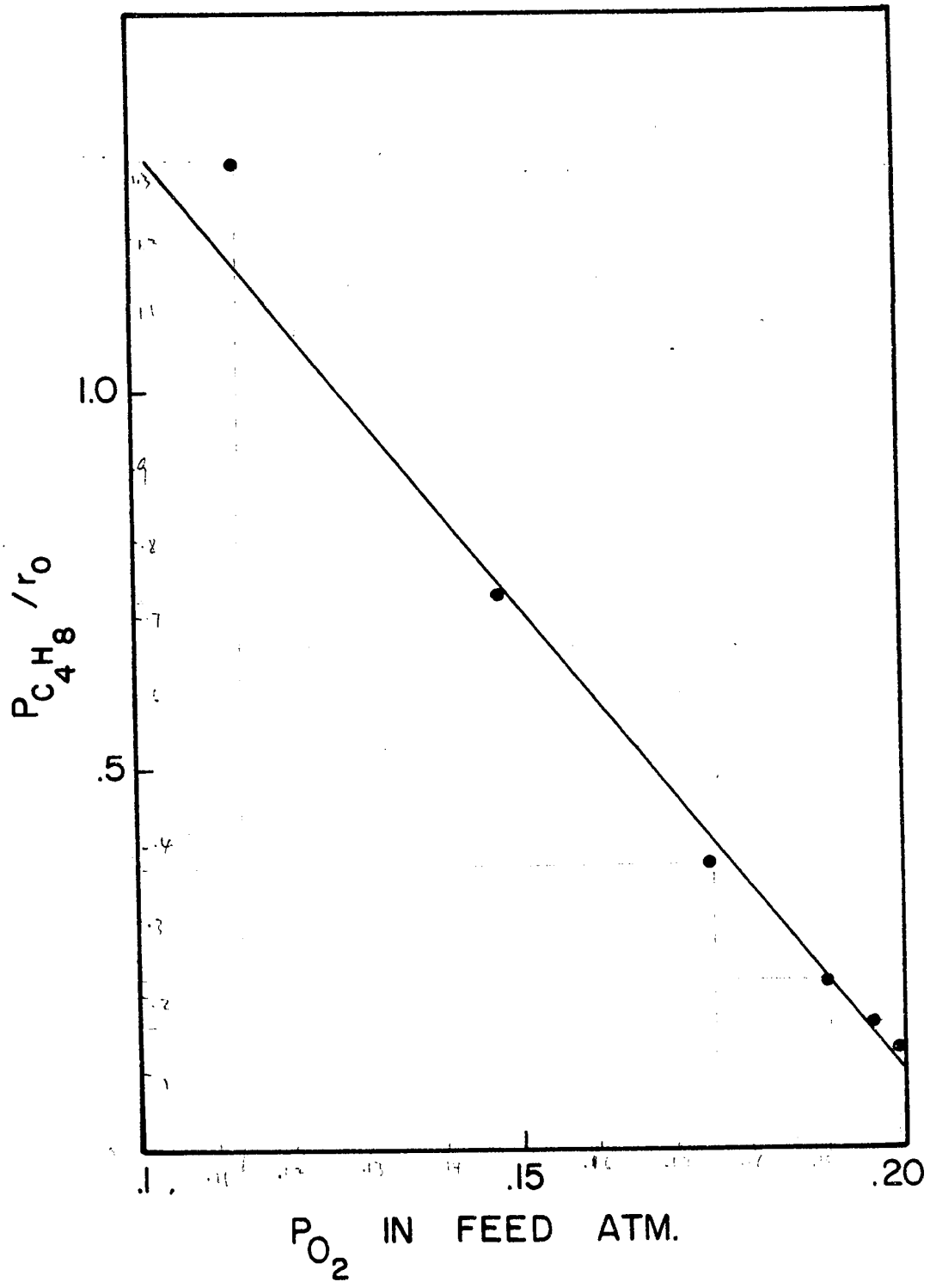

Figure 12 $f(r_o)$ Versus P_{O_2} in Feed for Equation (53a)

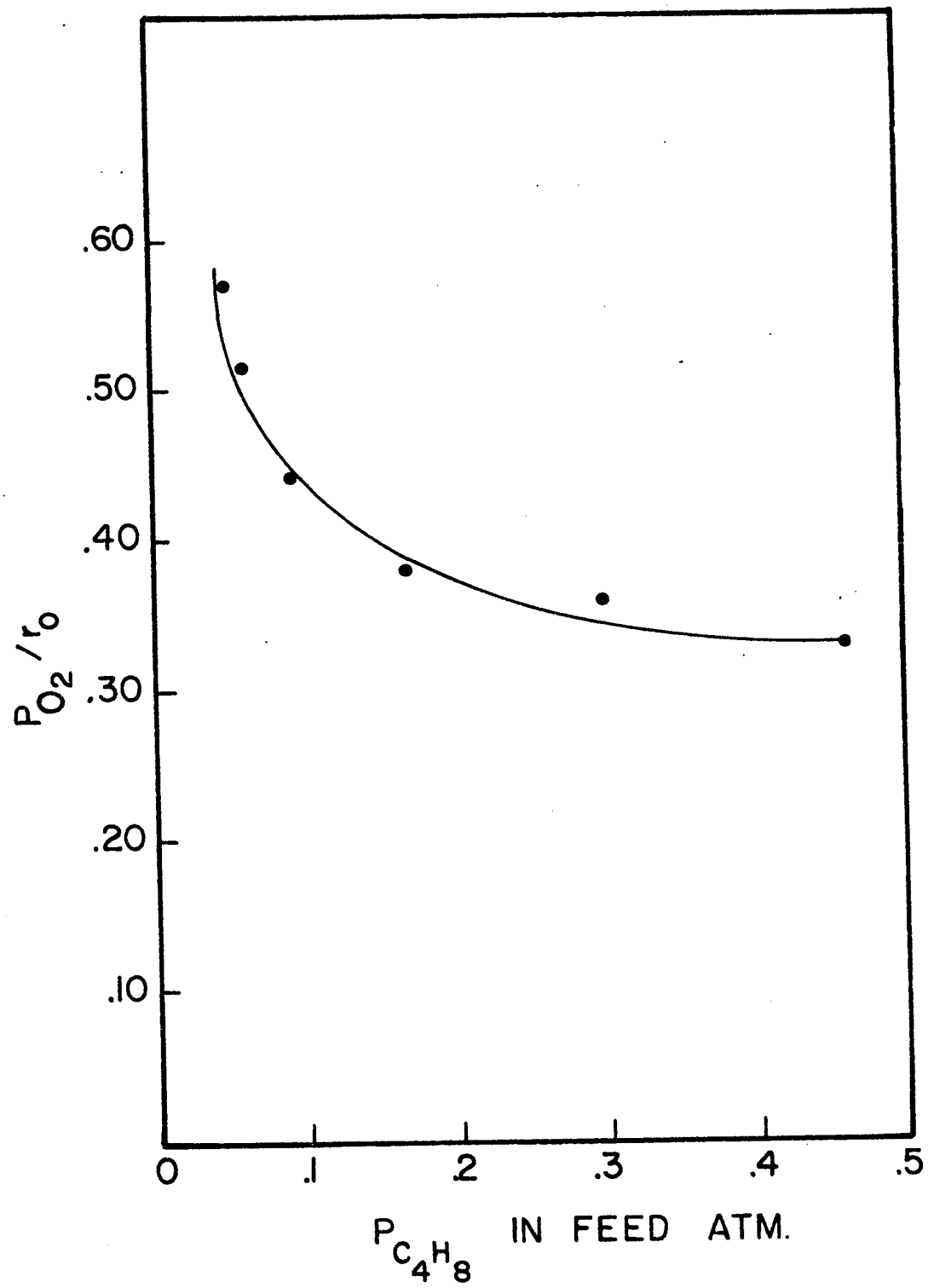

Fig. 13 $f(r_o)$ Versus $P_{C_4H_8}$ in Feed for Equation (55a)

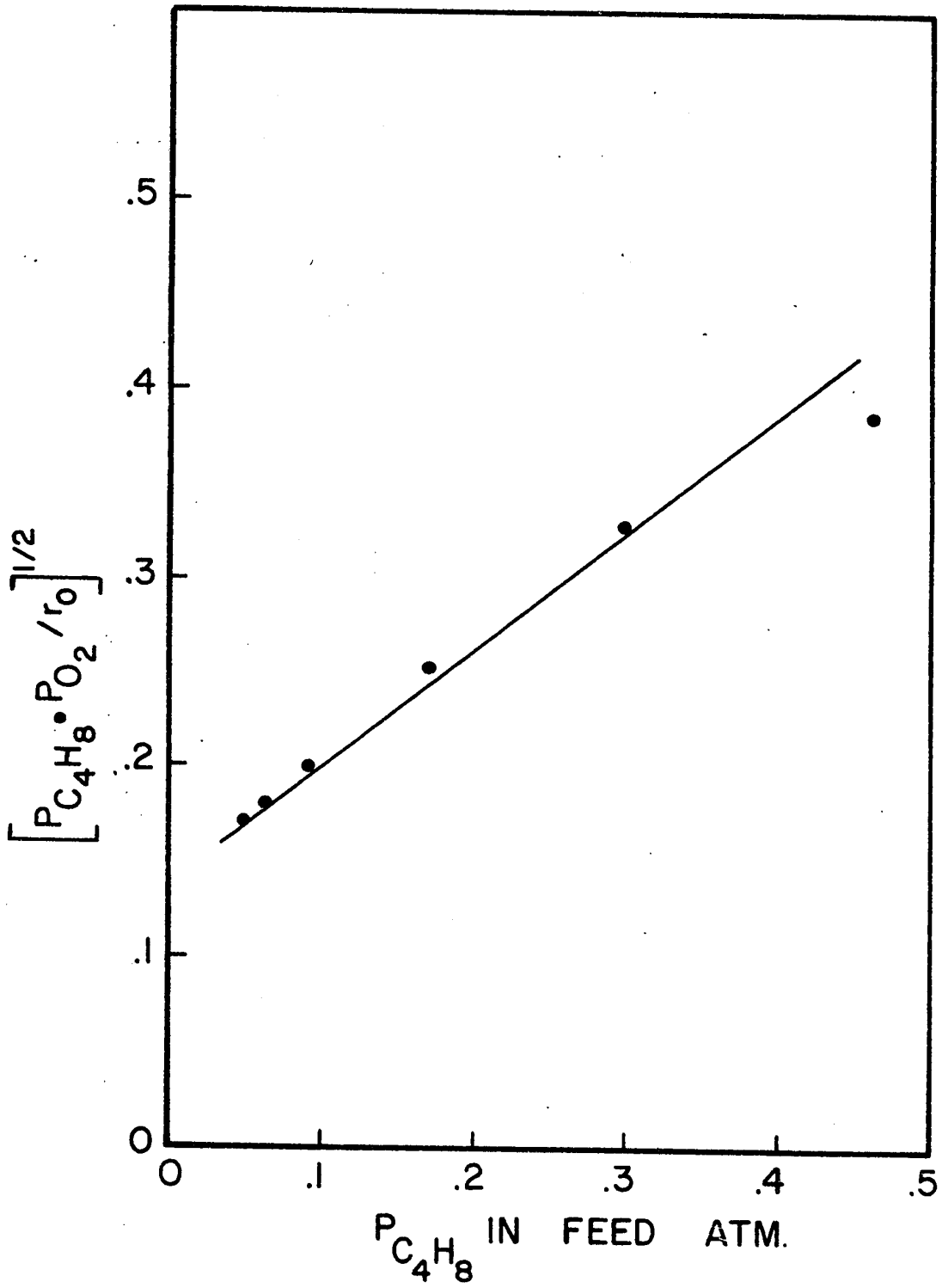

Fig. 14 $f(r_o)$ Versus $P_{C_4H_8}$ in Feed for Equation (57a)

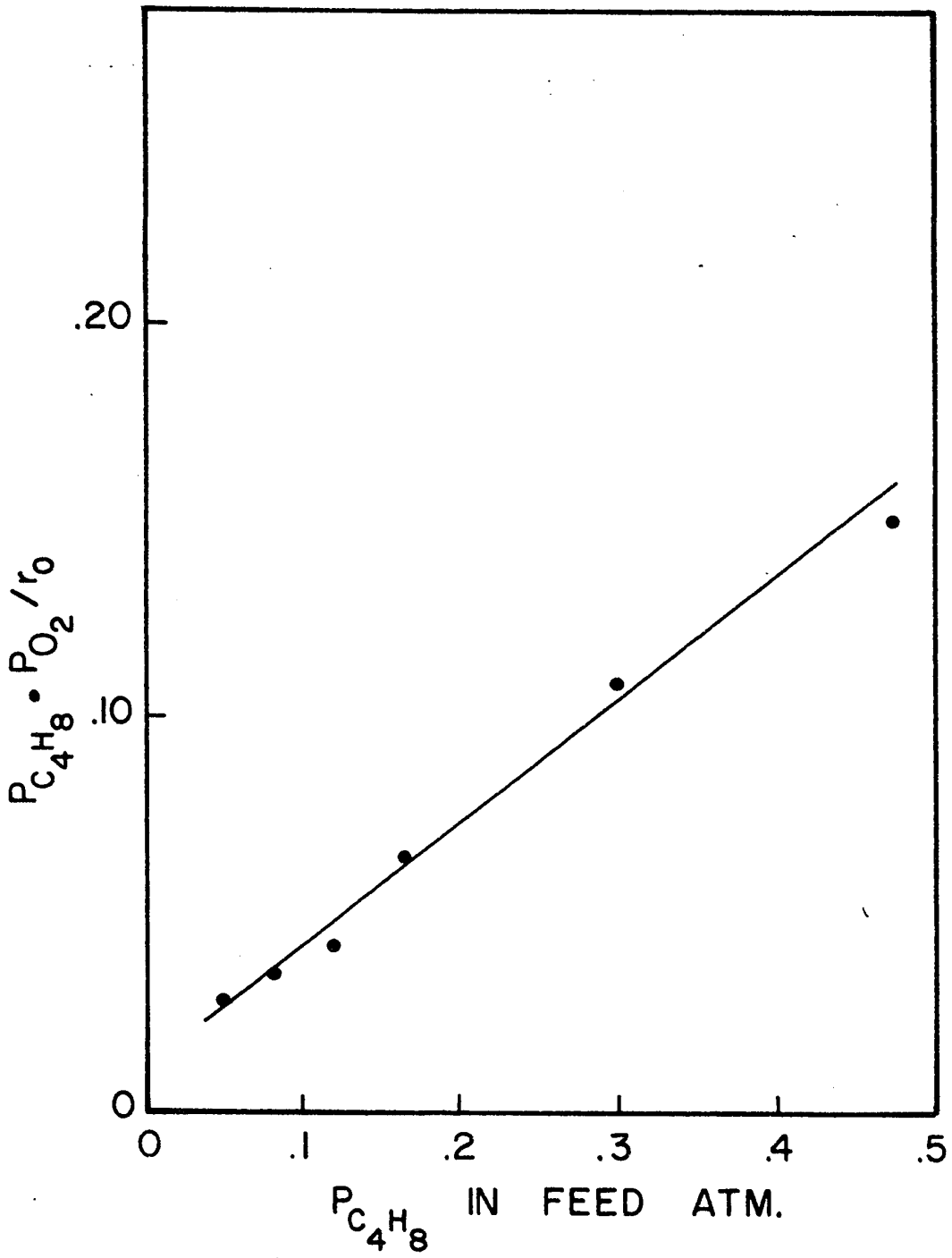

Fig. 15 $f(r_o)$ Versus $P_{C_4H_8}$ in Feed for Equation (58a)

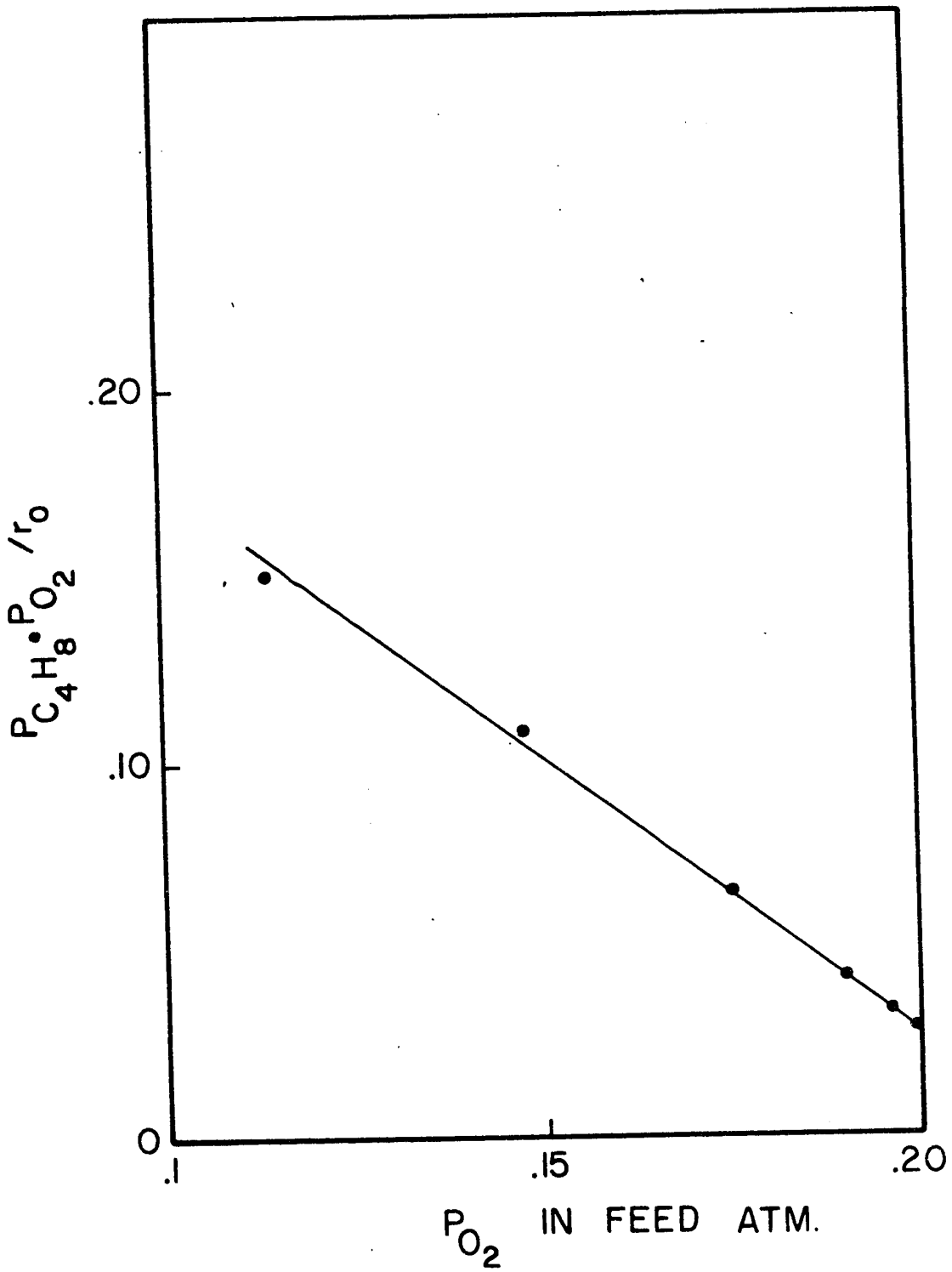

Fig. 16 $f(r_o)$ Versus P_{O_2} in Feed for Equation (59a)

$P_{C_4H_8}$ or P_{O_2} be a straight line. However mechanism 3 does not meet this requirement and is therefore rejected. This is shown in Figure 13. Similarly, mechanisms 2 and 4 are discarded since they do not meet the condition that $f(r_o)$ be a constant as required by equations (54a) and (56a) respectively.

H. Correlation of Conversion Data

By means of an isotope method, Vogue, Wagner and Stevenson (9) were able to establish that the carbon dioxide in the oxidation of propylene to acrolein came mainly from the complete oxidation of acrolein. Similarly, carbon dioxide from the oxidation of isobutylene to methacrolein could be considered as coming mainly from the complete oxidation of methacrolein. Experimental evidence seems to support this view. Selectivity was found to decrease with the conversion of isobutylene as required for consecutive reactions (see Figures 4, 5 and 6). Also, when methacrolein was oxidized with air in the gas phase at 400° C, large amounts of carbon dioxide and carbon monoxide were observed in the products. When this same reaction was carried out over a copper oxide catalyst the conversion was increased but this time the products contained mostly carbon dioxide and only traces of carbon monoxide. On the other hand, when isobutylene was oxidized with air in the gas phase at 400° C, no reaction products were observed. On the basis that the oxidation of isobutylene with air over a copper oxide catalyst is a consecutive reaction, a scheme has been developed to express all the components of the reaction in terms of the conversion of isobutylene. For the following consecutive reaction:

$$C_4H_8 + O_2 \rightleftharpoons C_4H_6O + H_2O \qquad (60)$$

$$C_4H_6O + 5O_2 \rightleftharpoons 4\,CO_2 + 3\,H_2O \qquad (61)$$

let X = moles of isobutylene reacting per hour by reaction (60)/ moles of isobutylene fed per hour

and Z = moles of methacrolein reacting per hour by reaction (61)/ moles of isobutylene fed per hour.

Since carbon dioxide comes solely from reaction (61), then

$$Z = 1/4\, X_{CO_2}$$

where X_{CO_2} = moles of carbon dioxide produced per hour/moles of isobutylene fed per hour.

Values of $X_{C_4H_8}$ and $1/4\, X_{CO_2}$ for different values of R at a temperature of 400° C from Table 5 were plotted as shown in Figure 17. A series of straight lines were obtained, each passing through the origin. The slope of these lines, which are given in Table 12, were plotted against the reactant ratio R in Figure 18 on logarithmic paper. From the curve of Figure 18, the following equation was derived:

$$Z = 0.555\, X\, R^{0.231} \qquad (62)$$

Having obtained a relationship between X and Z, it was possible to express the moles of each component as a function of X only. This is illustrated below.

Let $(N_{C_4H_8})_o$ = moles isobutylene in the feed

and $(N_{O_2})_o$ = moles of oxygen in the feed

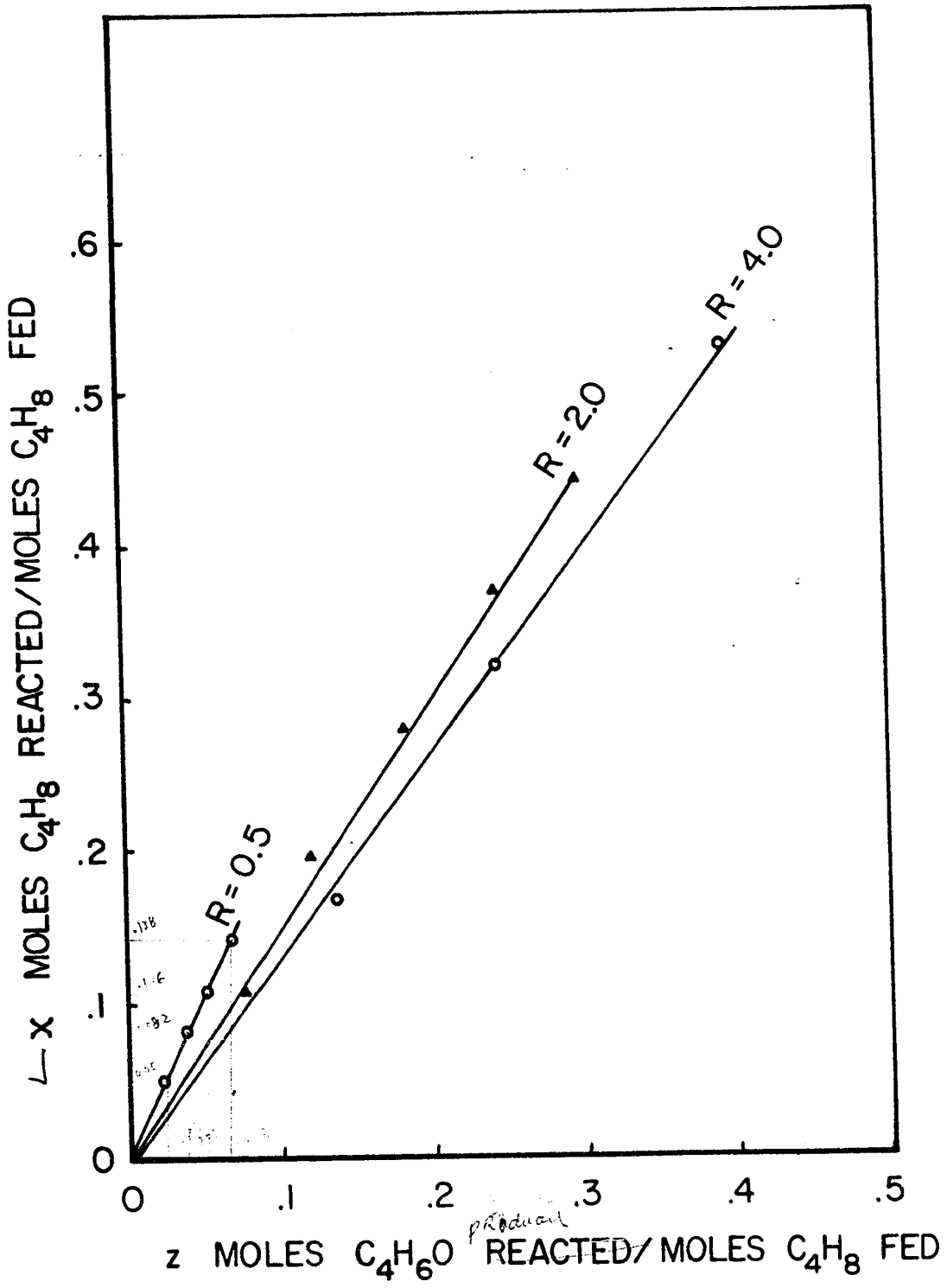

Fig. 17 Conversion of Isobutylene Versus Conversion to Methacrolein at 400° C

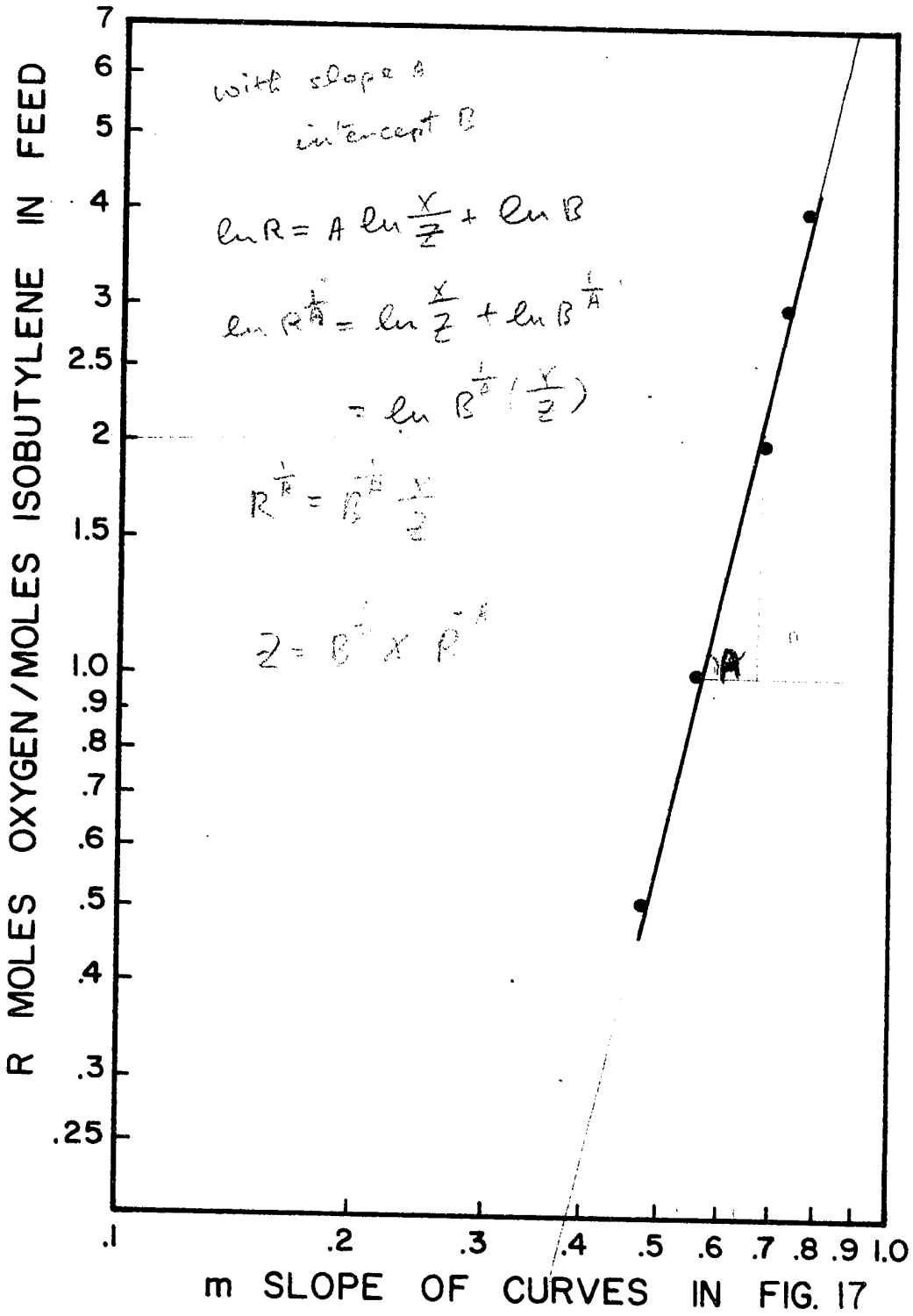

Fig. 18 Slope of Curves in Fig. 17 Versus Mole Ratio of Oxygen to Isobutylene at 400° C

Then, for any conversion, X

moles $C_4H_8 = (N_{C_4H_8})_o (1 - X)$

$C_4H_6O = (N_{C_4H_8})_o (X - Z) = (N_{C_4H_8})_o X (1 - 0.555 R^{0.231})$

$H_2O = (N_{C_4H_8})_o (X + 3Z) = (N_{C_4H_8})_o X (1 + 1.665 R^{0.231})$

$CO_2 = 4 (N_{C_4H_8})_o Z = 2.220 (N_{C_4H_8})_o X R^{0.231}$

$O_2 = (N_{O_2})_o - (N_{C_4H_8})_o (X + 5Z)$

$= (N_{O_2})_o - (N_{C_4H_8})_o X (1 + 2.775 R^{0.231})$

$N_2 = N_2$

Since the total moles did not vary by more than 5%, it was assumed constant and an arithmetic average used. If one lets

$(N_{C_4H_8})_o / (N_t)_{av.} = a$

$(N_{C_4H_8})_o (1 - 0.555 R^{0.231}) / (N_t)_{av.} = b$

$(N_{C_4H_8})_o (1 + 1.665 R^{0.231}) / (N_t)_{av.} = c$; $(N_{O_2})_o / (N_t)_{av.} = d$

and $(N_{C_4H_8})_o (1 + 2.775 R^{0.231}) / (N_t)_{av.} = e$

then the partial pressure of each component in the rate equation can be expressed in terms of conversion. Thus for any conversion X:

$$P_{C_4H_8} = a (1 - X)$$

$$P_{O_2} = d - eX$$

$$P_{C_4H_6O} = bX$$

$$P_{H_2O} = cX$$

These values of the partial pressures were substituted in the rate equations for those mechanisms that had not been eliminated and the equations put in the form

$$f(r) = f(\text{conversion})$$

Mechanism 1

$$\frac{a(1-X)}{r} = \frac{1+K_2 d}{a} - \left(\frac{K_2 e - K_3 b - K_4 c}{a}\right) X \qquad (53b)$$

Mechanism 5

$$\left[\frac{a(1-X)(d-eX)}{r}\right]^{1/2} = \frac{1+K_1 a+K_2 d}{\sqrt{aK_1K_2}} - \frac{(K_1 a+K_2 e-K_3 b-K_4 c)}{\sqrt{aK_1K_2}} X \qquad (57b)$$

Mechanism 6

$$\frac{a(1-X)(d-eX)}{r} = \frac{1+K_1 a}{aK_1} - \frac{(K_1 a - K_3 b}{aK_1} X \qquad (58b)$$

Mechanism 7

$$\frac{a(1-X)(d-eX)}{r} = \frac{1+K_2 d}{aK_2} - \frac{(K_2 e - K_3 b)}{aK_2} X \qquad (59b)$$

where $K_1 = K_{C_4H_8}$, $K_2 = K_{O_2}$, $K_3 = K_{C_4H_6O}$, $K_4 = K_{H_2O}$

The functions of rate f(r) for equations (53b) and (57b) were plotted against conversion and are shown in Figures 19 and 20 respectively. In Figure 21 are the curves for equations (58b) and (59b). The data for these graphs were taken from Table 10 in Appendix G. Since, on solving the simultaneous equations, a negative value was obtained for the adsorption equilibrium constant of oxygen (K_2), mechanism 5 was discarded.

The intercepts from Figures 19 and 21 were plotted against the partial pressure of one of the reactants in the feed and are shown in Figures 22, 23 and 24. Both the intercept and the slope of the resulting curves should be positive, otherwise some of the constants in the rate equation will have negative values and this would violate one of the postulates made in the derivation of the rate equations. Only equation (58b) was found to satisfy this condition. From the intercept and the slope of Figure 23, the following approximate values for the constants in equation (58) were obtained.

$$\alpha = 3.0 \qquad K_{C_4H_8} = 27 \qquad K_{C_4H_6O} = 27$$

From the foregoing analysis of the experimental data, it appears that mechanism 6 (surface reaction between adsorbed isobutylene and gaseous oxygen) would give a satisfactory explanation for the oxidation of isobutylene to methacrolein on a copper oxide catalyst. In order to correlate the laboratory data, the rate equation has to be integrated over the length of the catalyst bed. The conversion data calculated from this integrated rate equation is then compared with the experimental points. Subsequently, conclusions are drawn

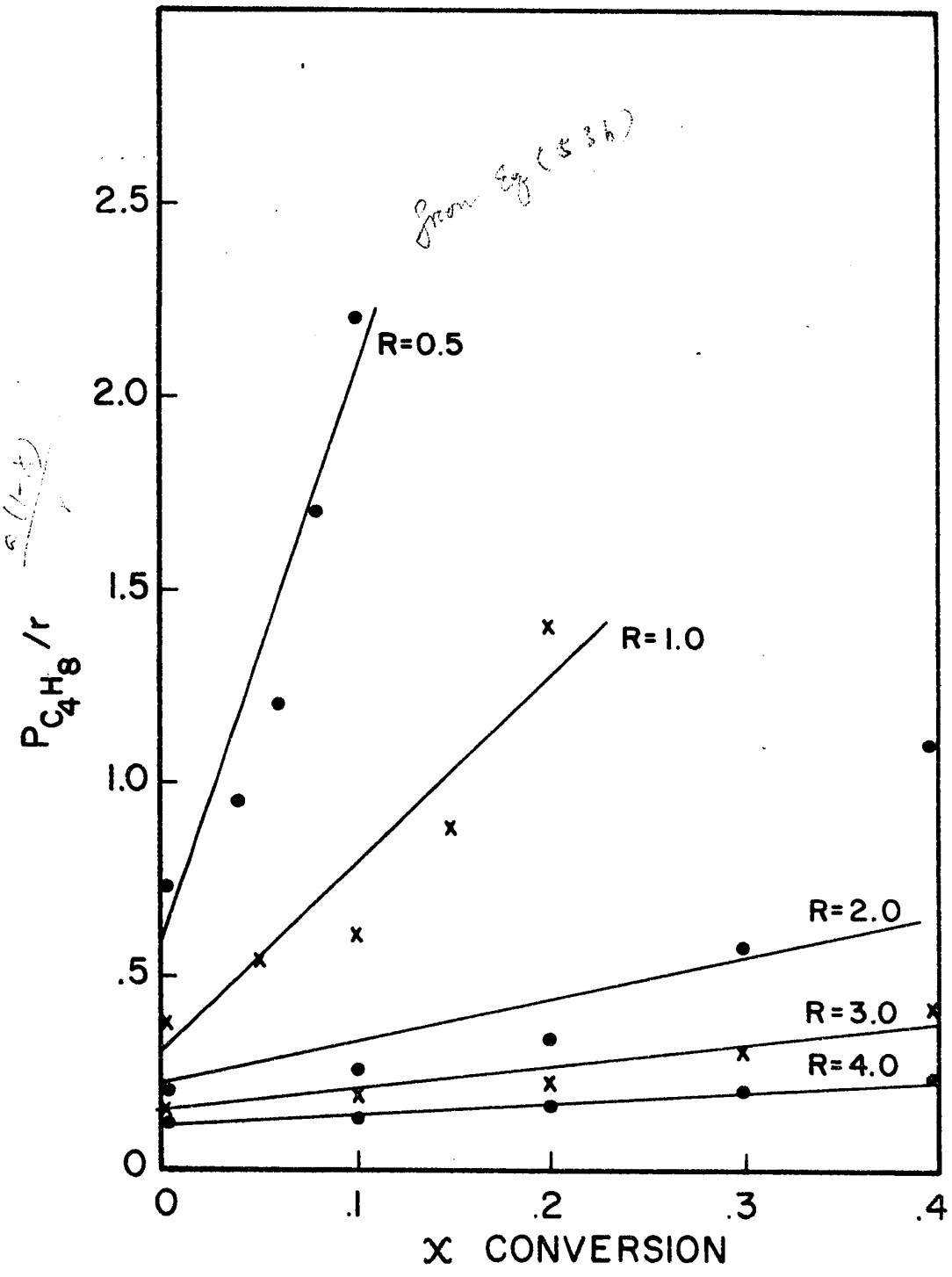

Fig. 19 f(r) Versus Conversion for Equation (53b)

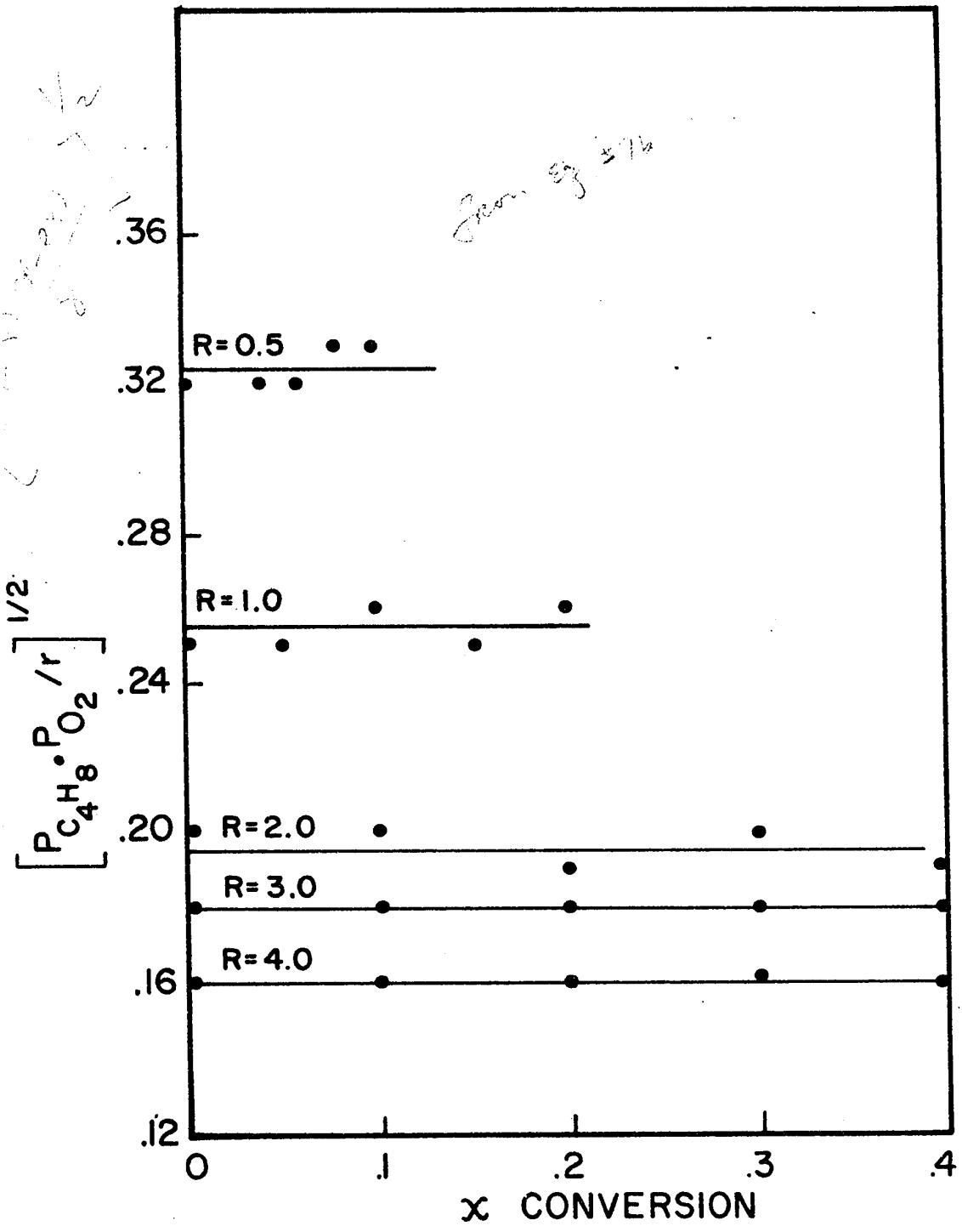

Fig. 20 . f(r) Versus Conversion for Equation (57b)

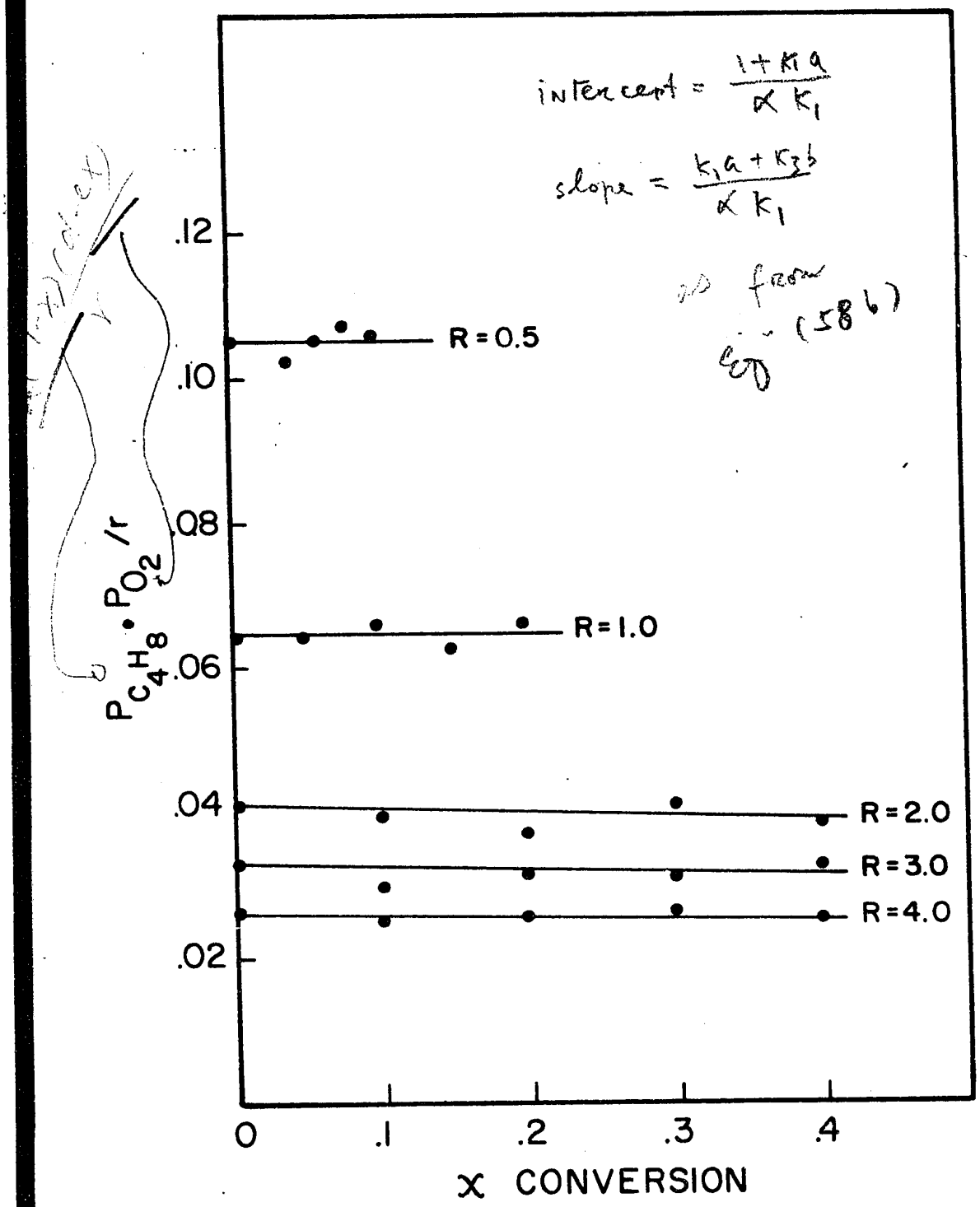

Fig. 21 . f(r) Versus Conversion for Equations (58b) and (59b)

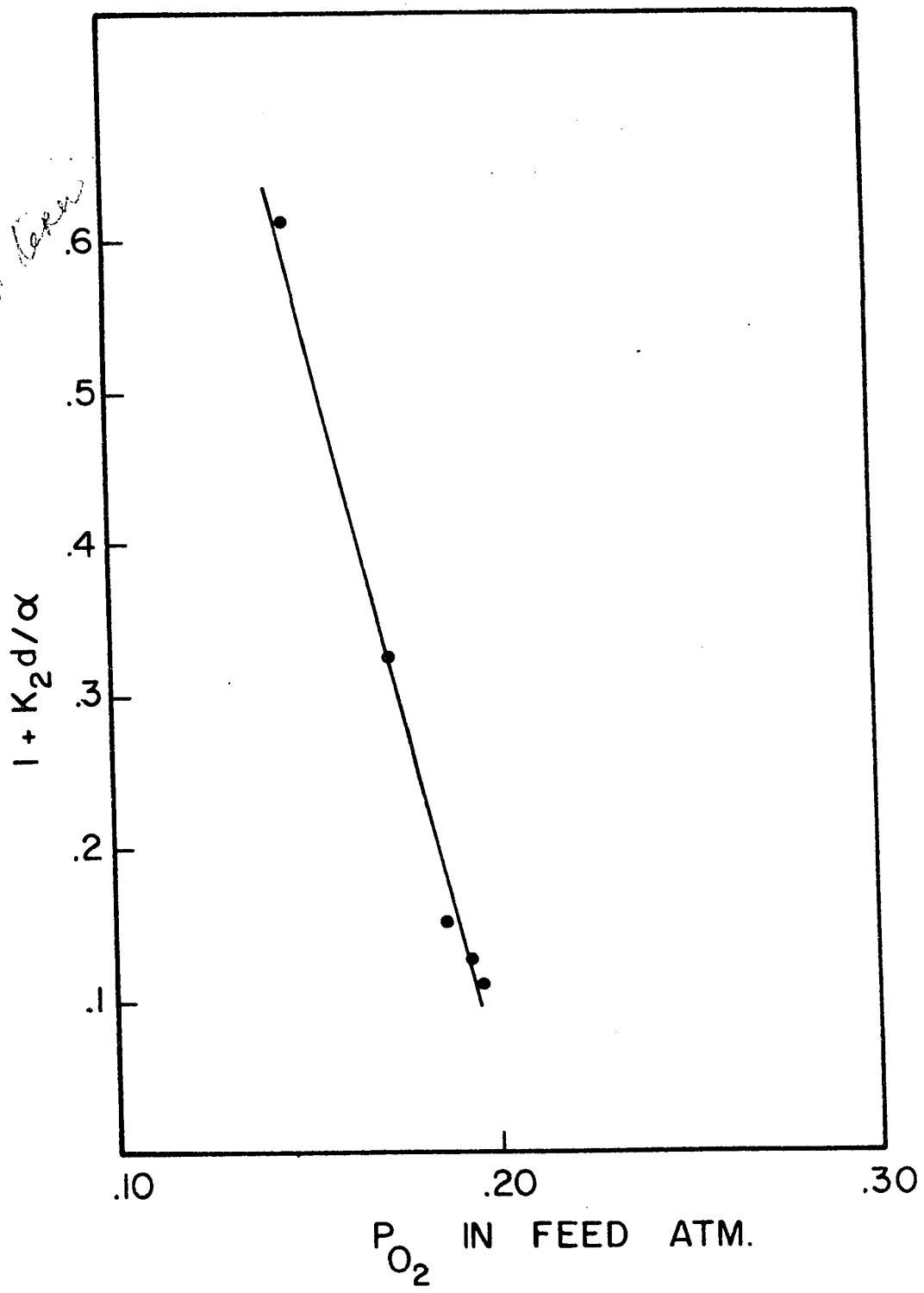

Fig. 22 Intercept of Fig. 19 Versus P_{O_2} in Feed

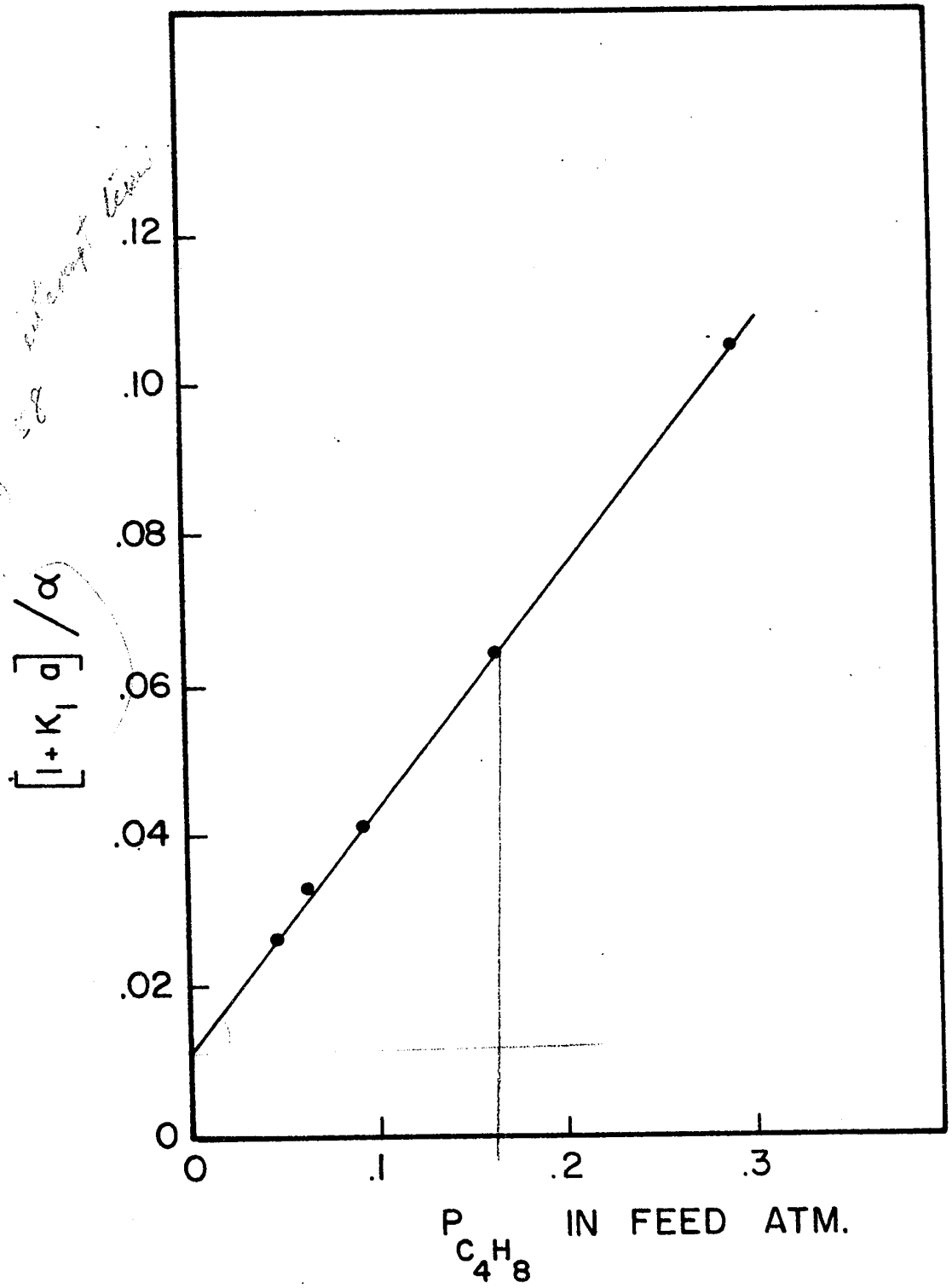

Fig. 23 Intercept of Fig. 21 Versus $P_{C_4H_8}$ in Feed

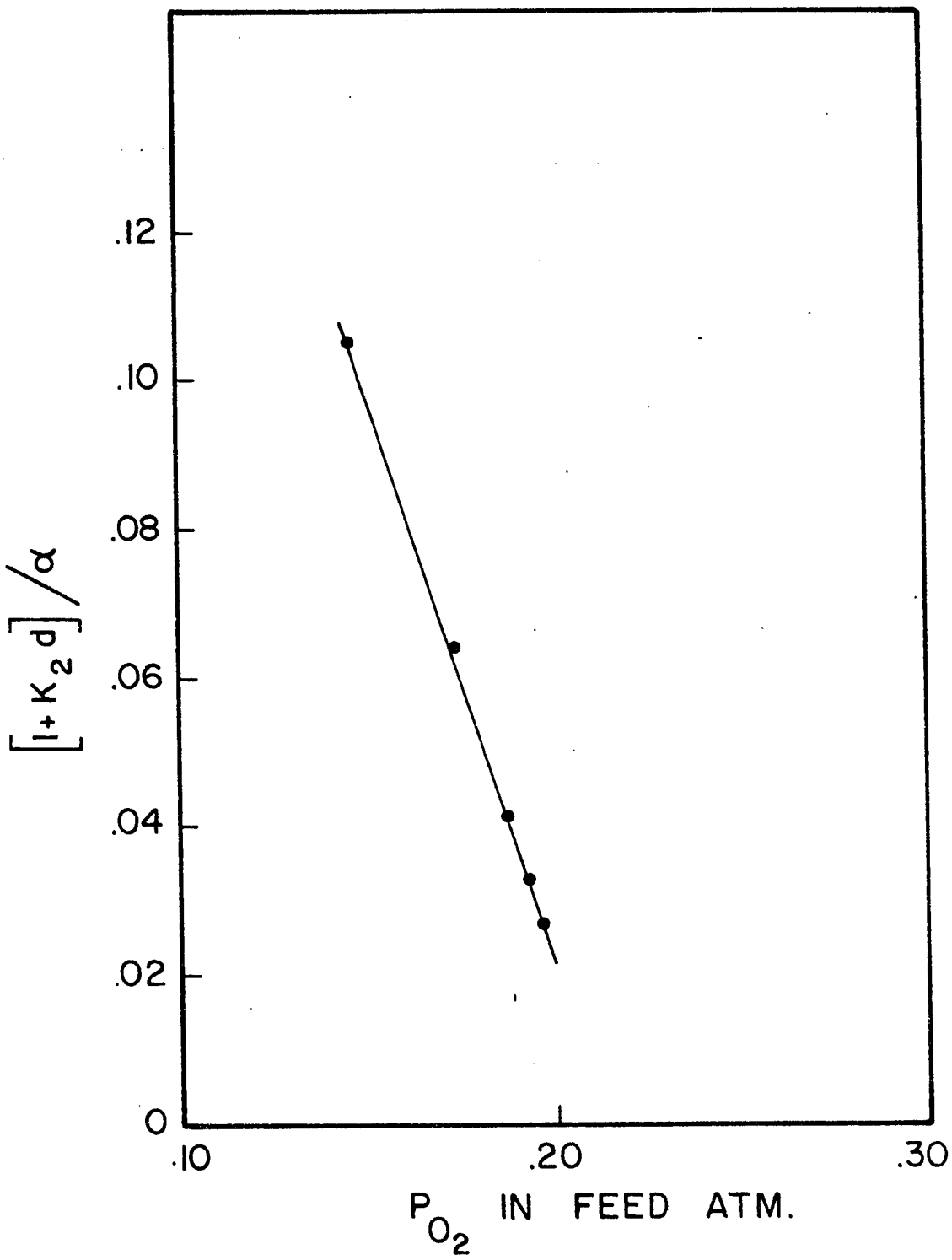

Fig. 24 Intercept of Fig. 21 Versus P_{O_2} in Feed

regarding the correctness of the assumed rate mechanism.

In a steady-state flow system, the relationship between space velocity or its reciprocal, the time factor W/F, and conversion is obtained by consideration of an elementary section of reactor containing a mass of catalyst dW in which a conversion dX is produced. Then a material balance gives

$$r\,dW = F\,dX \qquad (63)$$

where r = reaction rate, moles isobutylene reacted/(mass of catalyst) (hour)

W = mass of catalyst in reactor, gms

F = ~~moles/hour of isobutylene~~ Moles of iC$_4$ = fed to the reactor

X = moles isobutylene reacted/moles isobutylene fed

Integration yields

$$W/F = \int_0^x \frac{dX}{r} \qquad (64)$$

When integrating equation (63), one must make the assumption that the gases are passing through the catalyst bed under conditions of plug flow i. e. that the velocity profile across the width of the reactor is flat. This can be verified in large reactors by inserting pitot tubes inside the reactor and then establishing the velocity profile. However, in small reactors such as the one used in this kinetic study (1/2 inches in diameter), the use of pitot tubes was not considered very practicable, hence the velocity profile was not determined. However, a porous stainless steel plate was inserted at the entrance of the reactor so as to brake the velocity pattern of the incoming gases and create conditions approaching plug flow in

the catalyst bed. It appears that no appreciable errors were produced due to this assumption as the composition of the products did not change very much with velocity (see Figure 7). If the assumption of plug flow had not been justified, large variations in product composition would have been observed since the velocity profile is a function of velocity.

Equation (64) can be integrated easily by expressing r as a function of X. Since the partial pressures were expressed in terms of conversion, these values can be substituted into equation (58) to give

$$r = \frac{K_1 \alpha a(1 - X)(d - eX)}{1 + K_1 a (1 - X) + K_3 bX} \tag{65}$$

$$\text{and } 1/r = \frac{1}{\alpha K_1 a (1 - X)(d - eX)} + \frac{1}{\alpha (d - eX} + \frac{K_3 b X}{\alpha K_1 a (1 - X)(d - eX)} \tag{66}$$

Substituting equation (66) into equation (64)

$$W/F = \frac{1}{\alpha K_1 a} \int_o^x \frac{dX}{(1 - X)(d - eX)} + \frac{1}{\alpha} \int_o^x \frac{dX}{(d - eX)} + \frac{K_3 b}{\alpha K_1 a} \int_o^x \frac{X\, dX}{(1 - X)(d - eX)} \tag{67}$$

Integrating between the limits o and X yields

$$W/F = \frac{1}{\alpha K_1 a (e-d)} \left[- \ln \left(\frac{1 - eX/d}{1 - X} \right) \right] + \frac{1}{\alpha} \left[- \frac{1}{e} \ln (1 - eX/d) \right] + \frac{K_3 b}{\alpha K_1 a (e-d)} \left[\ln (1 - X) - \frac{d}{e} \ln (1 - eX/d) \right] \tag{68}$$

The values of a, b, e, d, α, K_1 and K_3 were substituted into equation (68) and the value of the integral plotted against conversion for different reactant ratios. These curves were then compared with the experimental data and the values of α, K_1 and K_3 adjusted by trial and error so as to give the best fit to the experimental points. The results as calculated from equation (68) are compared with the experimental points at a temperature of 400° C for reactant ratios of 0.25, 0.50, 1.0, 2.0, 3.0 and 4.0 in Figures 25, 26, 27, 28, 29 and 30 respectively. The solid lines indicate the curves as predicted from equation (68). The experimental points are given in Table 5 and the values for the calculated solid line in Table 10. The calculated values of $1/4\ X_{CO_2}$ from Table 10 were obtained from equation (62) and those of $X_{C_4H_6O}$ were obtained by difference ($X_{C_4H_6O} = X_{C_4H_8} - 1/4\ X_{CO_2}$).

The temperature dependent constants, α, K_1, and K_3 were similarly evaluated at temperatures of 350°, 425°, and 450° C. The values of these constants are given in Table 14. The conversion curves calculated from equation (68) for a reactant ratio of 4.0 are compared with the experimental data at temperatures of 350°, 375°, 425°, and 450° C in Figures 31, 32, 33 and 34 respectively. As before, the calculated cuves are represented by solid lines.

Since the constants α, $K_{C_4H_8}$ and $K_{C_4H_6O}$ obey Arrhenius behavior, they were correlated by a plot of their logarithms against

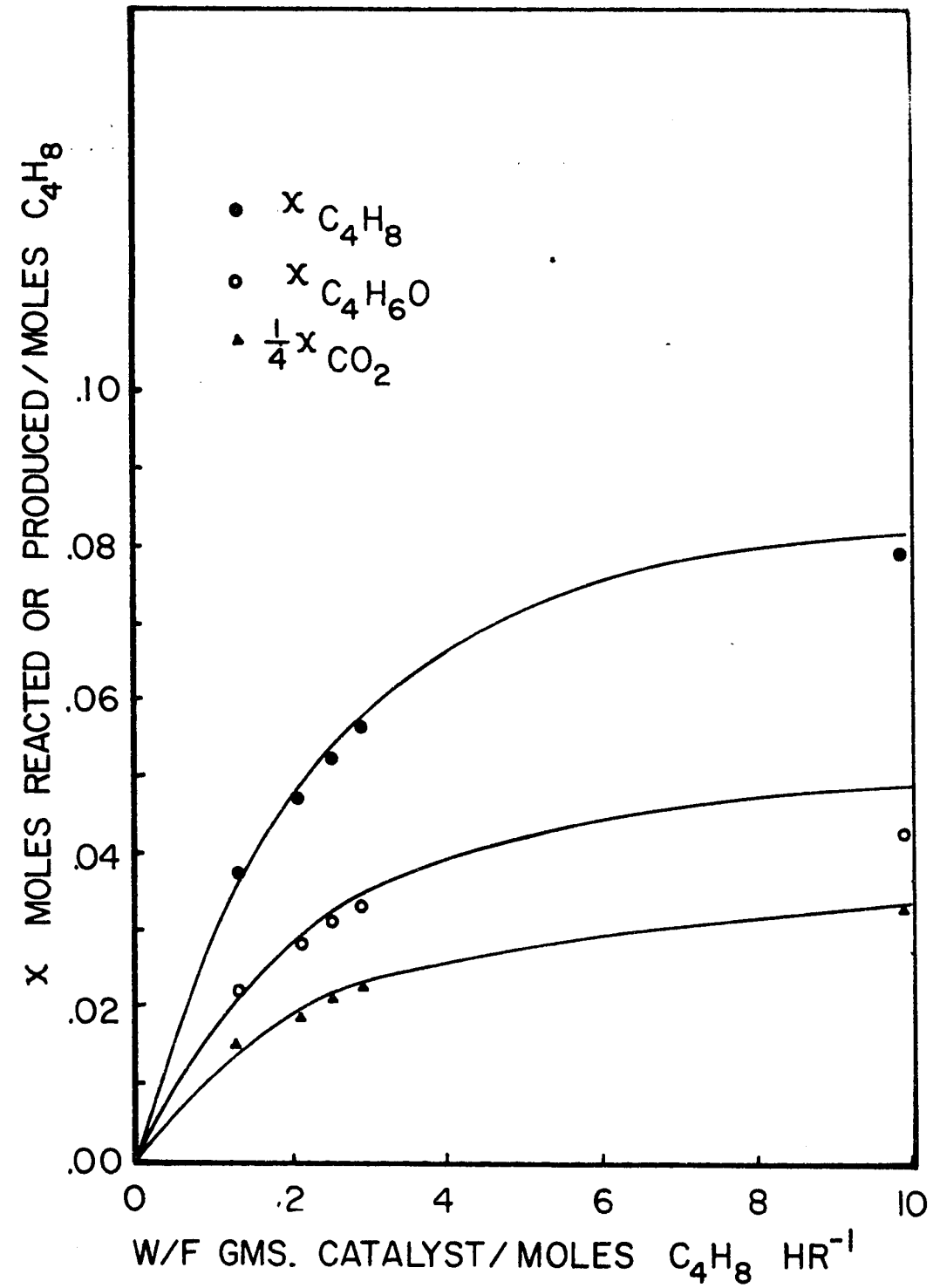

Fig. 2b - Conversion Curve at 400° C. to R = .2

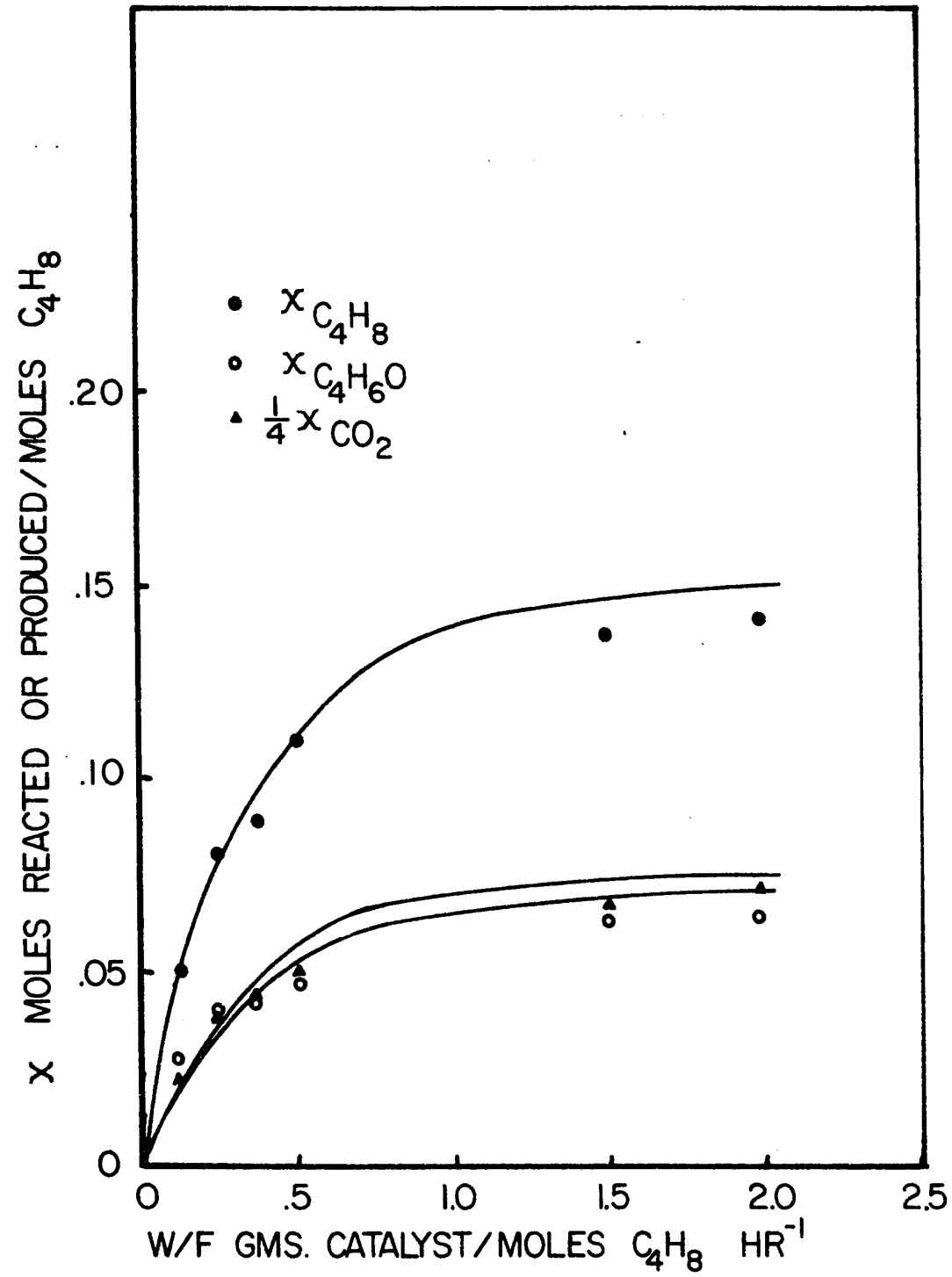

Fig. 26 Conversion Curves at 400° C for R = 0.5

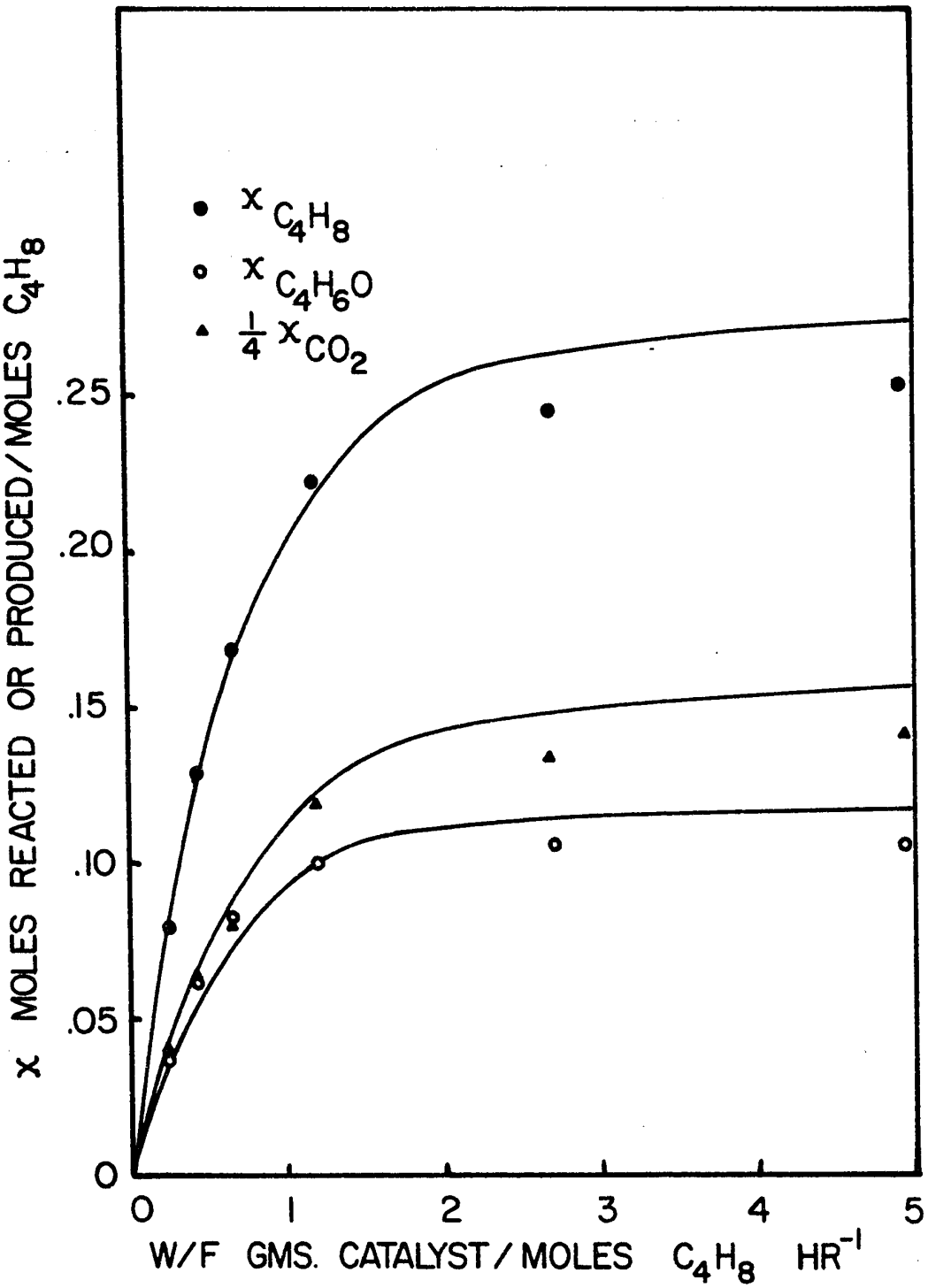

Fig. 27 Conversion Curves at 400° C for R = 1.0

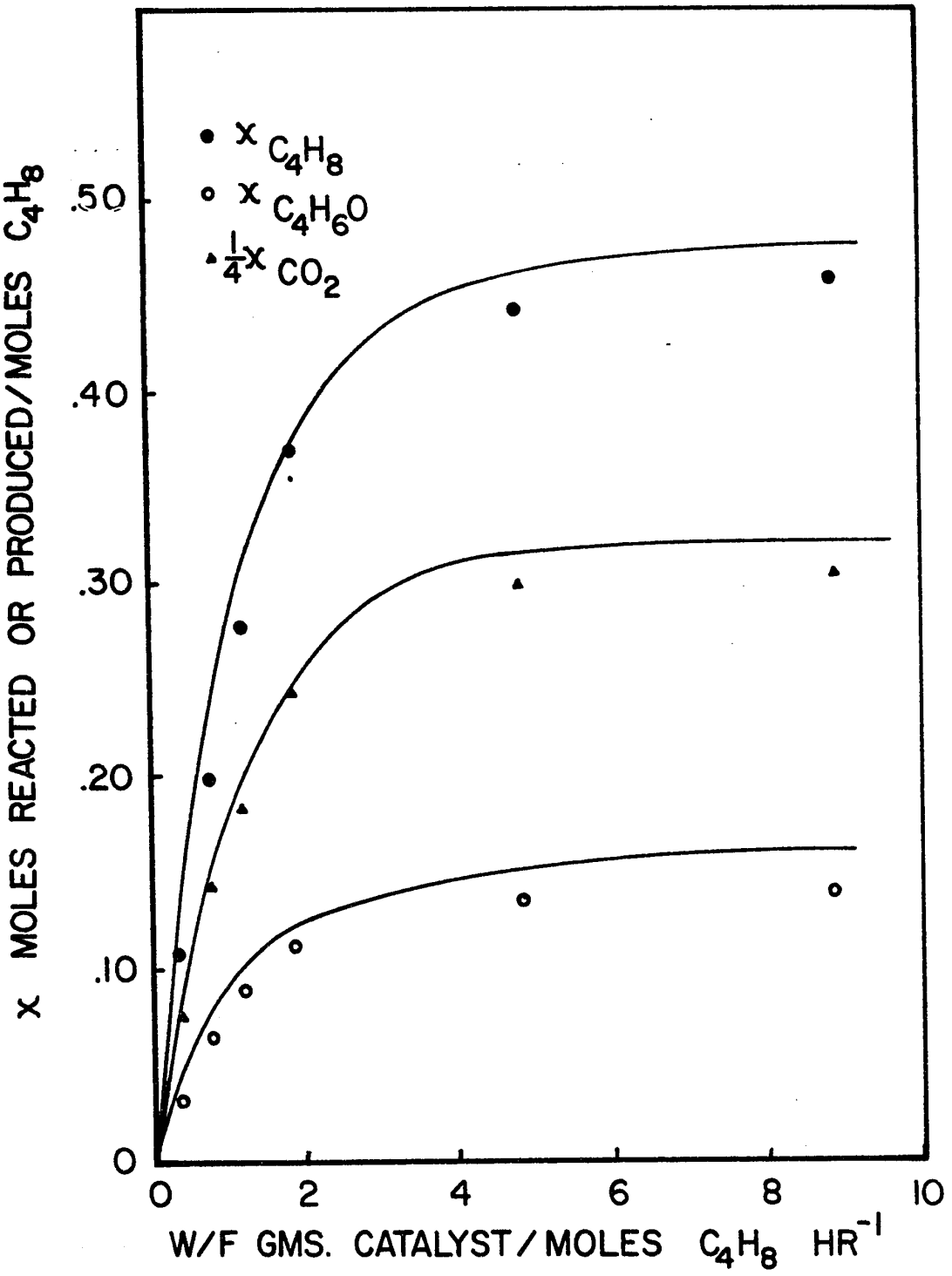

Fig. 28 Conversion Curves at 400° C for R = 2.0

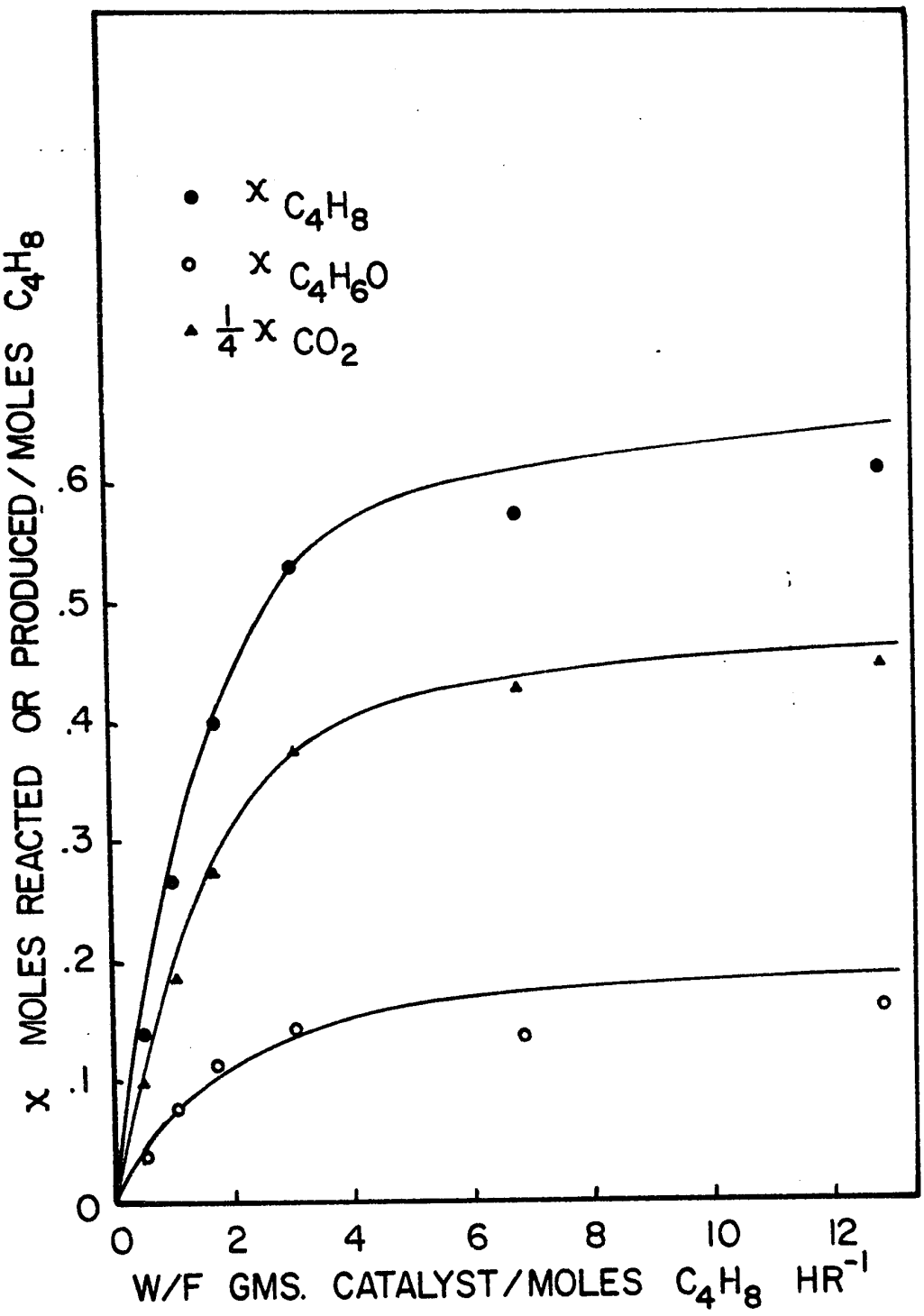

Fig. 29 - Conversion Curves at 400° C for R =

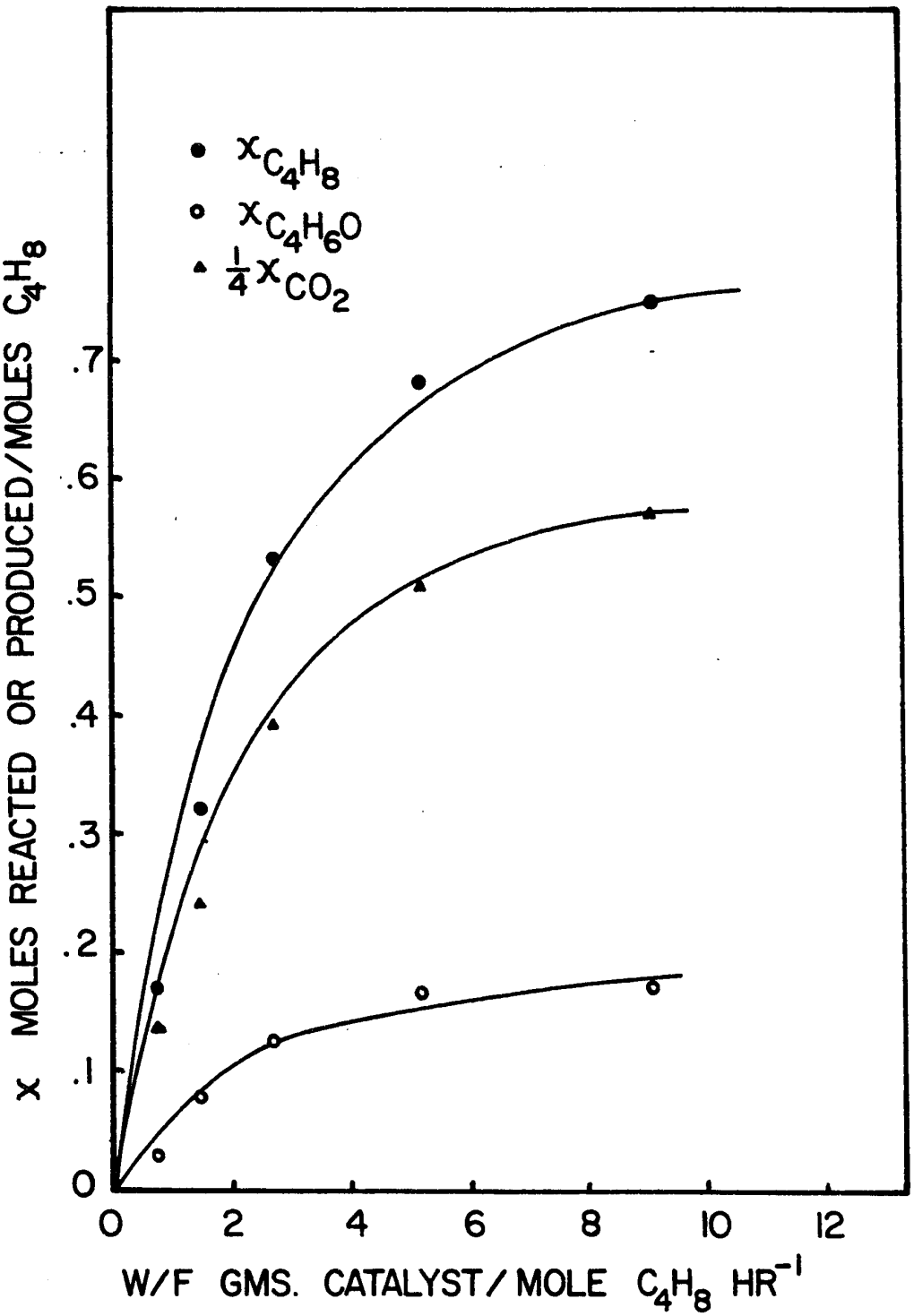

Fig. 30. Conversion Curves at 400° C for R - 4.0

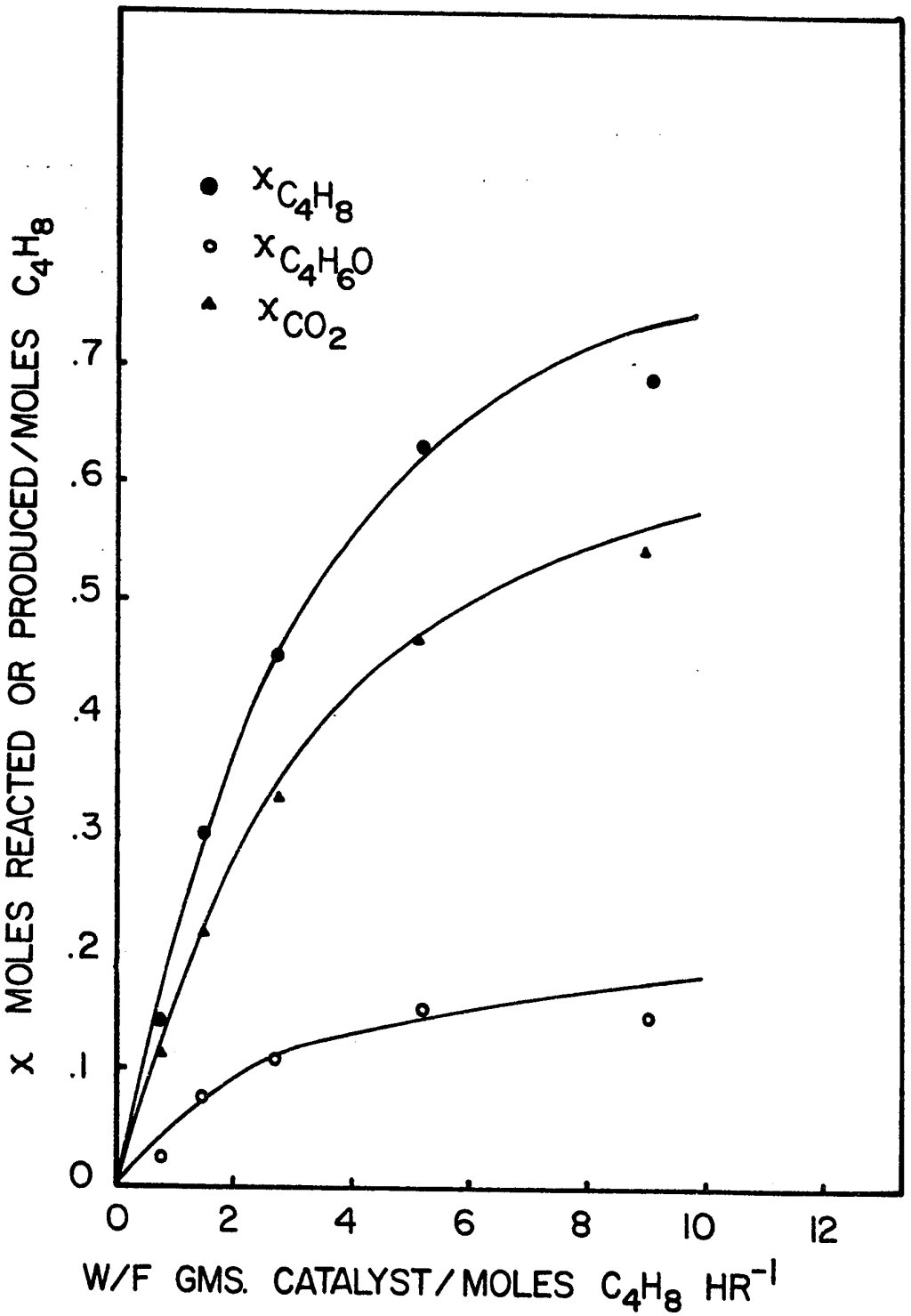

Fig. 31 - Conversion Curves at 350° C for R = 4.0

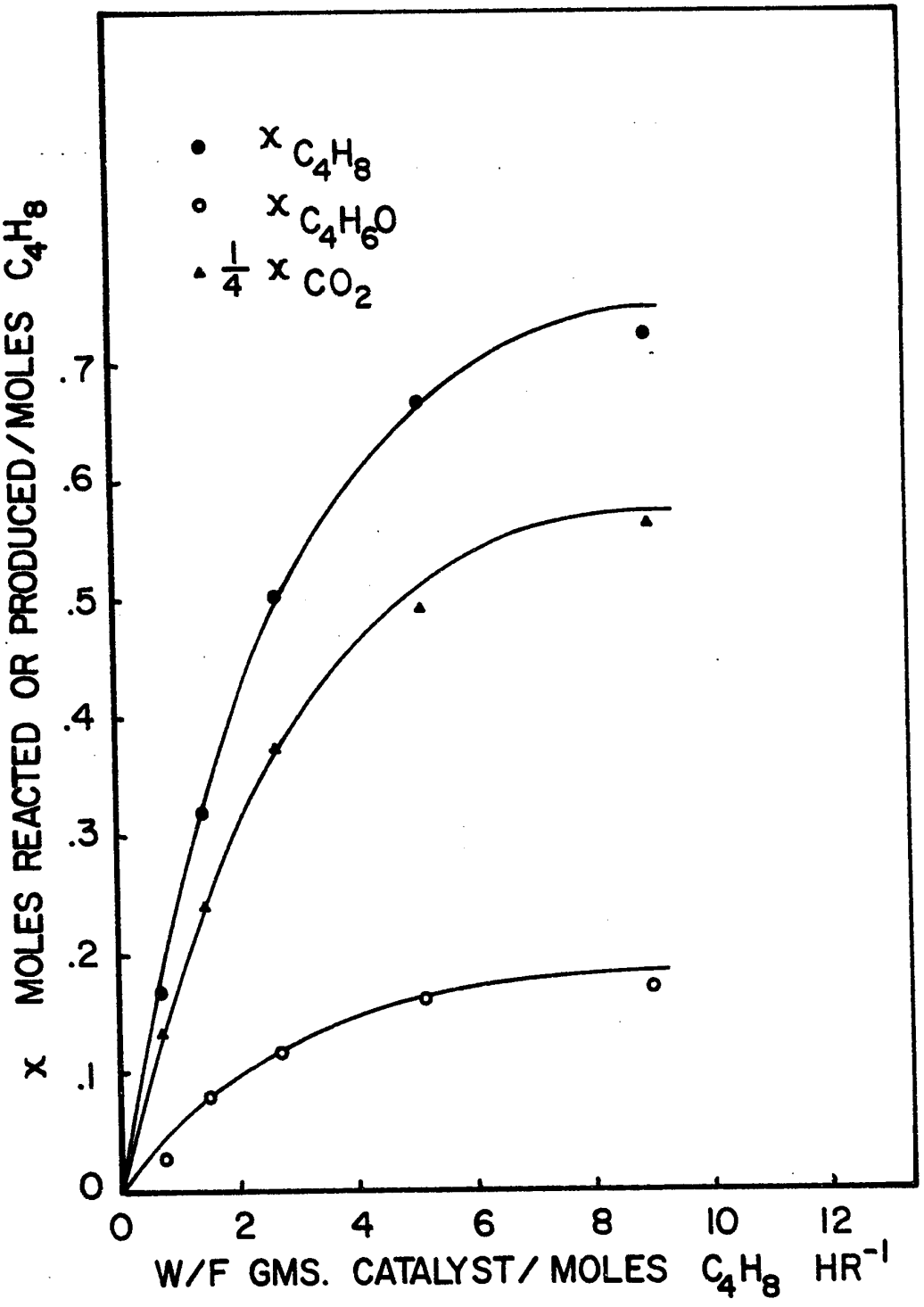

Fig. 32 . Conversion Curves at 375° C for R = 4.0

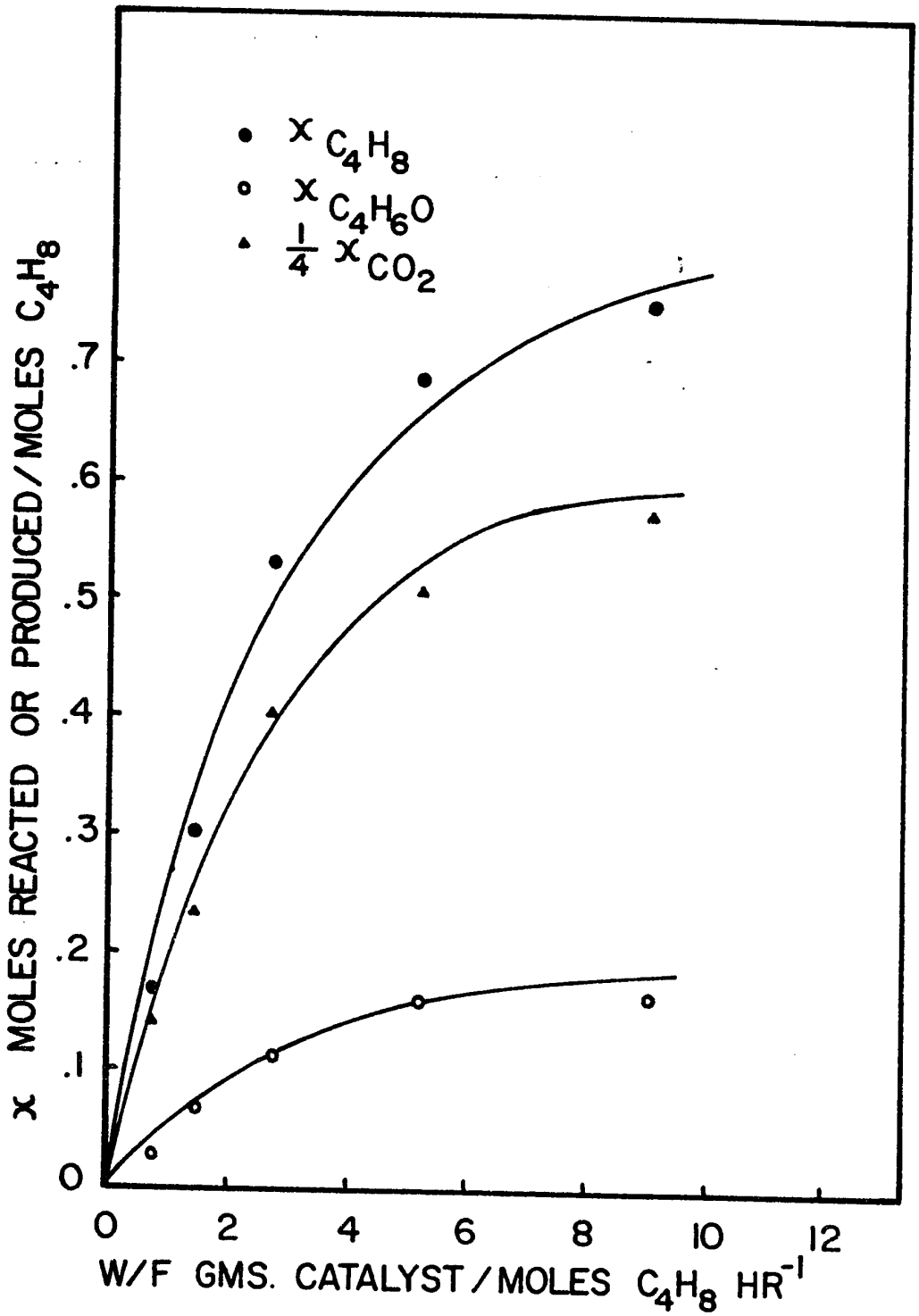

Fig. 33 Conversion Curves at 425 C for R = 4.0

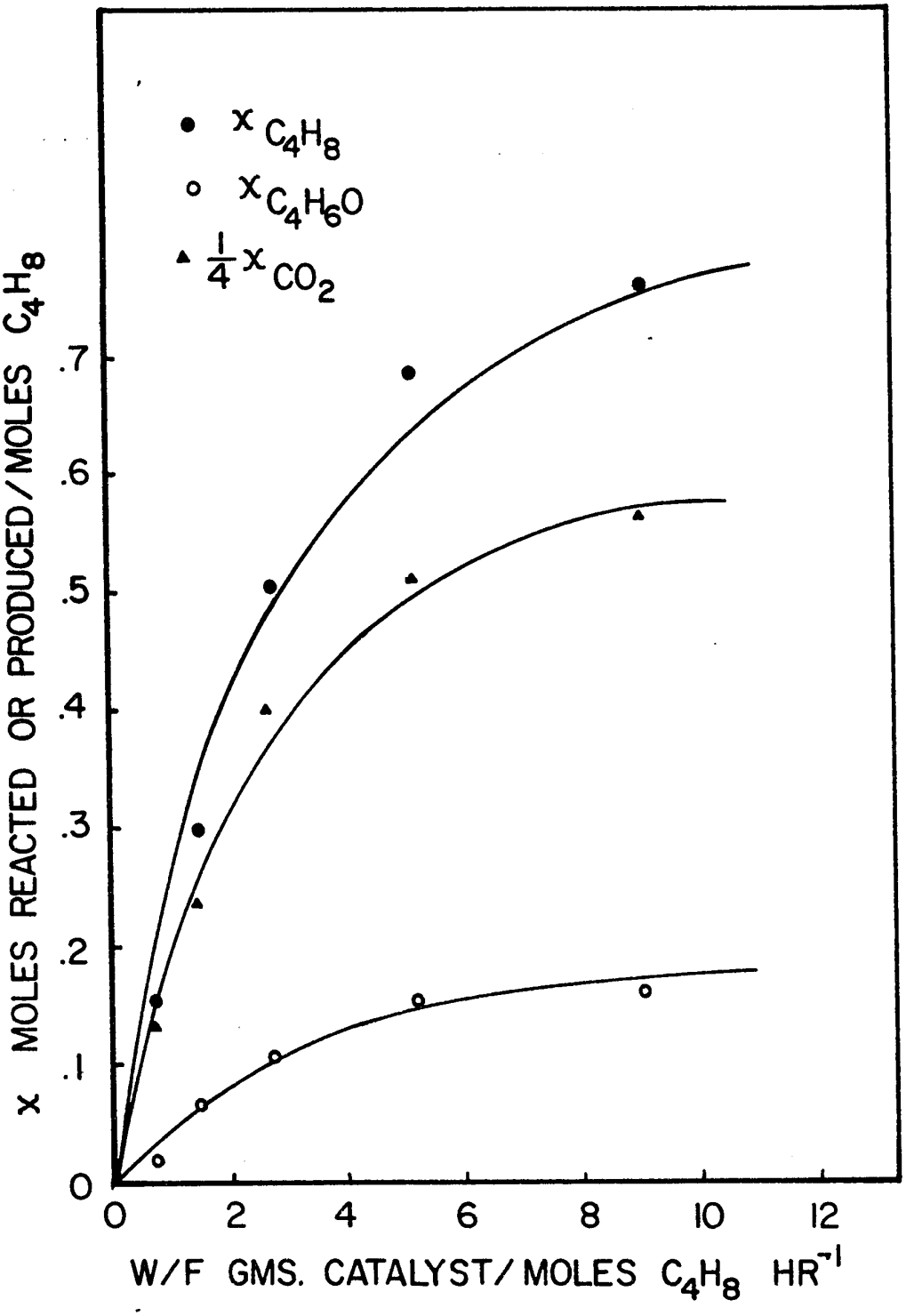

Fig. 34 - Conversion Curves at 450° C for R = 4.0

reciprocal temperatures. Figure 35 shows the isothermal values for α, $K_{C_4H_8}$ and $K_{C_4H_6O}$, along with the best line for each constant. From these lines, the following analytical expressions describing the temperature dependence of α, $K_{C_4H_8}$ and $K_{C_4H_6O}$ were obtained:

$$\ln \alpha = \frac{12,100}{RT} + \frac{20.1}{R} \qquad (69)$$

$$\ln K_{C_4H_8} = \frac{22,800}{RT} - \frac{26.8}{R} \qquad (70)$$

$$\ln K_{C_4H_6O} = \frac{22,800}{RT} - \frac{26.8}{R} \qquad (71)$$

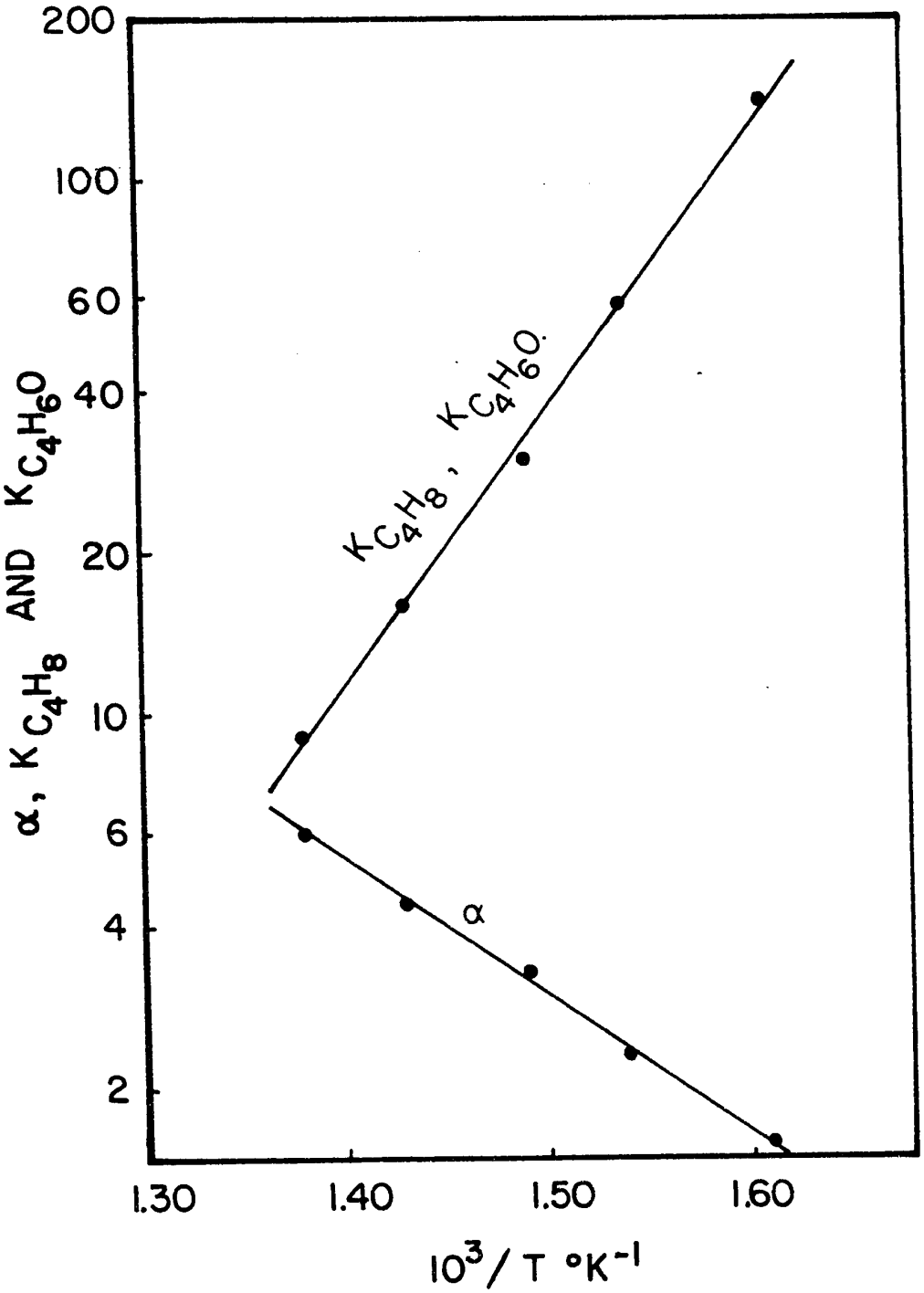

Fig. Temperature dependence of $K_{C_4H_8}$ and $K_{C_4H_6O}$

VII. DISCUSSION OF THE FINAL CORRELATION

A. The Isobutylene Adsorption Constant $K_{C_4H_8}$

The adsorption equilibrium constant of isobutylene follows Arrhenius behavior closely, as may be seen from Figure 35. The fact that the magnitude of the constant decreases with increasing temperature indicates that the copper oxide adsorbs isobutylene exothermally. Equation (70) shows that the enthalpy of chemisorption is -22,800 cal/mole. This could indicate that molecularly adsorbed isobutylene is attached to the catalyst surface by a rather strong bond, or alternately, that only strong adsorbing active sites participate to any great extent in the oxidation reaction.

The entropy of adsorption from equation (70) is -26.8 e.u. The entropy of adsorption shows a negative value in agreement with the theory that upon adsorption the isobutylene molecule loses translational and rotational degrees of freedom.

B. The Methacrolein Adsorption Constant $K_{C_4H_6O}$

The adsorption equilibrium constant of methacrolein was assumed to be the same as for isobutylene. The reason for this being that a change in $K_{C_4H_6O}$ had little effect on the correlation and therefore the numerical value of this constant could not be determined accurately. Although it could not be estimated precisely, the best fit to the data was obtained when the value of $K_{C_4H_6O}$ was of the same order of magnitude as $K_{C_4H_8}$. The slight influence of the adsorption equilibrium

constant $K_{C_4H_6O}$ on the correlation can be attributed to the fact that the concentration of methacrolein in the products was small in comparison with isobutylene.

The slope of the line in Figure 35 is positive, indicating a negative standard enthalpy of adsorption. This is in agreement with the general theory that adsorption is an exothermic process, unless dissociation occurs in which case the enthalpy may increase if heat of dissociation is included.

C. The Rate Constant a

The rate constant a follows Arrhenius behavior closely, as may be seen from Figure 35, and increases with temperature as required by theory. Equation (69) states that the enthalpy of formation for the activated complex is 12,100 cal./gm. mole. The entropy of activation however, is not easy to determine. We see from equation (69) that

$$a = k\,s\,L = e^{20.1/R - 12,100/RT} \qquad (72)$$

where k is the true specific reaction rate velocity constant for the surface reaction, and is given by equation (49) which states that

$$k = \left[\frac{kT}{h}\, e^{\frac{\Delta S^{\neq}}{R}}\right]\left[e^{-\frac{\Delta H^{\neq}}{RT}}\right]$$

Although s can be determined from the crystalline structure of the solid, L, the concentration of active sites per unit mass of catalyst, is unknown. Therefore, the value of $\Delta S^{\neq}$ cannot be determined.

D. The Rate Equation

The rate equation which successfully correlated the experimental

data is:

$$r = \frac{\alpha K_1 P_{C_4H_8} P_{O_2}}{1 + K_1 P_{C_4H_8} + K_3 P_{C_4H_6O}} \qquad (58)$$

The fact that equation (58) could be used to correlate the data within the limits of experimental error, is the main justification for the acceptance of the above reaction model. This equation gave a very good fit to the experimental points except in the region of high values of W/F where deviations of up to 14% were observed. This might be justified on the basis that the percentage error in the analysis of the products was approximately 2%, the change in catalyst activity accounted for about 3%, and the use of equation (62) to express the partial pressures in terms of conversions contributed another 5%.

Also, this equation was in agreement with theoretical arguments. A Langmuir isotherm for isobutylene adsorption was used. Due to the random distribution of active and inactive sites, the adsorbed isobutylene molecules are much farther apart than they would be if all the surface sites were active. This reduces the interaction among the adsorbed molecules and therefore the Langmuir isotherm for activated adsorption is more likely to hold. In pure adsorption studies, it was found that a semi-empirical isotherm would correlate the data better. This is possibly due to the fact that in pure adsorption studies, repulsion forces exist among identical molecules so that the heat of adsorption decreases with surface coverage. But in an actual kinetic study, more than one specie is involved. This may result in some attraction forces among the different species randomly distributed on the surface. The attraction and repulsion

may therefore compensate with each other so that the Langmuir isotherm holds. In most kinetic studies, Langmuir behavior is almost invariably assumed or implied.

Surface reaction was observed to be the rate controlling step in the oxidation of isobutylene to methacrolein over a pumice supported copper oxide catalyst. A surface reaction between adsorbed isobutylene and gaseous oxygen to yield adsorbed methacrolein and water in the gas phase was the postulated mechanism associated with this rate controlling step. A fraction of the adsorbed methacrolein would react with more oxygen from the gas phase to decompose into carbon dioxide and water. The other fraction would be desorbed from the surface to account for the methacrolein in the products. Of all the postulated mechanisms, this was the only one that fitted the experimental data satisfactorily. However, one must be aware of the fact that a large number of other mechanisms could be postulated and that some of them might even give a better fit to the experimental points.

Since the adsorption equilibrium constant for isobutylene is so large, this rate equation could also be made to explain the reaction between strongly adsorbed isobutylene molecules and weakly adsorbed oxygen molecules. If the value of the adsorption equilibrium constant for oxygen K_{O_2} was very small, it could be neglected in comparison with the other terms and therefore would not appear in the rate equation.

VIII. CONCLUSIONS AND RECOMMENDATIONS

The air oxidation of isobutylene was investigated over supported and unsupported copper oxide catalyst between 350° -450° C, for a W/F ratio of 0.12 to 16.8 and an oxygen/isobutylene ratio of 0.25 to 4.0 to establish the conditions for maximum conversions and yields, derive a rate equation and propose a possible reaction mechanism. It has been found that the oxidation of isobutylene was entirely due to the catalytic effect of copper oxide in the temperature range studied. It has also been possible to establish that methacrolein and carbon dioxide are produced through a consecutive reaction rather than a simultaneous reaction.

It was found that with an increase in the process variables of temperature, reactant ratio, copper concentration and reciprocal of space velocity, the conversion of isobutylene would increase and the yield of methacrolein decrease. As required for consecutive reactions, the selectivity of the reaction towards the formation of methacrolein decreased with increasing isobutylene conversion. Of all the catalyst tested, a pumice supported copper oxide catalyst was found to be the most suitable for kinetic studies.

A Hougen-Watson type approach based on Langmuir isotherm was used to derive the rate equation which could correlate the experimental conversion data. Surface reaction was found to be the rate-controlling step. The reaction on the surface of the catalyst could be visualized as taking place either between adsorbed isobutylene and oxygen in the gas phase or between strongly adsorbed isobutylene

and weakly adsorbed oxygen. A portion of the methacrolein, adsorbed on the surface, reacted further with oxygen to form carbon dioxide and water. The rest of the methacrolein molecules was desorbed from the surface to account for the methacrolein in the products.

The constants α, $K_{C_4H_8}$ and $K_{C_4H_6O}$ all have reasonable magnitudes and are temperature dependent. The enthalpies of adsorption, determined kinetically for isobutylene and methacrolein were of the same magnitude as the values which would be expected from independent adsorption studies. This indicated that only sites on which the adsorption is strongest were active for the partial oxidation of isobutylene to methacrolein. Also, the rate constant α followedArrhenius behavior and increased with increasing temperature as required by theory.

The experimental methods and procedures used in this kinetic study enabled the reaction to be run under conditions closely approximating the hypothetical isothermal, integral reactor. The use of chromatographic techniques as an analytical tool made feasible an accurate analysis of the reaction products. Appreciable heat and mass transfer resistances exterior to the catalyst particles, which could greatly complicate the correct interpretation of kinetic data, were made very small by maintaining a large gas velocity through the reactor, and by using very small catalyst particles. The catalyst granules, 20-40 mesh in size, had an effectiveness factor approaching unity.

It is recommended that the partial oxidation of other light olefins over a copper oxide supported on pumice catalyst be studied. In this way, the validity of the proposed kinetic model could easily be tested further and the effect of the molecular structure on the rate of catalytic oxidation established. If the proposed model is correct, the values of the adsorption equilibrium constants should be of the same magnitude and show a similar temperature dependence. Finally, the reactor design could be improved so as to approach more closely isothermal conditions.

IX NOMENCLATURE

A	component A
A	frequency factor
A_2	diatomic gas molecule
As	a state in which A is adsorbed on an active site
As_2	a state in which A is adsorbed on an active site and ready to jump to an adjacent one
A_2s_2	a diatomic molecule ready to be dissociatively adsorbed on two adjacent sites
As'	an atom of dissociated molecule A_2 after final jump to site s'
a	activity
a	$(N_{C_4H_8})_o/(N_t)$ av.
a_m	external particle surface area per unit mass
a_v	external particle surface area per unit volume
a, b, ..., r, s	coefficient of components A, B, ..., R, S respectively, in a reaction equation
B	component B
B	constant in Arrhenius Equation corresponding to - E/R
b	constant for Langmuir isotherm
b	$a\,(1 - 0.555\,R^{0.231})$
C_p	specific heat of gas
c	molal concentration (of adsorbed molecules or of active sites) per unit mass of catalyst
c	average radius of pores in a catalyst particle

D_{A_m}	average diffusivity of component A
D_p	diameter of particle
D_p'	effective particle diameter for Thiele modulus
D_v	diffusion coefficient
d	$(N_{O_2})_o/(N_t)$ av.
E	activation energy
E_A	effectiveness factor of catalyst particles
e	base of natural logarithm
e	a $(1+2.775\ R^{0.231})$
F	feed rate, moles C_4H_8 fed per hour
f	function proposed
f	total partition function
$f_{l.v.}$	partition function for the loose vibrational degree of freedom
$f^{\neq}$	total partition for activated complex
$f_{\neq}$	partition function of activated complex with one less vibrational degree of freedom
f (S)	adjacency of sites
G	mass velocity of gas flow based on the total cross-sectional area of catalyst bed
G_M	molal mass velocity of gas flow based on the total cross-sectional area of catalyst bed
$\Delta G°$	standard-state Gibbs free energy change
$\Delta H°$	standard-state enthalpy change
ΔH_A	heat of reaction per mole of A reacted

ΔH°_{A}	standard-state enthalpy change during the adsorption of component A
$\Delta H^{\neq}$	standard enthalpy of activation per mole
h	Planck constant
h_G	heat transfer coefficient
I	component I (inert)
j_d	Chilton-Colburn mass transfer factor
j_h	Chilton-Colburn heat-transfer factor
K	thermodynamic equilibrium constant, or for overall reaction
K	adsorption equilibrium constant (with subscripts A, B ....)
K'	equilibrium constant of dissociation step on adsorption (with subscript A, B, ...)
k	thermal conductivity of gas
k	reaction velocity constant
k	velocity constant of forward reaction or of adsorption
k'	velocity constant of reverse reaction or of desorption
$\underline{k}$	Boltzmann constant
k_c	thermal conductivity of copper
k_e	effective thermal conductivity
k_G	mass transfer coefficient
k_p	thermal conductivity of pumice
L	molal concentration of active sites per unit mass
M	molecular weight

M_m	mean molecular weight
m_T	the Thiele modulus
N	normality of solution
p	partial pressure
p_f	film pressure factor
P_r	Prandtl number, $\frac{C_p \mu}{k}$
Δp	partial pressure drop across gas film
Q	$\frac{r \quad \Delta H_A}{a_m \phi C_p G_M}$
q_m	rate of heat transfer per unit mass of catalyst
R	component R
R	gas constant
R	reactant feed ratio, moles oxygen/moles isobutylene
R	$\frac{r_A}{a_m \phi G_M}$
Re	Reynolds number, $\frac{D_p G}{\mu}$ or $\frac{G}{a_v \phi \mu}$
r	net forward reaction rate
r'	reverse reaction rate
r_A	rate of reaction or mass transfer of A per unit mass of catalyst
	rate of adsorption of A
r'_A	rate of desorption of A
r_f	forward reaction rate
r_o	initial reaction rate

S	component S
S	sphericity
Sc	Schmidt number $\frac{\mu}{D_{A_m}}$
s	active site
s_2	dual active site
s'	one of the active sites to which a dissociated molecule jumps
$\Delta S^{\neq}$	entropy of activation
$\Delta S°$	standard-state entropy change
$\Delta S°_A$	standard-state entropy change during the adsorption of A
T	temperature
ΔT	$T_i - T$, temperature drop across gas film
W	mass of catalyst
X	conversion, moles reacted or produced/moles isobutylene fed
$X^{\neq}$	activated complex
Y	yield, moles produced/moles isobutylene reacted
y_f	mole fraction of pressure factor, p_f/Π
Δy	concentration drop across gas film
Z	moles methacrolein reacted/moles isobutylene fed

Greek Symbols

α	surface reaction rate constant combined with surface parameters
Δ	finite increment or change of property

ϵ_1	activation energy per molecule at absolute zero
θ	fractional coverage of catalyst surface by a certain component
μ	viscosity
ν	frequency of vibration
π	total pressure
π	3.1416
ρ	density of gas
ρ_B	bulk density of catalyst bed
ϕ	shape factor

Subscripts

A	component A
A_2	diatomic gas molecule
AB	adjacently adsorbed A and B molecules
As	adsorbed A with an adjacen vacant active site
As_2	a state in which A is adsorbed on an active site and ready to jump to an adjacent one
A_2s_2	a diatomic molecule ready to dissociatively adsorbed on two adjacent sites
As'	an atom of dissociated molecule A_2 after final jump to site s'
a	adsorption
B	component B
d	desorption
f	property at average condition of gas film
f	forward

I	component I
i	interfacial quantity
o	initial
R	component R
S	component S
s	surface reaction
s	vacant active site
s_2	dual site
s'	one of the active sites to which a dissociated molecule jumps
$X^{\neq}$	activated complex

X BIBLIOGRAPHY

1. Hougen, O.A., and Watson, K.M., "Chemical Process Principles", Part III, John Wiley and Sons, New York (1947).
2. Isaev, O.V., and Margolis, L. Ya., Kinetika i Kataliz, Vol. 1, No. 2, pp. 237-241 July-August 1960.
3. Enikeev, E. Kh., Isaev, O.V., and Margolis, L. Ya., Kinetika i Kataliz, Vol. 1, No. 3, pp. 431-439 (1960).
4. Roginskii, S.Z., Collection: Problems in Kinetics and Catalysis, 10 (Moscow Acad. Sci. USSR Press, 1960).
5. Ishikawa, T., Government Chemical Industrial Research Institute, Tokyo, Vol. 55, No. 3 (1960).
6. Agamennone, M., Chem. and Eng. News, 39, No. 41, 56-57, (10/9/61).
7. Adams, C.R., and Jennings, T.S., Journal of Catalysis, 2, 63-68 (1963).
8. Sachtler, W.M.H., Rec. Trav. Chim., 82, 243 (1963).
9. Voge, H.H., Wagner, C.D., Stevenson, D.P., Journal of Catalysis 2, 58-62 (1963).
10. Isaev, O.V., Margolis, L. Ya., and Sazahova, I.S., Proc. Acad. Sci. USSR, Phys. Chem. Sect. 129, 905 (1959).
11. Bretton, R.H., Wan, S.U., and Dodge, B.F., Ind. Eng. Chem. 44 594 (1952).
12. Waters, W.A., Trans. Faraday Soc. 42, 184 (1946).
13. Baldwin, M.M., (to Olin Mathieson Chemical Corp.) U.S. 2,776,316 Jan. 1 1957.
14. Dowdon, D.A., and Caldwell, A.M.U., Brit. 828,812, Feb. 24, 1960.
15. Kitahara, and Moriya, Reports Inst. Phy. Chem. Res., 38 (1962).

16. Popova, N.I., Mil'man, F.A., and Latysheva, L.E., Izvest. Sibir. Otdel. Akad. Nauk S.S.S.R., No. 7, 77-82, 1961.

17. Skirrow, G., and Williams, A., Proceedings of the Royal Society, A, Volume 268, pp. 537-552, 1962.

18. Popova, N.I., Vermel, E.E., and Mil'man, F.A., Kinetika, i, Kataliz 3, 241-6 (1962).

19. Emmett, H., "Catalysis" Volume 1 p. 252 (1954).

20. Yang, K.N., and Hougen, O.A., Chem. Eng. Prog., 46, 146 (1950).

21. Chilton, T.H., and Colburn, A.P., Ind. Eng. Chem., 26, 1183 (1934).

22. Gamson, B.W., Thodos, G., and Hougen, O.A., Trans. A.I.Ch.E., 39, 1 (1943).

23. Wilke, C.R., and Hougen, O.A. Trans. A.I.Ch.E., 61, 445 (1945).

24. Yoshida, F., Ramaswami, D., and Hougen, O.A., A.I.Ch.E. (Am. Inst. Chem. Engrs.) J. 8, 5-11 (1962).

25. Thiele, E.W., Ind. Eng. Chem., 31, 916 (1939).

26. Twigg, G.H., and Rideal, E.K., Proc. Roy. Soc. (London), A 171, 55 (1939).

27. Glasstone, S., Laidler, K.J., and Eyring, H., "The Theory of Rate Processes" McGraw-Hill, New York (1941).

28. Hougen, O.A., Ch.E. 219 Lectures, University of Wisconsin, Madison (1959).

29. Laidler, K.J., in "Catalysis" Vol. I (P.H. Emmett, Editor), Reinhold, New York (1954).

30. Dowden, D.A., Paper presented at the Gordon Research Conference, July 1955.

31. Langmuir, I., Trans. Frad. Soc., 17, 621 (1922).

32. Langmuir, I., J. Chem. Soc., 511 (1940).

33. Laidler, K. J., "Chemical Kinetics", McGraw-Hill, New York (1950).

34. Twigg, G.H., and Rideal, E.K., Trans. Faraday Soc., 36 533 (1940).

35. Perkin-Elmer Corporation, "Instructions for the Model 154-D Vapor Fractometer", Norwalk, Conn. (1963).

XI APPENDICES

Appendix A

Instrument Calibrations and Analysis of Products

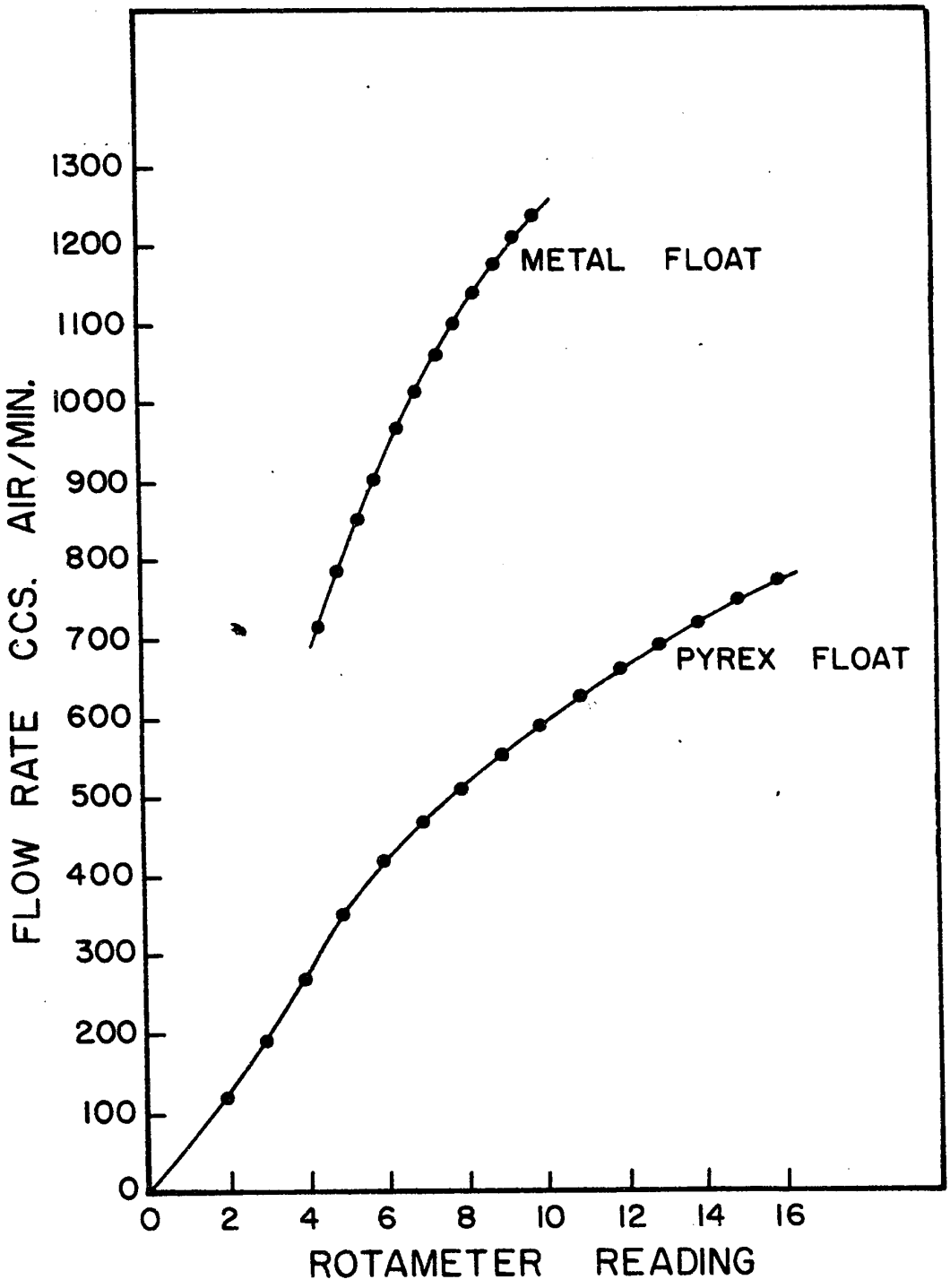

Fig. 36 Air Calibration 1 Atm and 32 F

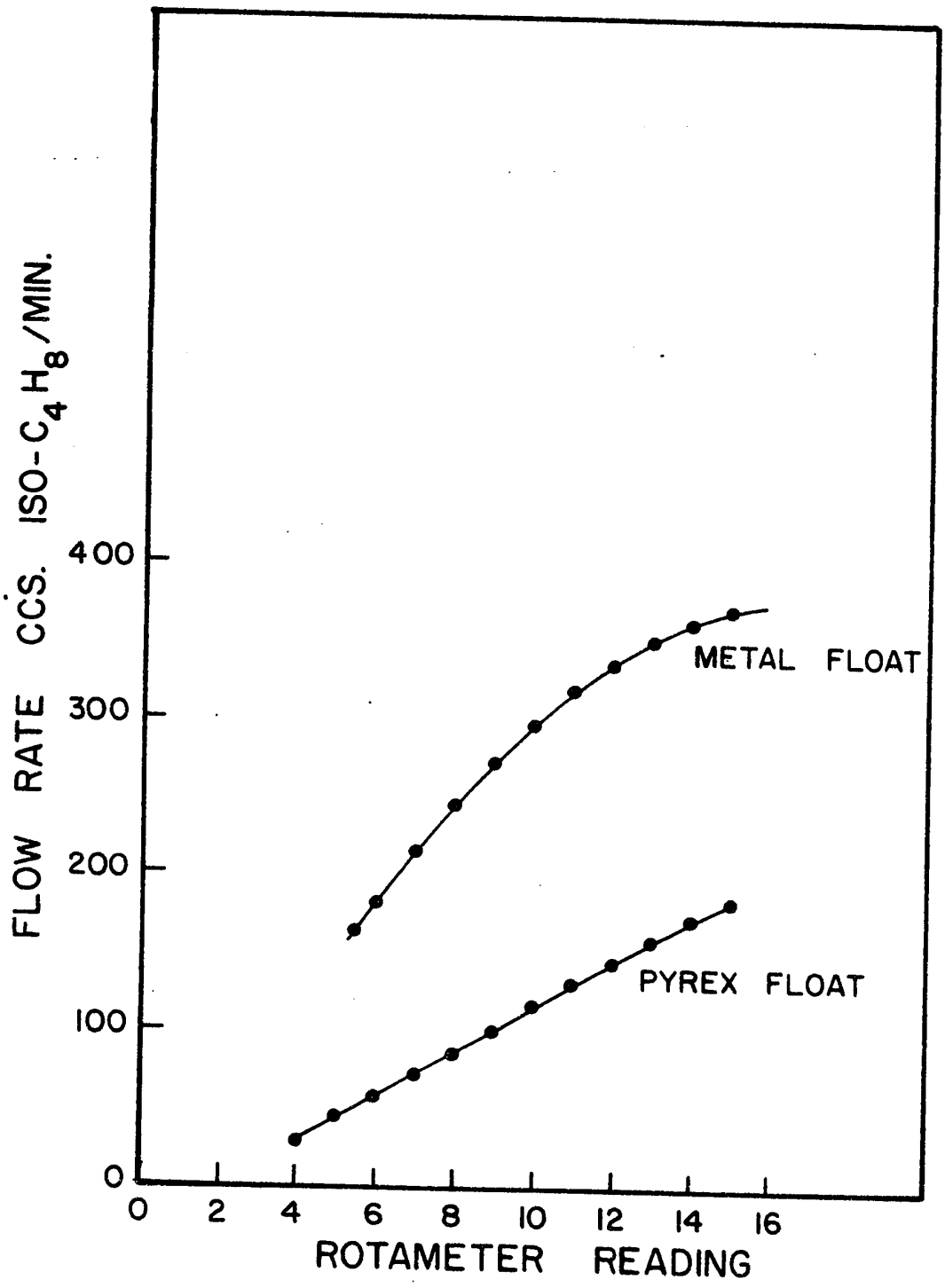

Fig. 37 Isobutylene Calibration 1 Atm. and 32 F

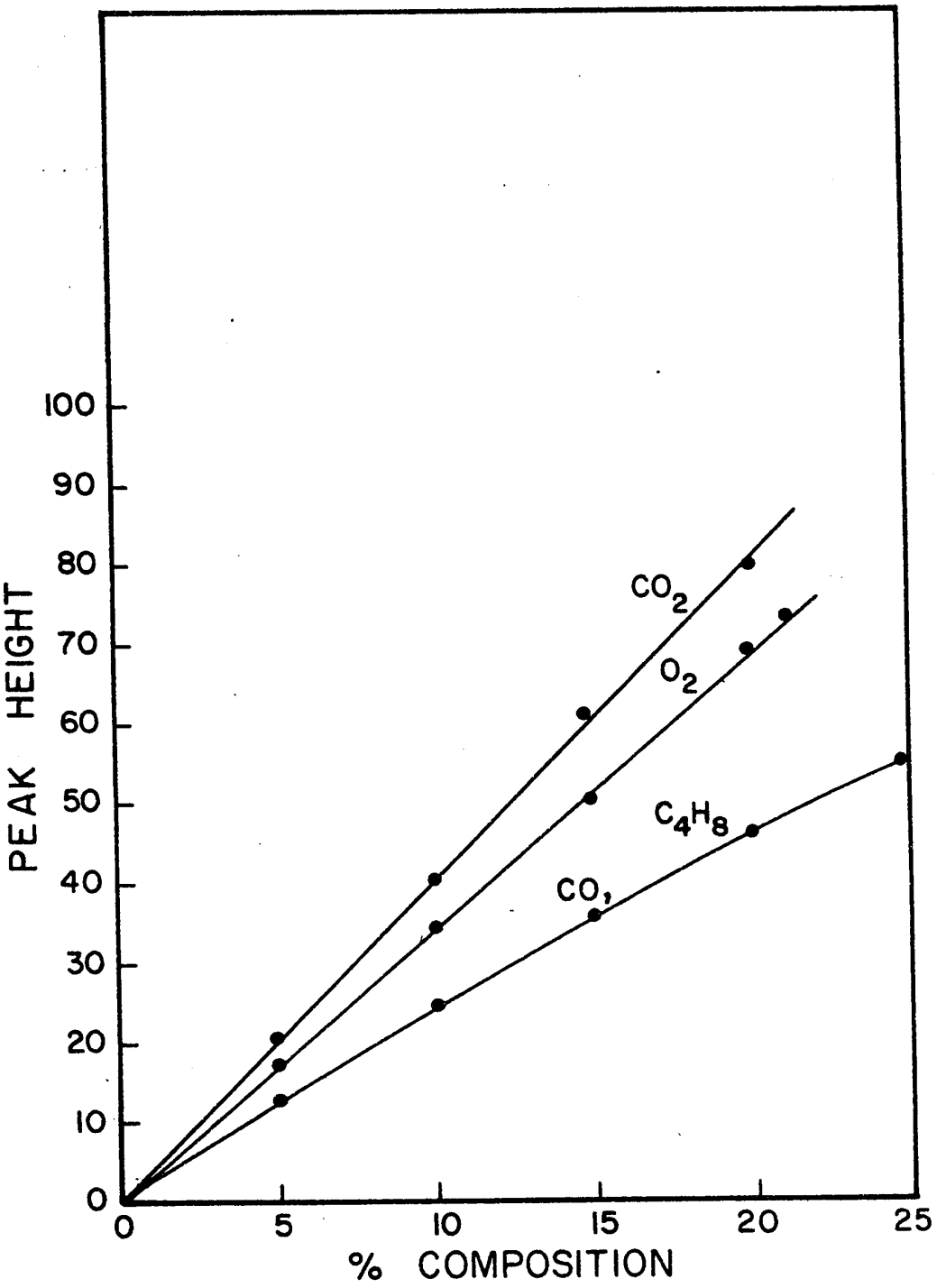

Fig. 38 Calibration of Gases 1 Atm. and 75° F.

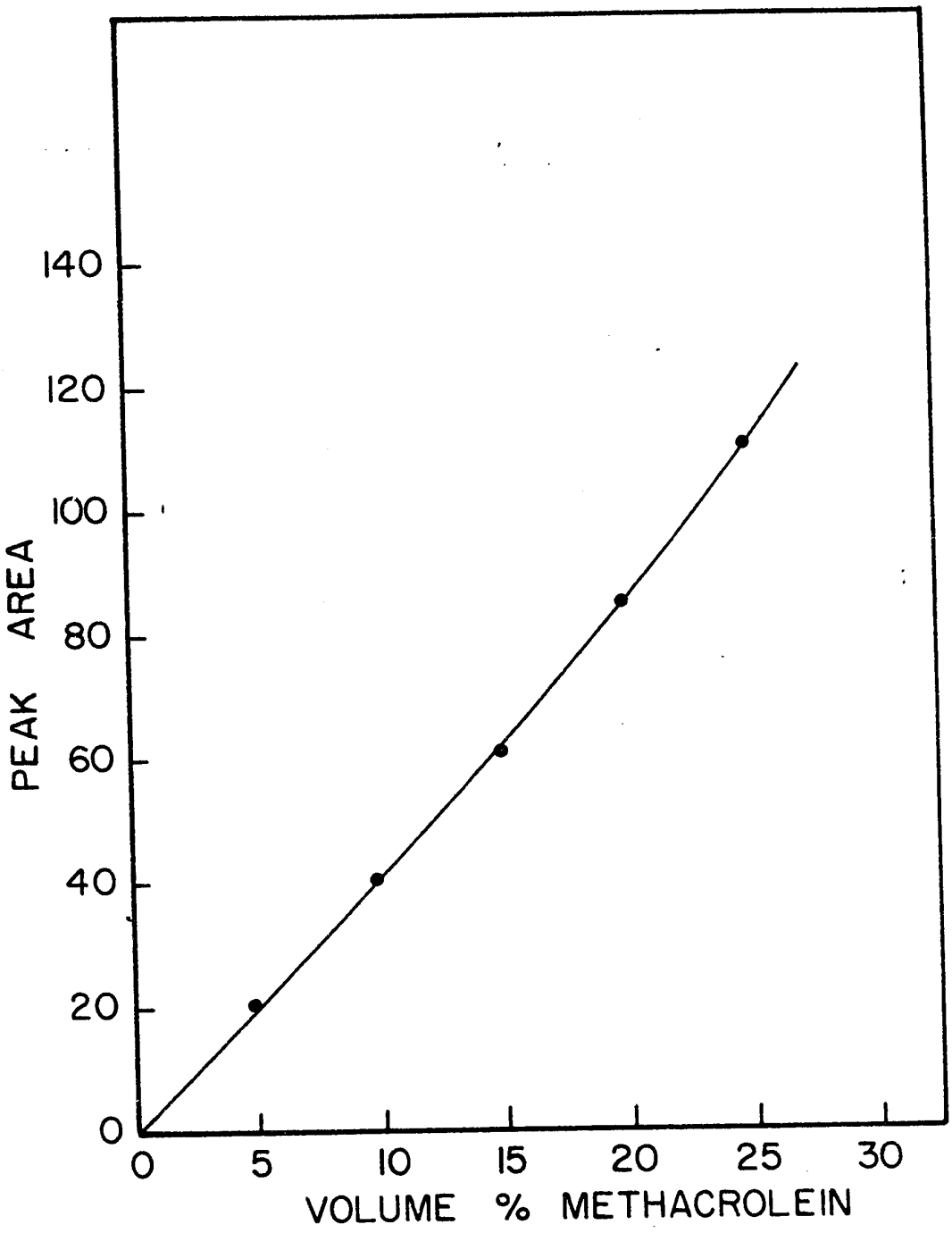

Fig. 39 Methacrolein Calibration Sensitivity 16 Temp. 110 C

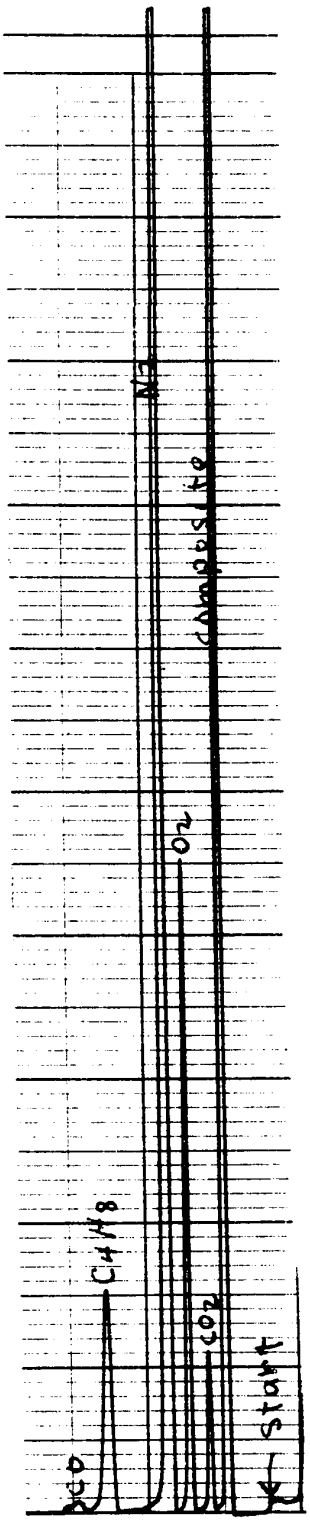

Fig. 40

Typical Analysis of the Gaseous Products

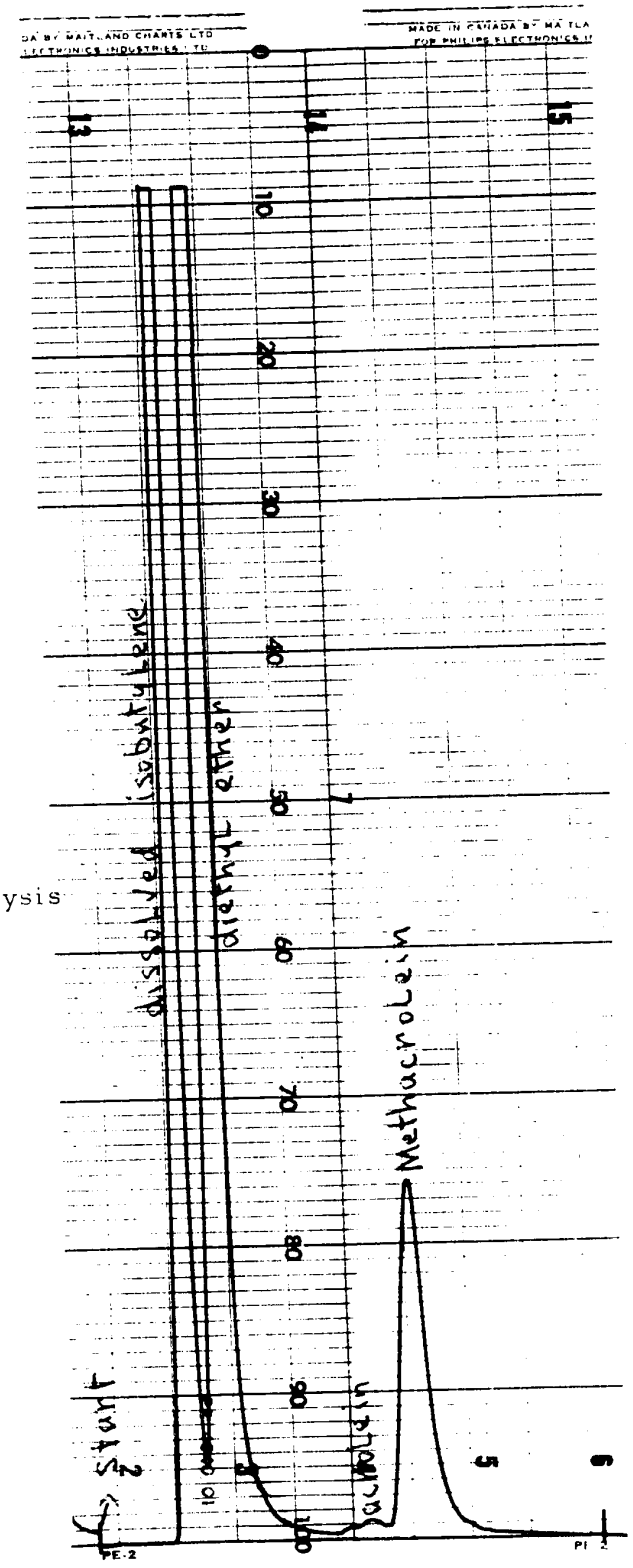

Fig. 41

Typical Analysis of the Liquid Products

Appendix B

Density Determination of Methacrolein

Temperature 25.0° C

Weight of dry pycnometer	=	28.11504 gms.
Weight of pycnometer with water	=	38.00283 gms.
Weight of water	=	9.88779 gms.
Density of water at 25.0° C	=	0.997074 gm/c.c.
Volume of pycnometer $= \frac{9.88779}{0.997074}$	=	0.99168 c.c.

Temperature 5° C

Weight of pycnometer with methacrolein	=	37.4616 gms.
Weight of methacrolein	=	9.3466 gms.
Density of methacrolein at 5° C $= \frac{9.3466}{0.99168}$	=	0.9425 gm/c.c.

Appendix C

Experimental Data

Table 5: Compositions of Feeds and Products and Conversions in Air Oxidation of Isobutylene over Catalyst 1

Temp. 350° C R = 1.0

Run No.	W/F	Feed moles/hr			Conversions		
		C_4H_8	O_2	N_2	$X_{C_4H_8}$	$X_{C_4H_6O}$	$1/4\,X_{CO_2}$
300	0.22	0.4821	0.5000	1.8833	0.074	0.038	0.035
301	0.43	0.4821	0.5000	1.8833	0.116	0.059	0.057
302	0.67	0.4821	0.5000	1.8833	0.116	0.084	0.076
303	1.20	0.4821	0.5000	1.8833	0.219	0.113	0.107
304	2.70	0.4821	0.5000	1.8833	0.235	0.112	0.118
305	4.96	0.4821	0.5000	1.8833	0.251	0.112	0.139

Run No.	Products			moles/hr			
	C_4H_8	O_2	N_2	C_4H_6O	CO_2	CO	H_2O
300	0.4464	0.3783	1.8833	0.0182	0.0665	-	0.085
301	0.4262	0.3051	1.8833	0.0285	0.1100	-	0.140
302	0.4021	0.2371	1.8833	0.0405	0.1465	-	0.190
303	0.3765	0.1254	1.8833	0.0544	0.2067	0.0026	0.262
304	0.3688	0.1261	1.8833	0.0539	0.2262	0.0079	0.287
305	0.3611	0.0384	1.8833	0.0540	0.2690	0.0077	0.327

Table 5 - Continued

Temp. 350° C R = 2.0

Run No.	W/F	Feed moles/hr			Conversions		
		C_4H_8	O_2	N_2	$X_{C_4H_8}$	$X_{C_4H_6O}$	$1/4\,X_{CO_2}$
306	0.39	0.2679	0.5456	2.0526	0.093	0.026	0.068
307	0.78	0.2679	0.5456	2.0526	0.198	0.064	0.145
308	1.20	0.2679	0.5456	2.0526	0.244	0.086	0.159
309	1.87	0.2679	0.5456	2.0526	0.313	0.105	0.197
310	4.85	0.2679	0.5456	2.0526	0.392	0.116	0.282
311	8.92	0.2679	0.5456	2.0526	0.405	0.123	0.278

Run No.	Products moles/hr						
	C_4H_8	O_2	N_2	C_4H_6O	CO_2	CO	H_2O
306	0.2430	0.4245	2.0526	0.0070	0.0726	-	0.080
307	0.2149	0.2937	2.0526	0.0170	0.1550	-	0.175
308	0.2025	0.2647	2.0526	0.0216	0.1702	0.0054	0.192
309	0.1840	0.1893	2.0526	0.0281	0.2106	0.0107	0.252
310	0.1629	0.0439	2.0526	0.0310	0.3024	0.0129	0.346
311	0.1594	0.0523	2.0526	0.0330	0.2981	0.0131	0.340

Table 5 - Continued

Temp. 350° C R = 3.0

Run No.	W/F	Feed moles/hr			Conversions		
		C_4H_8	O_2	N_2	$X_{C_4H_8}$	$X_{C_4H_6O}$	$1/4\,X_{CO_2}$
312	0.56	0.1875	0.5625	2.1161	0.113	0.029	0.083
313	1.11	0.1875	0.5625	2.1161	0.252	0.072	0.180
314	1.71	0.1875	0.5625	2.1161	0.363	0.113	0.250
315	3.01	0.1875	0.5625	2.1161	0.503	0.157	0.344
316	6.93	0.1875	0.5625	2.1161	0.545	0.157	0.383
317	12.8	0.1875	0.5625	2.1161	0.556	0.160	0.391

Run No.	Products moles/hr						
	C_4H_8	O_2	N_2	C_4H_6O	CO_2	CO	H_2O
312	0.1663	0.4598	2.1161	0.0054	0.0621	-	0.068
313	0.1402	0.3435	2.1161	0.0135	0.1347	-	0.150
314	0.1194	0.2604	2.1161	0.0211	0.1872	-	0.209
315	0.0932	0.1437	2.1161	0.0295	0.2582	0.0053	0.290
316	0.0853	0.0888	2.1161	0.0295	0.2872	0.0078	0.325
317	0.0832	0.0672	2.1161	0.0300	0.2931	0.0130	0.337

Table 5 - Continued

Temp. 350° C R = 4.0

Run No.	W/F	Feed moles/hr			Conversions		
		C_4H_8	O_2	N_2	$X_{C_4H_8}$	$X_{C_4H_6O}$	$1/4\ X_{CO_2}$
318	0.73	0.1420	0.5721	2.1520	0.142	0.025	0.115
319	1.47	0.1420	0.5721	2.1520	0.301	0.075	0.223
320	2.70	0.1420	0.5721	2.1520	0.451	0.113	0.336
321	5.21	0.1420	0.5721	2.1520	0.630	0.154	0.467
322	9.15	0.1420	0.5721	2.1520	0.689	0.149	0.545
323	16.8	0.1420	0.5721	2.1520	0.711	0.155	0.546

Run No.	Products				moles/hr		
	C_4H_8	O_2	N_2	C_4H_6O	CO_2	CO	H_2O
318	0.1218	0.4701	2.1520	0.0036	0.0651	-	0.071
319	0.0993	0.3669	2.1520	0.0106	0.1269	-	0.138
320	0.0780	0.2636	2.1520	0.0160	0.1910	-	0.208
321	0.0525	0.1496	2.1520	0.0218	0.2650	0.0053	0.290
322	0.0442	0.0755	2.1520	0.0212	0.3096	0.0026	0.330
323	0.0410	0.0638	2.1520	0.0220	0.3100	0.0128	0.345

Temp. 375° C R = 1.0

Run No.	W/F	Feed moles/hr			Conversions		
		C_4H_8	O_2	N_2	$X_{C_4H_8}$	$X_{C_4H_6O}$	$1/4\,X_{CO_2}$
324	0.22	0.4821	0.5000	1.8833	0.074	0.037	0.036
325	0.43	0.4821	0.5000	1.8833	0.128	0.064	0.062
326	0.67	0.4821	0.5000	1.8833	0.163	0.082	0.080
327	1.20	0.4821	0.5000	1.8833	0.219	0.113	0.107
328	2.70	0.4821	0.5000	1.8833	0.240	0.115	0.119
329	4.96	0.4821	0.5000	1.8833	0.253	0.114	0.135

Run No.	Products moles/hr						
	C_4H_8	O_2	N_2	C_4H_6O	CO_2	CO	H_2O
324	0.4464	0.3719	1.8833	0.0180	0.0700	-	0.090
325	0.4204	0.2920	1.8833	0.0309	0.1201	-	0.151
326	0.4035	0.2340	1.8833	0.0396	0.1533	-	0.193
327	0.3765	0.1334	1.8833	0.0544	0.2067	0.0026	0.262
328	0.3664	0.0935	1.8833	0.0552	0.2286	0.0104	0.292
329	0.3601	0.0372	1.8833	0.0550	0.2605	0.0129	0.328

Table 5 - Continued

Temp. 375° C R = 2.0

Run No.	W/F	Feed moles/hr			Conversions		
		C_4H_8	O_2	N_2	$X_{C_4H_8}$	$X_{C_4H_6O}$	$1/4\,X_{CO_2}$
330	0.39	0.2679	0.5456	2.0526	0.099	0.028	0.073
331	0.78	0.2679	0.5456	2.0526	0.198	0.064	0.145
332	1.20	0.2679	0.5456	2.0526	0.269	0.087	0.175
333	1.87	0.2679	0.5456	2.0526	0.352	0.119	0.219
334	4.85	0.2679	0.5456	2.0526	0.435	0.127	0.299
335	8.92	0.2679	0.5456	2.0526	0.440	0.129	0.298

Run No.	Products moles/hr						
	C_4H_8	O_2	N_2	C_4H_6O	CO_2	CO	H_2O
330	0.2414	0.4189	2.0526	0.0074	0.0777	-	0.086
331	0.2149	0.2937	2.0526	0.0170	0.1550	-	0.175
332	0.1958	0.2361	2.0526	0.0233	0.1878	0.0054	0.212
333	0.1736	0.1500	2.0526	0.0320	0.2343	0.0132	0.280
334	0.1514	0.0192	2.0526	0.0340	0.3200	0.0087	0.363
335	0.1500	0.0185	2.0526	0.0345	0.3197	0.0132	0.367

Table 5 - Continued

Temp. 375° C R = 3.0

Run No.	W/F	Feed moles/hr			Conversions		
		C_4H_8	O_2	N_2	$X_{C_4H_8}$	$X_{C_4H_6O}$	$1/4\ X_{CO_2}$
336	0.56	0.1875	0.5625	2.1161	0.128	0.032	0.094
337	1.11	0.1875	0.5625	2.1161	0.267	0.073	0.191
338	1.71	0.1875	0.5625	2.1161	0.382	0.118	0.259
339	3.01	0.1875	0.5625	2.1161	0.518	0.160	0.350
340	6.93	0.1875	0.5625	2.1161	0.559	0.165	0.380
341	12.8	0.1875	0.5625	2.1161	0.599	0.166	0.414

Run No.	Products moles/hr						
	C_4H_8	O_2	N_2	C_4H_6O	CO_2	CO	H_2O
336	0.1635	0.4542	2.1161	0.0060	0.0705	-	0.072
337	0.1374	0.3353	2.1161	0.0137	0.1429	-	0.158
338	0.1159	0.2453	2.1161	0.0222	0.1941	0.0027	0.218
339	0.0904	0.1381	2.1161	0.0300	0.2628	0.0053	0.288
340	0.0827	0.0955	2.1161	0.0310	0.2852	0.0077	0.324
341	0.0752	0.0501	2.1161	0.0312	0.3104	0.0130	0.353

Table 5 - Continued

Temp. 375° C R = 4.0

Run No.	W/F	Feed moles/hr			Conversions		
		C_4H_8	O_2	N_2	$X_{C_4H_8}$	$X_{C_4H_6O}$	$1/4\,X_{CO_2}$
342	0.73	0.1420	0.5721	2.1520	0.168	0.029	0.134
343	1.47	0.1420	0.5721	2.1520	0.320	0.076	0.243
344	2.70	0.1420	0.5721	2.1520	0.508	0.123	0.379
345	5.21	0.1420	0.5721	2.1520	0.668	0.159	0.494
346	9.15	0.1420	0.5721	2.1520	0.729	0.169	0.564
347	16.8	0.1420	0.5721	2.1520	0.746	0.169	0.560

Run No.	Products mcles/hr						
	C_4H_8	O_2	N_2	C_4H_6O	CO_2	CO	H_2O
342	0.1181	0.4557	2.1520	0.0041	0.0760	-	0.081
343	0.0966	0.3532	2.1520	0.0108	0.1380	-	0.151
344	0.0699	0.2287	2.1520	0.0174	0.2152	-	0.233
345	0.0471	0.1181	2.1520	0.0226	0.2808	0.0105	0.313
346	0.0385	0.0589	2.1520	0.0240	0.3203	0.0026	0.343
347	0.0361	0.0572	2.1520	0.0240	0.3178	0.0129	0.354

Table 5 - Continued

Temp. 400° C R = 0.25

Run No.	W/F	Feed moles/hr			Conversions		
		C_4H_8	O_2	N_2	$X_{C_4H_8}$	$X_{C_4H_6O}$	$1/4\,X_{CO_2}$
348	0.13	0.8400	0.2100	0.7900	0.038	0.022	0.015
349	0.21	0.8400	0.2100	0.7900	0.047	0.028	0.019
350	0.25	0.8400	0.2100	0.7900	0.052	0.031	0.021
351	0.29	0.8400	0.2100	0.7900	0.056	0.033	0.023
438	1.00	0.8400	0.2100	0.7900	0.079	0.043	0.033

Run No.	Products moles/hr						
	C_4H_8	O_2	N_2	C_4H_6O	CO_2	CO	H_2O
348	0.8085	0.1125	0.7900	0.0186	0.0511	-	0.070
349	0.8005	0.0902	0.7900	0.0235	0.0635	-	0.087
350	0.7960	0.0770	0.7900	0.0261	0.0709	-	0.097
351	0.7930	0.0679	0.7900	0.0277	0.0763	0.0018	0.103
438	0.7733	0.0028	0.7900	0.0360	0.1108	0.0039	0.150

Table 5 - Continued

Temp. 400° C R = 0.50

Run No.	W/F	Feed moles/hr			Conversions		
		C_4H_8	O_2	N_2	$X_{C_4H_8}$	$X_{C_4H_6O}$	$1/4\ X_{CO_2}$
352	0.12	0.8400	0.4200	1.5800	0.050	0.028	0.022
353	0.25	0.8400	0.4200	1.5800	0.081	0.041	0.039
354	0.37	0.8400	0.4200	1.5800	0.089	0.042	0.042
355	0.50	0.8400	0.4200	1.5800	0.110	0.048	0.052
356	1.49	0.8400	0.4200	1.5800	0.138	0.064	0.068
357	1.98	0.8400	0.4200	1.5800	0.142	0.065	0.073

Run No.	Products moles/hr						
	C_4H_8	O_2	N_2	C_4H_6O	CO_2	CO	H_2O
352	0.7980	0.2838	1.5800	0.0235	0.0739	-	0.098
353	0.7720	0.1867	1.5800	0.0342	0.1297	-	0.168
354	0.7652	0.1657	1.5800	0.0375	0.1408	-	0.181
355	0.7476	0.1152	1.5800	0.0400	0.1737	0.0026	0.215
356	0.7241	0.0220	1.5800	0.0538	0.2285	0.0028	0.283
357	0.7207	0.0030	1.5800	0.0546	0.2450	0.0029	0.295

Table 5 - Continued

Temp. 400° C R = 1.0

Run No.	W/F	Feed moles/hr			Conversions		
		C_4H_8	O_2	N_2	$X_{C_4H_8}$	$X_{C_4H_6O}$	$1/4 X_{CO_2}$
358	0.22	0.4821	0.5000	1.8833	0.081	0.038	0.041
359	0.43	0.4821	0.5000	1.8833	0.128	0.062	0.064
360	0.67	0.4821	0.5000	1.8833	0.169	0.083	0.082
361	1.20	0.4821	0.5000	1.8833	0.223	0.100	0.119
362	2.70	0.4821	0.5000	1.8833	0.245	0.106	0.133
363	4.96	0.4821	0.5000	1.8833	0.253	0.105	0.140

Run No.	Products moles/hr						
	C_4H_8	O_2	N_2	C_4H_6O	CO_2	CO	H_2O
358	0.4430	0.3523	1.8833	0.0185	0.0942	-	0.100
359	0.4204	0.2865	1.8833	0.0300	0.1228	-	0.153
360	0.4006	0.2260	1.8833	0.0400	0.1587	-	0.200
361	0.3746	0.1066	1.8833	0.0484	0.2289	0.0034	0.282
362	0.3640	0.0600	1.8833	0.0511	0.2558	0.0078	0.317
363	0.3601	0.0308	1.8833	0.0510	0.2702	0.0092	0.334

Table 5 — Continued

Temp. 400° C R = 2.0

Run No.	W/F	Feed moles/hr			Conversions		
		C_4H_8	O_2	N_2	$X_{C_4H_8}$	$X_{C_4H_6O}$	$1/4\,X_{CO_2}$
364	0.39	0.2679	0.5456	2.0526	0.109	0.031	0.078
365	0.78	0.2679	0.5456	2.0526	0.198	0.064	0.145
366	1.20	0.2679	0.5456	2.0526	0.279	0.090	0.183
367	1.87	0.2679	0.5456	2.0526	0.371	0.112	0.243
368	4.85	0.2679	0.5456	2.0526	0.442	0.136	0.300
369	8.92	0.2679	0.5456	2.0526	0.460	0.141	0.305

Run No.	Products moles/hr						
	C_4H_8	O_2	N_2	C_4H_6O	CO_2	CO	H_2O
364	0.2387	0.4106	2.0526	0.0084	0.0832	-	0.092
365	0.2149	0.2937	2.0526	0.0170	0.1550	-	0.175
366	0.1932	0.2281	2.0526	0.0240	0.1959	0.0054	0.220
367	0.1685	0.1105	2.0526	0.0300	0.2606	0.0132	0.306
368	0.1495	0.0152	2.0526	0.0364	0.3215	0.0130	0.366
369	0.1447	0.0110	2.0526	0.0378	0.3268	0.0120	0.366

Table 5 - Continued

Temp. 400° C R = 3.0

Run No.	W/F	Feed moles/hr			Conversions		
		C_4H_8	O_2	N_2	$X_{C_4H_8}$	$X_{C_4H_6O}$	$1/4\ X_{CO_2}$
370	0.56	0.1875	0.5625	2.1161	0.142	0.036	0.105
371	1.11	0.1875	0.5625	2.1161	0.267	0.073	0.191
372	1.71	0.1875	0.5625	2.1161	0.400	0.118	0.275
373	3.01	0.1875	0.5625	2.1161	0.531	0.147	0.376
374	6.93	0.1875	0.5625	2.1161	0.573	0.133	0.430
375	12.8	0.1875	0.5625	2.1161	0.613	0.156	0.450

Run No.	Products moles/hr						
	C_4H_8	O_2	N_2	C_4H_6O	CO_2	CO	H_2O
370	0.1609	0.4429	2.1161	0.0067	0.0790	-	0.086
371	0.1374	0.3353	2.1161	0.0137	0.1429	-	0.158
372	0.1125	0.2277	2.1161	0.0222	0.2063	0.0027	0.231
373	0.0879	0.1012	2.1161	0.0276	0.2822	0.0053	0.320
374	0.0801	0.0413	2.1161	0.0250	0.3226	0.0077	0.358
375	0.0726	0.0184	2.1161	0.0293	0.3375	0.0130	0.370

Table 5 - Continued

Temp. 400° C R = 4.0

Run No.	W/F	Feed moles/hr			Conversions		
		C_4H_8	O_2	N_2	$X_{C_4H_8}$	$X_{C_4H_6O}$	$1/4\ X_{CO_2}$
376	0.73	0.1420	0.5721	2.1520	0.168	0.026	0.139
377	1.47	0.1420	0.5721	2.1520	0.320	0.076	0.243
378	2.70	0.1420	0.5721	2.1520	0.530	0.123	0.395
379	5.21	0.1420	0.5721	2.1520	0.686	0.160	0.513
380	9.15	0.1420	0.5721	2.1520	0.747	0.169	0.568
381	16.8	0.1420	0.5721	2.1520	0.782	0.159	0.592

Run No.	Products moles/hr						
	C_4H_8	O_2	N_2	C_4H_6O	CO_2	CO	H_2O
376	0.1181	0.4501	2.1520	0.0037	0.0788	-	0.081
377	0.0966	0.3532	2.1520	0.0108	0.1380	-	0.151
378	0.0667	0.2192	2.1520	0.0175	0.2245	0.0027	0.242
379	0.0446	0.1050	2.1520	0.0227	0.2913	0.0105	0.327
380	0.0359	0.0589	2.1520	0.0240	0.3228	0.0027	0.351
381	0.0310	0.0300	2.1520	0.0226	0.3363	0.0129	0.370

Table 5 - Continued

Temp. 425° C R = 1.0

Run No.	W/F	Feed moles/hr.			Conversions		
		C_4H_8	O_2	N_2	$X_{C_4H_8}$	$X_{C_4H_6O}$	$1/4\ X_{CO_2}$
382	0.22	0.4821	0.5000	1.8833	0.087	0.039	0.047
383	0.43	0.4821	0.5000	1.8833	0.128	0.062	0.065
384	0.67	0.4821	0.5000	1.8833	0.169	0.083	0.082
385	1.20	0.4821	0.5000	1.8833	0.224	0.094	0.128
386	2.70	0.4821	0.5000	1.8833	0.245	0.099	0.138
387	4.96	0.4821	0.5000	1.8833	0.256	0.100	0.146

Run No.	Products moles/hr						
	C_4H_8	O_2	N_2	C_4H_6O	CO_2	CO	H_2O
382	0.4402	0.3424	1.8833	0.0188	0.0903	-	0.109
383	0.4204	0.2838	1.8833	0.0297	0.1255	-	0.156
384	0.4006	0.2260	1.8833	0.0400	0.1587	-	0.200
385	0.3741	0.0851	1.8833	0.0454	0.2477	0.0026	0.296
386	0.3640	0.0439	1.8833	0.0477	0.2657	0.0077	0.324
387	0.3587	0.0179	1.8833	0.0483	0.2818	0.0156	0.346

Table 5 - Continued

Temp. 425° C R = 2.0

Run No.	W/F	Feed moles/hr			Conversions		
		C_4H_8	O_2	N_2	$X_{C_4H_8}$	$X_{C_4H_6O}$	$1/4\ X_{CO_2}$
388	0.39	0.2679	0.5456	2.0526	0.109	0.027	0.083
389	0.78	0.2679	0.5456	2.0526	0.188	0.053	0.137
390	1.20	0.2679	0.5456	2.0526	0.289	0.084	0.198
391	1.87	0.2679	0.5456	2.0526	0.375	0.099	0.264
392	4.85	0.2679	0.5456	2.0526	0.455	0.118	0.332
393	8.92	0.2679	0.5456	2.0526	0.455	0.118	0.332

Run No.	Products moles/hr						
	C_4H_8	O_2	N_2	C_4H_6O	CO_2	CO	H_2O
388	0.2387	0.4078	2.0526	0.0072	0.0888		0.096
389	0.2175	0.3072	2.0526	0.0142	0.1468		0.162
390	0.1905	0.2093	2.0526	0.0225	0.2120	0.0054	0.237
391	0.1674	0.0811	2.0526	0.0265	0.2824	0.0131	0.321
392	0.1460	0.0025	2.0526	0.0315	0.3562	0.0142	0.382
393	0.1460	0.0025	2.0526	0.0315	0.3562	0.0142	0.382

Table 5 - Continued

Temp. 425° C R = 3.0

Run No.	W/F	Feed moles/hr			Conversions		
		C_4H_8	O_2	N_2	$X_{C_4H_8}$	$X_{C_4H_6O}$	$1/4\ X_{CO_2}$
394	0.56	0.1875	0.5625	2.1161	0.128	0.024	0.105
395	1.11	0.1875	0.5625	2.1161	0.267	0.073	0.191
396	1.71	0.1875	0.5625	2.1161	0.404	0.115	0.284
397	3.01	0.1875	0.5625	2.1161	0.546	0.145	0.394
398	6.93	0.1875	0.5625	2.1161	0.587	0.151	0.427
399	12.8	0.1875	0.5625	2.1161	0.625	0.151	0.453

Run No.	Products moles/hr						
	C_4H_8	O_2	N_2	C_4H_6O	CO_2	CO	H_2O
394	0.1635	0.4401	2.1161	0.0044	0.0790	-	0.082
395	0.1374	0.3353	2.1161	0.0137	0.1429	-	0.158
396	0.1117	0.2156	2.1161	0.0215	0.2130	0.0027	0.237
397	0.0851	0.0852	2.1161	0.0272	0.2955	0.0053	0.320
398	0.0774	0.0487	2.1161	0.0284	0.3201	0.0077	0.354
399	0.0703	0.0102	2.1161	0.0284	0.3397	0.0130	0.380

Table 5 - Continued

Temp. 425° C R = 4.0

Run No.	W/F	Feed moles/hr			Conversions		
		C_4H_8	O_2	N_2	$X_{C_4H_8}$	$X_{C_4H_6O}$	$1/4\ X_{CO_2}$
400	0.73	0.1420	0.5721	2.1520	0.168	0.024	0.144
401	1.47	0.1420	0.5721	2.1520	0.301	0.065	0.233
402	2.70	0.1420	0.5721	2.1520	0.530	0.118	0.405
403	5.21	0.1420	0.5721	2.1520	0.688	0.159	0.510
404	9.15	0.1420	0.5721	2.1520	0.747	0.162	0.577
405	16.8	0.1420	0.5721	2.1520	0.763	0.165	0.571

Run No.	Products moles/hr						
	C_4H_8	O_2	N_2	C_4H_6O	CO_2	CO	H_2O
400	0.1181	0.4445	2.1520	0.0034	0.0816		0.085
401	0.0993	0.3587	2.1520	0.0093	0.1324		0.143
402	0.0667	0.2138	2.1520	0.0168	0.2299	0.0027	0.246
403	0.0443	0.1017	2.1520	0.0225	0.2895	0.0104	0.325
404	0.0359	0.0564	2.1520	0.0230	0.3217	0.0026	0.352
405	0.0337	0.0500	2.1520	0.0235	0.3241	0.0129	0.361

Table 5 - Continued

Temp. 450° C R = 1.0

Run No.	W/F	Feed moles/hr			Conversions		
		C_4H_8	O_2	N_2	$X_{C_4H_8}$	$X_{C_4H_6O}$	$1/4\ X_{CO_2}$
406	0.22	0.4821	0.5000	1.8833	0.081	0.038	0.042
407	0.43	0.4821	0.5000	1.8833	0.123	0.058	0.064
408	0.67	0.4821	0.5000	1.8833	0.163	0.078	0.084
409	1.20	0.4821	0.5000	1.8833	0.215	0.086	0.130
410	2.70	0.4821	0.5000	1.8833	0.235	0.093	0.134
411	4.96	0.4821	0.5000	1.8833	0.251	0.098	0.146

Run No.	Products moles/hr						
	C_4H_8	O_2	N_2	C_4H_6O	CO_2	CO	H_2O
406	0.4430	0.3589	1.8833	0.0185	0.0807	-	0.100
407	0.4228	0.2893	1.8833	0.0280	0.1228	-	0.150
408	0.4035	0.2179	1.8833	0.0375	0.1614	-	0.200
409	0.3784	0.0751	1.8833	0.0415	0.2487	0.0052	0.298
410	0.3688	0.0593	1.[illegible]33	0.0450	[illegible]0	0.0077	0.314
411	0.3611	0.0205	1.8833	0.0470	0.2818	0.0128	0.343

Table 5 - Continued

Temp. 450° C R = 2.0

Run No.	W/F	Feed moles/hr			Conversions		
		C_4H_8	O_2	N_2	$X_{C_4H_8}$	$X_{C_4H_6O}$	$1/4\ X_{CO_2}$
412	0.39	0.2679	0.5456	2.0526	0.103	0.021	0.083
413	0.78	0.2679	0.5456	2.0526	0.188	0.053	0.137
414	1.20	0.2679	0.5456	2.0526	0.289	0.077	0.205
415	1.87	0.2679	0.5456	2.0526	0.375	0.094	0.271
416	4.85	0.2679	0.5456	2.0526	0.440	0.103	0.317
417	8.92	0.2679	0.5456	2.0526	0.440	0.103	0.317

Run No.	Products moles/hr						
	C_4H_8	O_2	N_2	C_4H_6O	CO_2	CO	H_2O
412	0.2403	0.4078	2.0526	0.0056	0.0894	-	0.095
413	0.2175	0.3072	2.0526	0.0142	0.1468	-	0.162
414	0.1995	0.1959	2.0526	0.0205	0.2200	0.0054	0.243
415	0.1674	0.0732	2.0526	0.0252	0.2903	0.0131	0.326
416	0.1500	0.0010	2.0526	0.0275	0.3402	0.0137	0.384
417	0.1500	0.0010	2.0526	0.0275	0.3402	0.0137	0.384

Table 5 - Continued

Temp. 450° C R = 3.0

Run No.	W/F	Feed moles/hr			Conversions		
		C_4H_8	O_2	N_2	$X_{C_4H_8}$	$X_{C_4H_6O}$	$1/4\ X_{CO_2}$
418	0.56	0.1875	0.5625	2.1161	0.128	0.019	0.109
419	1.11	0.1875	0.5625	2.1161	0.238	0.050	0.187
420	1.71	0.1875	0.5625	2.1161	0.404	0.107	0.291
421	3.01	0.1875	0.5625	2.1161	0.546	0.143	0.397
422	6.93	0.1875	0.5625	2.1161	0.587	0.147	0.427
423	12.8	0.1875	0.5625	2.1161	0.625	0.151	0.455

Run No.	Products moles/hr						
	C_4H_8	O_2	N_2	C_4H_6O	CO_2	CO	H_2O
418	0.1635	0.4373	2.1161	0.0035	0.0818	-	0.085
419	0.1429	0.3353	2.1161	0.0093	0.1402	-	0.152
420	0.1117	0.2130	2.1161	0.0200	0.2183	0.0027	0.240
421	0.0851	0.0799	2.1161	0.0268	0.2981	0.0027	0.325
422	0.0774	0.0468	2.1161	0.0276	0.3201	0.0077	0.355
423	0.0703	0.0093	2.1161	0.0283	0.3412	0.0130	0.382

Table 5 - Continued

Temp. 450° C R = 4.0

Run No.	W/F	Feed moles/hr			Conversions		
		C_4H_8	O_2	N_2	$X_{C_4H_8}$	$X_{C_4H_6O}$	$1/4\ X_{CO_2}$
424	0.73	0.1420	0.5721	2.1520	0.148	0.018	0.134
425	1.47	0.1420	0.5721	2.1520	0.301	0.062	0.238
426	2.70	0.1420	0.5721	2.1520	0.511	0.106	0.400
427	5.21	0.1420	0.5721	2.1520	0.688	0.153	0.514
428	9.15	0.1420	0.5721	2.1520	0.730	0.158	0.560
429	16.8	0.1420	0.5721	2.1520	0.763	0.162	0.575

Run No.	Products moles/hr						
	C_4H_8	O_2	N_2	C_4H_6O	CO_2	CO	H_2O
424	0.1209	0.4501	2.1520	0.0025	0.0760	-	0.080
425	0.0993	0.3559	2.1520	0.0088	0.1352	-	0.145
426	0.0674	0.2138	2.1520	0.0150	0.2272	0.0027	0.245
427	0.0443	0.0991	2.1520	0.0217	0.2921	0.0104	0.328
428	0.0383	0.0683	2.1520	0.0225	0.3180	0.0026	0.344
429	0.0337	0.0448	2.1520	0.0230	0.3268	0.0129	0.363

Appendix D

Effect of Process Variables on Conversion and Yield

Table 6: Effect of Feed Ratio on Conversion and Yield at 400° C for W/F = 1.0 over Catalyst 1

Run No.	R	Feed moles/hr			Yields		
		C_4H_8	O_2	N_2	$X_{C_4H_8}$	$Y_{C_4H_6O}$	$1/4\ Y_{CO_2}$
438	0.25	0.8400	0.2100	0.7900	0.079	0.540	0.415
439	0.50	0.8400	0.4200	1.5800	0.136	0.479	0.493
440	1.00	0.4821	0.5000	1.8833	0.203	0.449	0.552
441	2.00	0.2679	0.5456	2.0526	0.272	0.328	0.648
442	3.00	0.1875	0.5625	2.1161	0.266	0.277	0.702
443	4.00	0.1420	0.5721	2.1520	0.261	0.230	0.764

Run No.	Products moles/hr						
	C_4H_8	O_2	N_2	C_4H_6O	CO_2	CO	H_2O
438	0.7733	0.0028	0.7900	0.0360	0.1108	0.0039	0.150
439	0.7258	0.0271	1.5800	0.0547	0.2252	-	0.280
440	0.3842	0.1304	1.8833	0.0440	0.2162	-	0.260
441	0.1950	0.2384	2.0526	0.0239	0.1890	-	0.211
442	0.1376	0.3347	2.1161	0.0138	0.1401	-	0.156
443	0.1049	0.3923	2.1520	0.0085	0.1134	-	0.121

Table 7: Effect of Temperature on Conversion and Yield for R = 2.0, W/F = 1.20 over Catalyst 1

Run No.	Temp. °C	Feed moles/hr			Yields		
		C_4H_8	O_2	N_2	$X_{C_4H_8}$	$Y_{C_4H_6O}$	$1/4\ Y_{CO_2}$
308	350	0.2679	0.5456	2.0526	0.244	0.330	0.651
332	375	0.2679	0.5456	2.0526	0.269	0.323	0.652
366	400	0.2679	0.5456	2.0526	0.279	0.321	0.656
390	425	0.2679	0.5456	2.0526	0.289	0.291	0.685
414	450	0.2679	0.5456	2.0526	0.289	0.265	0.711

Run No.	Products moles/hr						
	C_4H_8	O_2	N_2	C_4H_6O	CO_2	CO	H_2O
308	0.2025	0.2647	2.0526	0.0216	0.1702	0.0054	0.192
332	0.1958	0.2361	2.0526	0.0233	0.1878	0.0054	0.212
366	0.1932	0.2281	2.0526	0.0240	0.1959	0.0054	0.220
390	0.1905	0.2093	2.0526	0.0225	0.2120	0.0054	0.237
414	0.1905	0.1959	2.0526	0.0205	0.2200	0.0054	0.243

Table 8: Effect of Copper Concentration on Conversion and Yield at 400° C for W/F = 1.71 and R = 3.0

Run No.	Catalyst No.	Feed moles/hr			Conversions - Yields		
		C_4H_8	O_2	N_2	$X_{C_4H_8}$	$Y_{C_4H_6O}$	$1/4\ Y_{CO_2}$
434	2	0.1875	0.5625	2.1161	0.272	0.333	0.651
435	3	0.1875	0.5625	2.1161	0.371	0.308	0.678
372	1	0.1875	0.5625	2.1161	0.400	0.296	0.688
436	4	0.1875	0.5625	2.1161	0.422	0.274	0.717
437	5	0.1875	0.5625	2.1161	0.467	0.069	0.840

Run No.	Products moles/hr						
	C_4H_8	O_2	N_2	C_4H_6O	CO_2	CO	H_2O
434	0.1365	0.3303	2.1161	0.0170	0.1329	0.0026	0.156
435	0.1179	0.2452	2.1161	0.0214	0.1888	0.0032	0.230
372	0.1125	0.2277	2.1161	0.0222	0.2063	0.0027	0.231
436	0.1084	0.1975	2.1161	0.0217	0.2269	0.0030	0.249
437	0.0999	0.0736	2.1161	0.0060	0.2944	0.0342	0.333

Table 9. Effect of Velocity on Conversion at 400° C for R = 2.0 over Catalyst 1

Run No.	W/F	Feed moles/hr			Conversions		
		C_4H_8	O_2	N_2	$X_{C_4H_8}$	$X_{C_4H_6O}$	$1/4\ X_{CO_2}$
430	1.55	0.2679	0.5456	2.0526	0.348	0.114	0.220
431	1.55	0.2009	0.4101	1.5429	0.346	0.112	0.223
432	1.55	0.1340	0.2729	1.0264	0.338	0.116	0.213
433	1.55	0.0670	0.1367	0.5143	0.342	0.112	0.215

Run No.	Products moles/hr						
	C_4H_8	O_2	N_2	C_4H_6O	CO_2	CO	H_2O
430	0.1748	0.1510	2.0526	0.0305	0.2358	0.0132	0.280
431	0.1314	0.1095	1.5429	0.0225	0.1792	0.0080	0.210
432	0.0887	0.0808	1.0264	0.0155	0.1139	0.0053	0.135
433	0.0441	0.0398	0.5143	0.0075	0.0577	0.0032	0.069

Appendix E

Calculation of Drops of Partial Pressures and Temperature from Ambient Gas Stream to the External Surface of Catalyst

A. Estimates of Partial Pressure Drops For Each Component For Run 362

Partial pressure drops from Yoshida, Ramaswami and Hougen's (24) plots of Δ_{p_j}/P_j vs. R/y_j were calculated in the following way

$$R = r_{m_A}/a_m \phi G_m$$

where ϕ = shape factor

G_m = molal mass velocity of gas based on total cross section of bed

r_{m_A} = molal reaction rate of component A per unit mass of catalyst particles

a_m = area of particle per unit mass

$$G_m = 2.866/(\frac{0.430}{12})^2 \quad \frac{\pi}{4} = 2843 \text{ gm. moles/hr. ft}^2$$

$\phi = 0.9$ (for irregular granules)

$a_m = 0.04 \text{ m}^2/\text{gm} = 0.43 \text{ ft}^2/\text{gm}$

Weight of catalyst = 1.298 gms

$$R = \frac{r'_{m_A}}{1.298 \times 0.43 \times 0.9 \times 2843} = 0.00070\, r'_{m_A} \quad \frac{\text{hr}}{\text{gm moles}}$$

where $r'_{m_A} = r_{m_A}/\text{weight of catalyst}$

Component	R	y	R/y	$(\Delta P_j/P_j)$ max.
C_4H_8	0.000083	0.168	0.0005	0.005
CO_2	0.000179	0.087	0.0021	0.009

Component	R	y	R/y	$(\Delta P_j/P_j)_{max.}$
C_4H_6O	0.000036	0.017	0.0021	0.009
H_2O	0.000220	0.108	0.0020	0.009
O_2	0.000310	0.175	0.0018	0.008

B. Calculation of Pressure Drop for Carbon Dioxide from Equation (15) For Run 362

$$\Delta y_A = \frac{\Delta P_A}{P_A} = R\,(j_d)^{-1}\; y_{f_A}\,(Sc)_f^{2/3} \qquad (15)$$

Inlet Composition

O_2	=	17.5%
N_2	=	65.7%
C_4H_8	=	16.8%

Outlet Composition

O_2	=	4.3%
N_2	=	64.3
C_4H_8	=	12.8
C_4H_6O	=	1.7
CO_2	=	7.2
H_2O	=	9.3
CO	=	0.3

Component	$C_{av.}$	M	(M) $(C_{av.})$	P_c	$(P_c)(C_{av.})$
O_2	10.9	32.0	3.49	49.7	5.42
N_2	65.0	28.0	18.21	33.5	21.78
C_4H_8	14.8	56.1	8.30	39.5	5.85
C_4H_6O	0.85	70.1	0.60	44.9	0.38
CO_2	3.60	44.0	1.58	72.9	2.62
H_2O	4.65	18.0	0.84	217.7	10.12
CO	0.15	28.0	0.04	35	0.05
			M' = 33.06		P'_c = 46.22

where $C_{av.}$ = average composition

M = molecular weight

P_c = critical pressure

$$P'_r = \frac{P}{P'_c} = \frac{1}{46.22} = 0.0216$$

Component	$C_{av.}$	T_c	$(T_c)(C_{av.})$	μ_c	$(\mu_c)(C_{av.})$
O_2	10.9	154.2	16.81	250	27.3
N_2	65.0	125.8	81.77	180	117.0
C_4H_8	14.8	417.7	61.82	250	37.0
C_4H_6O	0.85	522	4.44	287	2.4
CO_2	3.60	304.1	10.95	343	12.3
H_2O	4.65	647	30.09	495	23.0
CO	0.15	134	0.20	190	0.3
			T'_c = 206.08		μ_c = 219.3 X 10^{-2} poise

where T_c = critical temperature

μ_c = critical viscosity

$$T'_r = \frac{T}{T_c'} = \frac{673}{206.08} = 3.27$$

From the values of P'_r and T'_r and Figure 175 in C.P.P. by Hougen and Watson (1)

$$\mu'_r = 1.22$$

$$\mu = \mu_r \mu_c = 1.22 \times 219 \times 10^{-6} = 267 \times 10^{-6} \text{ poise}$$

$$\mu = 646 \times 10^{-4} \text{ lb/ft. hr}$$

$$\rho = \frac{PM'}{RT} = \frac{33.06}{82.1 \times 673} = 599 \times 10^{-6} \text{ gm/cm}^3$$

$$= 374 \times 10^{-4} \text{ lb/ft}^3$$

$G = 83.9 \text{ lb/ft}^2 \text{ hr}$

$a_v = 9750 \text{ ft}^2/\text{ft}^3$

$$Re = \frac{G}{a_v \phi} = \frac{83.9 \times 10^4}{9750 \times 0.9 \times 646} = 0.148$$

$$D_{M_A} = \frac{\sum_{j=1}^{n} y_{f_A}}{\frac{1}{D_{A_j}} (Y_j - Y_A \frac{N_j}{N_A})}$$

Let the overall reaction be represented by

$$2\ C_4H_8 + 7\ O_2 \rightleftharpoons 4\ CO_2 + C_4H_6O + 5\ H_2O$$

Then $y_{f_{CO_2}} = 1 + y_{CO_2} \left(\frac{2 + 7 - 4 - 1 - 5}{4}\right)$

$$y_{f_{CO_2}} = 1 - 0.25\, y_{CO_2}$$

where y_{CO_2} = mole fraction of CO_2

$D_{CO_2} - C_4H_6O = 0.296$

$D_{CO_2} - O_2 = 0.650$

$D_{CO_2} - N_2 = 0.656$

$D_{CO_2} - H_2O = 0.759$

$D_{CO_2} - C_4H_8 = 0.321$

and $D_{CO_2} - M = 0.560\ cm^2/sec$

$$(Sc)_{CO_2} = \frac{\mu'}{D_{CO_2 - M}} = \frac{267 \times 10^{-6}}{599 \times 10^{-6} \times 0.560} = 0.796$$

$(Sc)_{CO_2}^{2/3} = 0.859$

$R_{CO_2} = 0.000179$

Since π = 1 atm

$$P_{f_{CO_2}} = y_{f_{CO_2}} = 0.991$$

$$j_d = 0.84\ Re^{-0.51}$$

$$j_d = 0.84\,(0.148)^{-0.51} = 2.22$$

$$\Delta y_{CO_2} = \frac{R_{CO_2}\, y_{f_{CO_2}}\, (Sc)^{2/3}}{j_d} = \frac{0.000179 \times 0.991 \times 0.859}{2.22}$$

$$\Delta y_{CO_2} = 0.0000686$$

$$\left(\frac{\Delta P}{P}\right)_{CO_2} = \Delta y_{CO_2}\, \frac{\pi}{P_{CO_2}} = \frac{0.0000686}{0.036}$$

$$\left(\frac{\Delta P}{P}\right)_{CO_2} = 0.0019$$

C. Estimation of Temperature Drop From the Bulk Gas Phase to the Surface of the Catalyst for Run 362

The temperature drop from the plot of ΔT vs. Q of Yoshida, Ramaswami and Hougen (24) was obtained as follows

$$Q = \frac{r_{m_A}\, \Delta H_A}{a_m \rho\, C_p\, G_m}$$

where C_p = molal heat capacity at cst. P

ΔH_A = molal heat of reaction of component A

Component	$C_{av.}$	C_p		$(C_p)(C_{av.})$
O_2	0.109	7.8	=	0.850
N_2	0.650	7.3	=	4.745
C_4H_8	0.148	38.0	=	5.624
C_4H_6O	0.0085	41.0	=	0.349

Component	$C_{av.}$	C_p		$(C_p)(C_{av.})$
CO_2	0.036	11.8	=	0.425
H_2O	0.047	8.8	=	0.409
CO	0.0015	7.4	=	0.011
		C'_p	=	12.4 cal./g. mole °C

$(\Delta H_r)_{400° C}$ = 648,000 cal./g. mole

r_{m_A} = 0.0672 g. moles/hr.

a_m = 0.43 ft^2/gm., weight of catalyst = 1.298 gms

ϕ = 0.9

G_m = 2843 g. moles/hr. ft^2

$$Q = \frac{.0672 \times 648,000}{1.298 \times 0.43 \times 0.9 \times 12.4 \times 2843} = 2.5° C$$

and from the chart ΔT = 7° C

D. Estimation of Temperature Drop from the Center of the Catalyst Bed to the Liquid Metal Bath for Run 362

Neglecting heat transfer by radiation and convection and assuming a parallel heat transfer scheme, then:

$$q = \left[h_{air} A_1 + k_{Cu} A_2 + k_{steel} A_3\right] \Delta T$$

h_{air} = 2.8 k_{Cu} = 210 k_{steel} = 25

A_1 = 0.0785 A_2 = .0236 A_3 = .055 ft^2

$$q = \left[2.8 \times 0.0785 + 210 \times 0.0236 + 25 \times 0.055 \right] \Delta T$$

$$q = 6.6 \Delta T$$

$$q = 648,000 \times 0.0672 = 43,600 \text{ cal}$$

$$q = 173 \text{ Btu}$$

$$\Delta T = 173/6.6 = 26.3^\circ F$$

$$(\Delta T) = 15^\circ C$$

This is probably a maximum ΔT because the other sources of heat transfer were neglected.

Appendix F

Conversion Curves as Calculated by Equation (68)

Table 10: Conversion Data as Calculated by Equation (68)

Temp. 400° C R = 0.25

$(NO_2)_o$ = 0.2100 $(N_{C_4H_8})_o$ = 0.8400 N_2 = 0.7900 (N_t) av. = 1.8526

$d = (NO_2)_o/(N_t)$ av.	= 0.2100/1.8526	= 0.1134
$a = (N_{C_4H_8})_o/(N_t)$ av.	= 0.8400/1.8526	= 0.4534
$e = a(1 + 2.775\ R^{0.231})$	= 0.4534 X 3.015	= 1.367
$b = a(1 - 555\ R^{0.231})$	= 0.4534 X 0.5971	= 0.2707

$X_{C_4H_8}$	0.0200	0.0400	0.0600	0.0800
1 - X	0.9800	0.9600	0.9400	0.9200
eX/d	0.2411	0.4822	0.7233	0.9644
1-eX/d	0.7589	0.5178	0.2767	0.0356
(1-eX/d)/(1-X)	0.7744	0.5394	0.2944	0.0387
A	0.2562	0.6180	1.2242	3.2520
-ln (1-eX/d)	0.2758	0.6578	1.2837	3.3355
-ln (1-X)	0.0202	0.0408	0.0619	0.0834
B	0.2018	0.4812	0.9391	2.440
$-\frac{d}{e}$ ln (1-eX/d)	0.0229	0.0546	0.1065	0.2767
C	0.0027	0.0138	0.0446	0.1933

α = 3.33 K_1 = 30 K_3 = 30

$1/\alpha K_1 a(e-d)$ = 0.0176 $1/\alpha$ = 0.30 $K_3 b/\alpha a K_1 (e-d)$ = 0.143

$X_{C_4H_8}$	0.020	0.040	0.060	0.080
D	-	0.01	0.02	0.06
E	0.06	0.14	0.28	0.73
H	-	-	0.01	0.03

Table 10 - Continued

Temp. 400° C R = 0.25

W/F	0.06	0.15	0.31	0.82
$1/4\, X_{CO_2}$	0.008	0.016	0.024	0.032
$X_{C_4H_6O}$	0.012	0.024	0.036	0.048

$A = -\ln (1-eX/d)/(1-X)$

$B = -\frac{1}{e} \ln (1-eX/d)$

$C = -\frac{d}{e} \ln (1-eX/d) - \ln(1-X)$

$D = -1/\alpha K_1 a (e-d) \ln (1-eX/d)/(1-X)$

$E = -1/e\alpha \ln (1-eX/d)$

$H = -K_3 b/\alpha a (e-d) \frac{d}{e} \ln (1-eX/d) - \ln (1-X)$

Table 10 - Continued

Temp. 400° C R = 0.5

$(NO_2)_o = 0.4200$ $(N_{C_4H_8})_o = 0.8400$ $N_2 = 1.580$ (N_t) av. = 2.860

d = 0.147 a = 0.294 e = 0.989 b = 0.155

$\alpha = 3.33$ $K_1 = 30$ $K_3 = 30$

$1/\alpha K_1 a(e-d) = 0.0404$ $1/\alpha = 0.30$ $K_3 b/\alpha a K_1 (e-d) = 0.188$

$X_{C_4H_8}$	0.025	0.050	0.075	0.100	0.120	0.145
A	0.159	0.358	0.625	1.013	1.519	3.576
B	0.187	0.415	0.711	1.130	1.664	3.770
C	0.0022	0.0097	0.0265	0.0950	0.117	0.397
D	0.01	0.01	0.03	0.04	0.06	0.15
E	0.06	0.12	0.21	0.34	0.50	1.13
H	-	0.01	0.01	0.02	0.02	0.07
W/F	0.07	0.14	0.25	0.40	0.58	1.35
$1/4 X_{CO_2}$	0.012	0.024	0.036	0.048	0.057	0.069
$X_{C_4H_6O}$	0.013	0.026	0.039	0.052	0.063	0.076

Table 10 - Continued

Temp. 400° C R = 1.0

$(NO_2)_o$ = 0.5006 $(N_{C_4H_8\,o})$ = 0.4821 N_2 = 1.8833 (N_t) av. = 2.901

d = 0.173 a = 0.166 e = 0.627 b = 0.0739

α = 3.33 K_1 = 30 K_3 = 30

$1/\alpha K_1 a(e-d)$ = 0.133 $1/\alpha$ = 0.30 $K_3 b/\alpha a K_1 (e-d)$ = 0.295

$X_{C_4H_8}$	0.050	0.100	0.150	0.200	0.250
A	0.149	0.345	0.622	1.067	2.079
B	0.319	0.717	1.253	2.059	3.771
C	0.0038	0.0186	0.0542	0.133	0.365
D	0.04	0.09	0.17	0.29	0.56
E	0.09	0.22	0.38	0.62	1.13
H	-	0.01	0.02	0.04	0.11
W/F	0.13	0.32	0.57	0.95	1.80
$1/4\ X_{CO_2}$	0.028	0.055	0.083	0.110	0.138
$X_{C_4H_6O}$	0.022	0.045	0.067	0.090	0.112

Table 10 - Continued

Temp. 400° C R = 2.0

$(NO_2)_o = 0.5456$ $(N_{C_4H_8\,o}) = 0.2679$ $N_2 = 2.053$ (N_t) av. $= 2.904$

$d = 0.188$ $a = 0.0923$ $e = 0.393$ $b = 0.0321$

$\alpha = 3.33$ $K_1 = 30$ $K_3 = 30$

$1/\alpha K_1 a(e-d) = 0.529$ $1/\alpha = 0.30$ $K_3 b/\alpha a K_1 (e-d) = 0.509$

$X_{C_4H_8}$	0.100	0.200	0.300	0.400	0.475
A	0.129	0.318	0.629	1.298	4.343
B	0.598	1.377	2.509	4.601	12.63
C	0.007	0.036	0.114	0.353	1.73
D	0.07	0.17	0.33	0.69	2.30
E	0.18	0.41	0.75	1.38	3.79
H	-	0.02	0.06	0.18	0.88
W/F	0.25	0.60	1.14	2.25	6.97
$1/4\ X_{CO_2}$	0.067	0.134	0.202	0.269	0.319
$X_{C_4H_6O}$	0.033	0.066	0.098	0.131	0.161

Table 10 - Continued

Temp. 400° C R = 3.0

$(NO_2)_o = 0.5625$ $(N_{C_4H_8})_o = 0.1875$ $N_2 = 2.1161$ (N_t) av. = 2.908

d = 0.194 a = 0.0646 e = 0.296 b = 0.0184

$\alpha = 3.33$ $K_1 = 30$ $K_3 = 30$

$1/\alpha K_1 a(e-d) = 1.52$ $1/\alpha = 0.30$ $K_3 b/\alpha K_1 a(e-d) = 0.839$

$X_{C_4H_8}$	0.100	0.200	0.300	0.500	0.650
A	0.062	0.140	0.256	0.747	3.77
B	0.561	1.23	2.07	4.86	16.31
C	0.004	0.016	0.045	0.251	2.11
D	0.09	0.21	0.39	1.14	5.73
E	0.17	0.37	0.62	1.46	4.89
H	-	0.01	0.04	0.21	1.77
W/F	0.26	0.59	1.05	2.81	12.39
$1/4\ X_{CO_2}$	0.072	0.143	0.215	0.358	0.465
$X_{C_4H_6O}$	0.028	0.057	0.085	0.142	0.185

Table 10 - Continued

Temp. 400° C R = 4.0

$(NO_2)_o$ = 0.5721 $(N_{C_4H_8\,o})$ = 0.1420 N_2 = 2.152 (N_t) av. = 2.915

d = 0.196 a = 0.0487 e = 0.235 b = 0.0115

α = 3.33 K_1 = 30 K_3 = 30

$1/\alpha K_1 a(e-d)$ = 5.26 $1/\alpha$ = 0.30 $K_3 b/\alpha K_1 a(e-d)$ = 1.81

$X_{C_4H_8}$	0.100	0.300	0.500	0.600	0.750
A	0.0223	0.0888	0.222	0.354	0.909
B	0.544	1.899	3.888	5.401	9.771
C	0.0012	0.0155	0.0689	0.142	0.529
D	0.12	0.47	1.17	1.86	4.78
E	0.16	0.57	1.17	1.62	2.93
H	-	0.03	0.12	0.26	0.95
W/F	0.28	1.07	2.46	3.74	8.66
$1/4\ X_{CO_2}$	0.076	0.228	0.380	0.456	0.570
$X_{C_4H_6O}$	0.024	0.072	0.120	0.144	0.180

Table 10 - Continued

Temp. 350° C R = 4.0

α = 1.60 K_1 = 140 K_3 = 140

$1/\alpha K_i a(e-d)$ = 2.35 $1/\alpha$ = 0.625 $K_3 b/\alpha K_1 a(e-d)$ = 3.78

$X_{C_4H_8}$	0.100	0.300	0.500	0.600	0.750
W/F	0.39	1.46	3.21	4.75	10.24
$1/4\ X_{CO_2}$	0.076	0.228	0.380	0.456	0.570
$X_{C_4H_6O}$	0.024	0.072	0.120	0.144	0.180

Table 10 - Continued

Temp. 375° C R = 4.0

$\alpha = 2.30$		$K_1 = 58$		$K_3 = 58$	
$1/\alpha K_1 a(e-d) = 3.95$		$1/\alpha = 0.435$		$K_3 b/\alpha K_1 a(e-d) = 2.63$	
$X_{C_4H_8}$	0.100	0.300	0.500	0.600	0.750
W/F	0.33	1.22	2.76	4.1	9.3
$1/4\ X_{CO_2}$	0.076	0.228	0.380	0.456	0.570
$X_{C_4H_6O}$	0.024	0.072	0.120	0.144	0.180

Table 10 - Continued

Temp. 425° C R = 4.0

$\alpha = 4.4$ $K_1 = 16$ $K_3 = 16$

$1/\alpha K_1 a(e-d) = 7.65$ $1/\alpha = 0.233$ $K_3 b/\alpha K_1 a(e-d) = 1.41$

$X_{C_4H_8}$	0.100	0.300	0.500	0.600	0.750
W/F	0.30	1.14	2.71	4.17	9.98
$1/4\ X_{CO_2}$	0.076	0.228	0.380	0.456	0.570
$X_{C_4H_6O}$	0.024	0.072	0.120	0.144	0.180

Table 10 - Continued

Temp. 450° C R = 4.0

$a = 6.0$ $K_1 = 9.0$ $K_3 = 9.0$

$1/a\,K_1\,a\,(e-d) = 9.75$ $1/a = .167$ $K_3 b/a\,K_1\,a\,(e-d) = 1.01$

$X_{C_4H_8}$	0.100	0.300	0.500	0.600	0.750
W/F	0.31	1.21	2.88	4.49	11.02
$1/4\ X_{CO_2}$	0.076	0.228	0.380	0.456	0.570
$X_{C_4H_6O}$	0.024	0.072	0.120	0.144	0.180

Appendix G

Calculations of $f(r_o)$ and $f(r)$

Table 11: $f(r_o)$ As Calculated From the Different Rate Equations

R	r_o	P_{O_2}	$P_{C_4H_8}$	P_{O_2}/r_o	$P_{C_4H_8}/r_o$	$\frac{P_{O_2}P_{C_4H_8}}{r_o}$	$\left[\frac{P_{O_2}P_{C_4H_8}}{r_o}\right]^{1/2}$
0.25	0.35	0.114	0.46	0.326	1.31	0.150	0.387
0.50	0.41	0.148	0.30	0.361	0.732	0.108	0.329
1.0	0.46	0.175	0.17	0.380	0.370	0.065	0.255
2.0	0.43	0.190	0.094	0.442	0.219	0.042	0.205
3.0	0.38	0.196	0.064	0.516	0.168	0.033	0.182
4.0	0.35	0.200	0.050	0.571	0.143	0.029	0.170

Table 12: Calculated Slopes from Curves of Figure 17

R	Slope
0.5	0.475
1.0	0.552
2.0	0.672
3.0	0.715
4.0	0.760

Table 13: f(r) As Calculated From the Different Rate Equations

	X	r	a(1-X)	a(1-X)(d-eX)	$\frac{a(1-X)}{r}$	$\frac{a(1-X)(d-eX)}{r}$	$\frac{[a(1-X)(d-eX)]^{1/2}}{r}$
R = 0.5	0	0.41	0.294	0.0432	0.72	0.105	0.32
	0.04	0.30	0.282	0.0303	0.94	0.101	0.32
	0.06	0.23	0.276	0.0242	1.20	0.105	0.32
	0.08	0.17	0.270	0.0184	1.59	0.108	0.33
	0.10	0.12	0.265	0.0127	2.20	0.106	0.33
R = 1.0	0	0.46	0.166	0.0287	0.37	0.064	0.25
	0.05	0.35	0.158	0.0224	0.45	0.064	0.25
	0.10	0.25	0.149	0.0164	0.60	0.066	0.26
	0.15	0.18	0.141	0.0111	0.78	0.062	0.25
	0.20	0.095	0.133	0.0063	1.40	0.067	0.26
R = 2.0	0	0.43	0.0923	0.0174	0.21	0.041	0.20
	0.10	0.32	0.0831	0.0124	0.26	0.039	0.20
	0.20	0.22	0.0738	0.00805	0.34	0.037	0.19
	0.30	0.11	0.0646	0.00453	0.59	0.041	0.20
	0.40	0.045	0.0554	0.00171	1.20	0.038	0.19

Table 13 - Continued

	X	r	a(1-X)	a(1-X)(d-eX)	$\frac{a(1-X)}{r}$	$\frac{a(1-X)(d-eX)}{r}$	$\frac{[a(1-X)(d-eX)]^{1/2}}{r}$
R = 3.0	0	0.38	0.0646	0.0125	0.17	0.033	0.18
	0.10	0.33	0.0581	0.0096	0.18	0.029	0.17
	0.20	0.23	0.0517	0.0070	0.22	0.031	0.18
	0.30	0.15	0.0452	0.0048	0.30	0.032	0.18
	0.40	0.090	0.0388	0.0029	0.43	0.033	0.18
R = 4.0	0	0.35	0.0487	0.0096	0.14	0.027	0.16
	0.10	0.31	0.0438	0.0760	0.14	0.025	0.16
	0.20	0.22	0.0390	0.0580	0.18	0.026	0.16
	0.30	0.16	0.0341	0.0430	0.21	0.027	0.16
	0.40	0.12	0.0292	0.0298	0.24	0.025	0.16

Appendix H

Temperature Dependence of a, $K_{C_4H_8}$ and $K_{C_4H_6O}$

Table 14: Temperature Dependence Of α, $K_{C_4H_8}$ and $K_{C_4H_6O}$

T °K	$10^3/T$ $°K^{-1}$	α	$K_{C_4H_8}$	$K_{C_4H_6O}$
623	1.61	1.60	140	140
648	1.54	2.30	58	58
673	1.49	3.33	30	30
698	1.43	4.40	16	16
723	1.38	6.00	9.0	9.0

Appendix I

Conversions and Yields for Different Catalysts

Table 15: Conversion and Yields For Different Catalysts at 400° C For R = 2.0 and W/F = 1.71

Run No.	Catalyst	$X_{C_4H_8}$	Yield C_4H_6O	Yield CO_2	Yield CO	Yield Total Acids	Yield Other Aldehydes
372	1	0.400	0.296	0.688	0.009	-	-
434	2	0.272	0.333	0.651	0.013	-	-
435	3	0.371	0.308	0.678	0.012	-	-
436	4	0.422	0.274	0.717	0.009	-	-
437	5	0.467	0.069	0.840	0.098	-	-
444	6	-	-	-	-	-	-
445	7	0.386	0.301	0.682	0.009	-	-
446	8	0.526	0.181	0.532	0.171	0.010	0.106
447	9	0.618	0.273	0.383	0.083	0.046	0.215